Modelling Tile Drains Under Present and Future Climate Conditions

by

Patrick O'Neill

A thesis
presented to the University of Waterloo
in fulfillment of the
thesis requirement for the degree of
Master of Applied Science
in
Civil Engineering

Waterloo, Ontario, Canada, 2008

I hereby declare that I am the sole author of this thesis. This is a true copy of the thesis, including any required final revisions, as accepted by my examiners.

I understand that my thesis may be made electronically available to the public.

Abstract

Modelling the impact of climate change on the water from agricultural areas on a regional scale over a 40 year time period is the subject of this thesis. The Grand River watershed spans approximately 290 km with an area of approximately 6,800 km^2. Approximately 90% of the watershed is agricultural land some of which is tile drained. These tile drains, which cover approximately 15% of the total land of the watershed, are installed to augment field drainage. The tile drains usually outlet somewhere along the perimeter of a property; the discharge then typically moves along the surface until it discharges into a surface water body such as a river, pond, or lake. Investigating the impact of climate change on agricultural tile drainage at a watershed scale can be achieved using modelling. The tile drains can affect both the water quality and the water quantity of a watershed. With the potential climatic changes, the storm intensity, and growing season also could change.

Spatial data for the Grand River watershed was gathered to allow for further simulation. The data for tile drained areas was added to land use/land class and soil data for the watershed to produce a map of tile drained agricultural areas.

Climate change scenarios were then simulated for each cell. Three climate change scenarios were investigated to determine the impact on tile drain discharge and the hydrological process for the watershed. The climate change scenarios that were chosen were the A2, A1B, and the B1 scenario of the Intergovernmental Panel on Climate Change.

After the simulations were completed for the tiled areas and the results collected, the simulations showed the greatest impact of tile drain discharge in the spring season as well as the fall season.

For the tiled cells the annual average discharge was approximately 0.22 m^3/ha for 1999. The average discharge was approximately 0.15 m^3/ha for April of 1999. April accounted for approximately 65% of the annual tile drainage for 1999.

The climate change scenarios were simulated and the average annual discharge increased approximately 0.023 m^3/ha and 0.021 m^3/ha for the A2 and A1B scenarios respectively. The B1 scenario had an average annual decrease of approximately 0.022 m^3/ha.

Acknowledgements

I would like to thank Prof. Jon Sykes for giving me the opportunity to complete my thesis under his guidance. I would also like to thank Prof. James Craig and Stefano Normani for all of the GIS and database help when I was looking for help, Mikko Jyrkama for guiding me with the recharge and climate change modelling. I would also like to thank my family who supported me while I was attending the University of Waterloo. I would like to thank all of my friends who helped me get through the long journey that is university.

Dedication

This is dedicated to my family and friends who supported me through my time at the University of Waterloo.

Contents

List of Tables

List of Figures

Chapter 1

Introduction

The Grand River watershed (GRW) spans approximately 290 km with an area of approximately 6,800 km^2 (*Jyrkama and Sykes*, 2007). Approximately 90% of the watershed is agricultural land. Tile drains are located on agricultural land where the soils such as heavy clays and silts do not allow the groundwater to readily drain. Tile drains cover approximately 99,800 ha of agricultural land in the GRW with this being approximately 15%, of the total GRW area. The tile drains prevent the fields from becoming water logged with this potentially having an effect on the crop yield. The tile drains must outlet somewhere along the perimeter of a farm property. This discharge typically then moves along the surface to a surface water body such as a river, pond, or lake.

The water courses for these discharges potentially can be experiencing conditions of eutrophication as well as hypoxia (*Anderson et al.*, 2006). These conditions are a result of contaminated runoff and tile drainage discharge from agricultural fields (*Burkart and James*, 1999). The discharge waters are often contaminated with nitrates, which were applied to the field as fertilizer. Nitrates that migrate into the drinking water sources can be potentially fatal to both humans and animals that ingest the contaminated drinking water (*Prakasa Rao and Puttanna*, 2000; *Toghi et al.*, 1998; *Irvine et al.*, 1993).

Climate change is a reality that the earth is undergoing. Modelling the potential changes to the earth's temperatures and precipitation has been done by others (*Jyrkama and Sykes*, 2007; *McGregor*, 1997). Modelling the potential impact of climate change effects on the transport of discharge waters from tile drains from agricultural sources will also be examined in this thesis.

1.1 Research Motivation

Large scale watershed modelling is not done very often. However, to understand the potential outcomes of a system on a watershed scale, modelling is a useful tool. One of the variables that can be examined is tile drains and how they affect the watershed. The tile drains can impact both the water quality and water quantity of a watershed.

Many of the agricultural fields in the Grand River watershed have had some form of tile drains installed, with these potentially carrying harmful nitrates and other contaminants into drinking water supplies. Predicting how and when the nitrates will arrive can be crucial to mitigating the problem. The flow from tile drained farms can be considerable, especially after a major rain storm or snow melt event. With the potential climatic changes to the weather patterns, storm intensity, and growing seasons that could take place within the next 40 years, the ability to predict how much water to expect and where potential contaminants will travel can be a very useful tool.

With a complex and large watershed scale model, the appropriate software has to be used. Geographical information systems (GIS), as well as database software such as Microsoft Access, allows modelling on the watershed scale with the complexities of varying Land Use/Land Classes, soil variability, and climatic variability.

1.2 Objectives

The objective of this thesis is to simulate the impact of tile drains on the hydrological processes in the Grand River Watershed. Another objective of this thesis is to simulate climate change scenarios on the Grand River Watershed. This is done to examine the potential impacts on the tile drain discharges as well as the other hydrological processes.

1.3 Focus

The main focus of this study is to investigate the potential risks that tile drains can have to surrounding area surface water bodies for the Grand River

watershed. This will be done by using a spatial database and a physically based model to simulate conditions for the 40 year period from 1960 to 1999 using meteorological data that has been collected by the Grand River Conservation Authority (GRCA). This simulation will illustrate how much water the tile drains are collecting on an annual basis and transporting to adjacent surface waters.

The other focus of this thesis includes predicting how potential climate change scenarios will impact how the tile drains work and if more or less water is extracted from the tile drains by using the Intergovernmental Panel on Climate Change (IPCC) climate change scenario projections *IPCC* (2007c). These projections will be used to modify the base-case weather data that has been collected for 40 years and then run the tile drain model to examine what the effect differing scenarios will have on the drainage from the watershed tile drains and the recharge to the groundwater.

Chapter 2

Background

The Grand River watershed (GRW) contains large agricultural areas as well as some significant urban areas. The inhabitants of the GRW use the many rivers and lakes, as well as the groundwater, for drinking water and irrigation for the land. The quantity of water that is extracted from the watershed each year puts stress on the hydrological processes in the watershed. With the effects of climate change occurring in the watershed those stresses on the hydrological processes will likely be impacted. On the agricultural lands in the GRW fertilization, irrigation and drainage of the fields is critical to the crop yields. If any of these three processes are impacted, crop yields will suffer and drinking water can potentially become contaminated. This chapter will discuss how tile drains are involved with the watershed and how they will be modelled for this thesis.

2.1 Grand River Watershed

The GRW is located in southwestern Ontario, Canada. Figure 2.1 shows the location of the watershed relative to some of the major cities. The GRW is approximately 6,800 km^2 and drains into Lake Erie. The main river stretches approximately 290 km with an overall elevation change of approximately 362 m from source to mouth (*Jyrkama and Sykes*, 2007). Located in the GRW are some urban centres such as Kitchener-Waterloo, Cambridge, Guelph, and Brantford. These cities comprise a small percentage of the GRW area; up to 90% of the watershed is rural land (*Jyrkama and Sykes*, 2007).

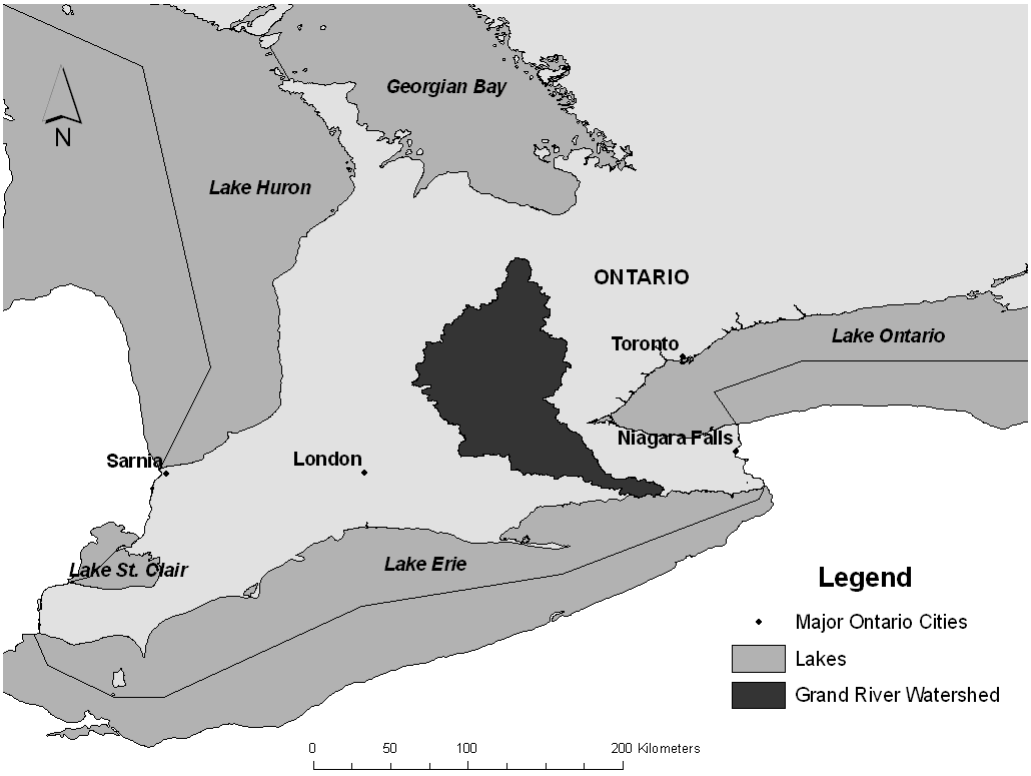

Figure 2.1: Grand River Watershed

Southwestern Ontario was heavily influenced by the last glacial retreat. When the last glaciers left, they created an area of highly variable soil type. The southern and northern sections of the GRW have lower permeability soils, while the central area, the Kitchener-Waterloo region, is made up of higher permeability soils (*Holysh et al.*, 2000).

The Grand River Conservation Authority (GRCA) constantly monitors and protects the watershed because the rivers in the watershed are a valuable resource for both drinking water and water for irrigation (*Grand River Conservation Authority*, 2008). With the increasing urbanization of the city areas, more stress is being put on the GRW. Not only is water quantity being stressed but so is water quality. As a result, the GRCA is constantly monitoring the watershed for both water quantity and quality.

2.2 Hydrological Cycle

The hydrological cycle describes how water moves on the earth and the various pathways that it takes. Water can take three different forms, specifically liquid (rain), solid (ice) and gas (water vapour), as it moves around the earth. The pathways of water result from interaction with vegetation, as well as various meteorological and geological conditions. Figure 2.2 depicts the hydrological cycle.

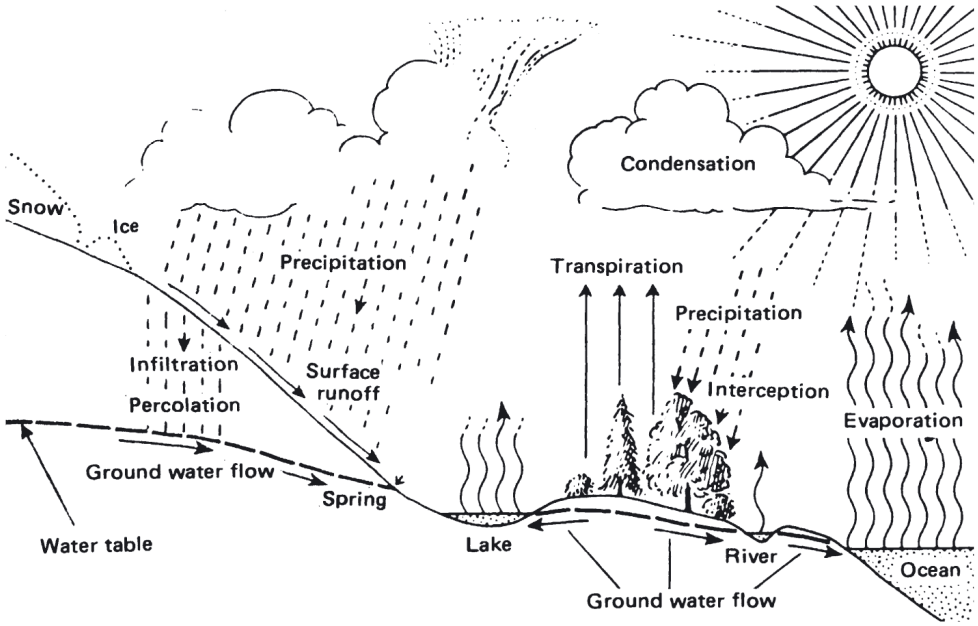

Figure 2.2: Hydrological cycle concept (*Busse and Hinkelmann*, 2006)

The hydrological cycle is made up of many components and can be described as the continuous movement of water above, below, and on the surface of the Earth. Precipitation can be described as the driving force of water movement over and through land surfaces. Precipitation forms when water vapour accumulates in the atmosphere in the form of clouds. These clouds will eventually deliver freshwater to the land, fresh water bodies, and oceans as precipitation. Precipitation mainly occurs in a liquid form but can also take on a solid state as snow or hail.

Precipitation that falls on land will accumulate to form lakes and rivers or as snow on the surface. Precipitation can also be intercepted by vegetation. Some of this intercepted water can still reach the ground through stemflow and throughflow. However, most of the water captured by vegetation is evaporated

back into the atmosphere. However, in liquid form, precipitation can migrate into the ground. Surface topology and precipitation intensity and duration are all large factors that determine if the precipitation will infiltrate and move into the subsurface. Once the water infiltrates into the subsurface and migrates below the root zone of the local vegetation it can move as interflow in the unsaturated zone or migrate into the saturated zone of the subsurface where it can stay for many years. Groundwater generally moves very slowly with respect to surface water.

If the precipitation does not move into the subsurface it will move across the land as overland flow. Overland flow will move towards streams, rivers, and lakes if it does not migrate eventually into the subsurface. In urban areas, the overland flow is captured and transported using the storm water sewer systems to areas such as lakes, rivers and groundwater recharge areas. In new subdivisions it is common practice to collect the overland flow and try to return that water to the subsurface in a natural way by using a storm water detention pond. Instead of collecting all of the storm water from an urban area and transporting it to central location, these ponds spread out the distribution of the storm water. Finally the last transport method in the water cycle is the evaporation and sublimation of water. This occurs on land, from the precipitation that is intercepted by plants and from the surface water bodies. Water evaporates from the surface of water such as rivers and lakes as well as a very limited amount of water can evaporate during precipitation events. This evaporate accumulates to form clouds and the cycle starts all over again.

In the past the groundwater and surface water portions of the hydrological cycle have been treated as separate entities. This was done to simplify the problem as solutions could not be derived for the integrated system due to the overwhelming computational power required. With the power available in computers today we are able to treat the groundwater and surface water as two very interactive parts in the hydrological cycle.

2.3 Changes in the Hydrological Cycle

According to the Intergovernmental Panel on Climate Change (IPCC) and their fourth assessment report, the annual mean precipitation is very likely

to increase in northeast Canada and the United States of America (USA), and likely to decrease in the southwest USA (*IPCC*, 2007a). In south-eastern Canada, precipitation is likely to increase in winter and spring, but decrease in the summer months (*IPCC*, 2007a). Snow season length and snow depths are very likely to decrease in most of North America, except in the northernmost parts of Canada where maximum snow depth is likely to increase (*IPCC*, 2007a).

The IPCC also predicted that storm systems, such as tropical storms and hurricanes, are likely to increase in intensity and frequency (*IPCC*, 2007a). This has already become evident during the 2005 hurricane season for the southern United States of America. The 2005 season had the most hurricanes and tropical storms on record with 28 compared to the average of 10 per season (*National Oceanic and Atmospheric Administration (NOAA)*, 2008).

2.3.1 Greenhouse Warming

Climate change is both a man made and a naturally occurring phenomenon. The climate of the Earth's surface and lower atmosphere is warming up and is likely to impact the global circulation of water vapour (*Loaiciga et al.*, 1995). To understand how climate change is affecting the hydrologic cycle we must first look at the basic concept of the greenhouse effect.

The greenhouse effect has been described as greenhouse gasses such as chlorofluorocarbons, carbon dioxide (CO_2), methane (CH_4), nitrous oxide, water vapour, and ozone that are emitted into the atmosphere and trap infrared radiation resulting in the warming of the Earth's surface. Of the gasses listed previously, CO_2, water vapour, along with cloud particles are the biggest greenhouse gasses and contribute to approximately 95% of the greenhouse effect (*Loaiciga et al.*, 1995). The sun's solar radiation is absorbed on the Earth's surface as well as by the atmosphere. Some of the solar radiation is reflected back into space. As this is occurring, the Earth emits infrared radiation into the atmosphere. With the green house gasses collecting in the atmosphere less of this infrared radiation is escaping and instead it is either bouncing back to the earth or trapped by the greenhouse gasses resulting in the warming of the Earth's atmosphere and surface (*Loaiciga et al.*, 1995). Due to the greenhouse gasses the radiative equilibrium on the Earth has resulted in an

average global temperature increase to approximately 15°C as compared to the Earth's atmospheric temperature of approximately -18°C, which is caused by the greenhouse effect (*Loaiciga et al.*, 1995).

2.3.2 Water Vapour Feedback on Greenhouse Warming

The first feedback mechanism that would have an effect on the temperature of the Earth is that of water vapour. This feedback loop starts with direct CO_2 emissions into the troposphere (portion of the atmosphere that is within the first 10 km of the Earth's surface). This will result in increased infrared emissions to the Earth surface, effectively increasing the temperature on the surface. With this heat, more water evaporates from the oceans and land. This then increases atmospheric humidity and simultaneously releases latent heat into the atmosphere, raising the tropospheric temperature. The tropospheric temperature is again raised by the adsorption of infrared radiation of greenhouse gasses. With this increased tropospheric temperature, the water holding capacity of the atmosphere increases. The increased water vapour in the atmosphere will also help trap more infrared radiation and again will increase the surface temperature, which completes the feedback loop when more surface water is evaporated (*Loaiciga et al.*, 1995). However, blackbody cooling emissions moderate the temperature increase. Essentially, blackbody cooling occurs when the radiative state reaches equilibrium, with this occurring when the infrared radiation emissions balance the net energy input from the sun (*Loaiciga et al.*, 1995).

2.3.3 Cloud Cover Feedback on Greenhouse Warming

Another lesser understood feedback mechanism that has much uncertainty surrounding it, is the feedback caused by clouds. Performing climate modelling on a regional and global scale with cloud cover can create problems. Clouds have the ability to absorb, reflect and emit radiation, which can cool and heat up the earth (*Jyrkama and Sykes*, 2007). The amount of cloud cover can present a source of error when simulating climate modelling predictions. This level of complexity may not be feasible to integrate into present climate models since there can be a high level of randomness associated with the formation of cloud cover.

Loaiciga et al. (1995) determined that the approximate global cloudiness was at 50%. Clouds have both a positive (warming) and negative (cooling) effect on the Earth's surface. Clouds can trap infrared radiation since they are essentially water vapour, which causes a warming effect. However clouds also reflect a lot of the sun's radiation back into space, which has a negative (cooling) effect on the Earth's surface. Overall, clouds have been shown to have a net negative effect on the Earth's surface (*Ramanathan and Collins*, 1991). Thus, if the Earth's cloudiness were to decrease then more solar radiation would reach the surface and increase the surface temperature.

2.3.4 Soil Moisture Feedback on Greenhouse Warming

Another feedback mechanism is through soil moisture. The role of soils is at best poorly understood when it comes to climate change. Even if the role(s) were understood and modelled, it would be very difficult to calibrate and validate the soil moisture effects in a climate change model on a global scale. However, even if this parameter is not as well known, the process of how it would most likely impact climate change has been theorized.

Soil moisture is most likely to affect areas where precipitation is predicted to decline. Soil moisture feedback would be more on a regional scale as opposed to the water vapour feedback, which is more on a global scale (*Loaiciga et al.*, 1995). As the precipitation decreases, soil moisture also decreases, which in turn decreases the evapotranspiration of the region. With less moisture evaporating, less cloud cover is likely to occur, which would reflect less solar energy and increase the surface temperature. This leads to more evaporation from the soil, which brings the feedback loop full circle having a net positive (warming) effect on the surface (*Loaiciga et al.*, 1995).

2.3.5 Vegetation Feedback on Greenhouse Warming

An additional feedback mechanism that has been documented is the feedback produced by the vegetation on the Earth's surface. Along with the soil moisture, the role of vegetation on feedback is poorly understood. The role that vegetation has on climate patterns can also be hard to calibrate on a global scale.

The vegetation feedback involves the biosphere (*Manabe and Wetherland*, 1987). One main cause in vegetation feedback is thought to be major changes in vegetated cover (i.e. clear cutting, or a major tree re-planting). These changes in vegetated cover can do multiple things to the surface temperature. First this would change the surface albedo, extent of how the surface diffusely reflects light from the sun, of the vegetated areas. A second change would be the CO_2 exchange between the vegetation and the atmosphere. For a plant to grow, it needs CO_2 from the atmosphere, proper temperature and a source of water. If any of these variables are not within an acceptable range for the plant, then the plant will not reach its potential growth or simply die. Too much surface temperature and the plant will likely lose most, if not all, of the soil moisture that it needs to grow (*Loaiciga et al.*, 1995).

2.3.6 Surface Albedo Feedback on Greenhouse Warming

The final feedback mechanism that occurs on the Earth is the feedback caused by surface albedo. Surface albedo is mainly concentrated at areas that contain large ice formations (i.e., glaciers and polar regions) (*Loaiciga et al.*, 1995). In the event of a surface temperature increase, ice and snow will melt. It is important to note that surface temperature increases are magnified at higher latitudes (*Loaiciga et al.*, 1995). With more surface melting of ice and snow the global surface albedo will be decreased, which will increase the amount of solar radiation being absorbed on the planet. This will increase the surface temperature, which completes the surface albedo feedback loop.

These feedback loops and the resulting surface warming are only one part of greenhouse consequences. Seasonal modifications to the hydrologic cycle, seen on a global scale, are also evident. Changes to precipitation and runoff are very important to water collection for water supply in many regions of the world (*Loaiciga et al.*, 1995). Also, the amplification of the magnitude of flooding, major storms (i.e., hurricanes, monsoons, etc.) along with the severity of droughts is a concern. All of these concerns are related to the hydrological cycle and their impact can change how the cycle can operate on not only a regional scale but a global scale as well.

2.4 The Nitrogen Cycle

The modelling of the nitrogen cycle is beyond the scope of this thesis. However, the impact of tile drains is to moderate or alter the distribution of nitrates in both the surface water and groundwater. This section describes the nitrogen cycle and the impact of tile drains on this cycle.

The nitrogen cycle describes the transformation of nitrogen and nitrogen-containing compounds within nature (*Biocrawler*, 2005). The largest source of nitrogen on the Earth is the atmosphere; air containing approximately 78% by volume in the gaseous state N_2. Nitrogen is an essential part of many biological processes, especially in vegetation. Plant life is essential in the conversion of atmospheric nitrogen into useable forms of nitrogen for other organisms. All nitrogen acquired by animals can be traced back to plants somewhere in the food chain. Herbivores and omnivores get nitrogen directly when they ingest the plant material. Carnivores will obtain their nitrogen through the ingestion of other animals. Plants are not the only things able to fix nitrogen. Nitrogen fixing is the process of taking nitrogen from the atmosphere and converting it into a useable form of nitrogen. Nitrogen fixing bacteria that live in the soil, such as Azobacter vinelandii and Rhizobium, are needed to produce another form of nitrogen that can be used by other nitrifying bacteria (*Biocrawler*, 2005).

After the process known as nitrification has been completed, then the vegetation can assimilate the nitrogen in the form of nitrate, which is then used by the plant for growth. If there is an abundance of nitrates in the soil, then further denitrifying bacteria, such as Thiobacillus Denitrificans, in the soil will return the nitrate into its gaseous N_2 state and the nitrogen cycle will start over (*Biocrawler*, 2005). Figure 2.3 describes the general concept of the nitrogen cycle.

2.4.1 Nitrates

For common crops found in North America, such as corn, there is normally not enough nitrogen in the soil to produce large crop yields every year. To maximize crop growth and size, without increasing cultivated land needed to sustain larger crops, nitrate (NO_3^-) rich organic and inorganic fertilizers are applied

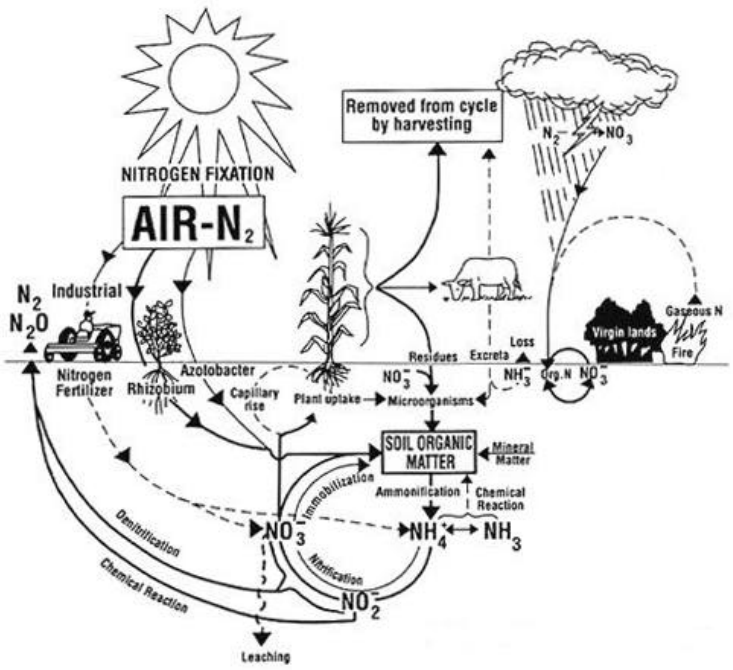

Figure 2.3: Conceptual nitrogen cycle (*Ohio State University*, 1991)

to the crop to ensure that nitrogen is not a limiting nutrient (*Prakasa Rao and Puttanna*, 2000). However, crop yields can be negatively affected from previous fertilization if excess nitrogen is left in the ground (*Kladivko et al.*, 2004).

After the fertilizer is applied to the soil it will infiltrate the ground and be converted from organic nitrogen into inorganic nitrogen via subsurface transformations. The first of these possible transformations is known as mineralization (*Prakasa Rao and Puttanna*, 2000). Mineralization occurs in the soil when there is a substantial amount of organic nitrogen available (*Burkart and James*, 1999). Another transformation of Nitrogen is known as nitrification, which is described in equation 2.1. This process occurs rapidly through oxidation with bacteria and occurs when ammonium (NH_4^+) or ammonia (NH_3) is converted into nitrite (NO_2^-) and nitrobacter bacteria then convert this form of nitrogen into nitrate (*Prakasa Rao and Puttanna*, 2000). Depending on the crop and soil type, the plants will absorb the nitrogen in either the ammonia or nitrate form.

$$NH_3 + 2O_2 \rightarrow NO_3^- + H_2O + H^+ \tag{2.1}$$

Under some soil conditions, and in an anaerobic environment, the process of denitrification can occur and will break the nitrate down into nitrogen gas (N_2), nitrous oxide (N_2O), or potentially nitric oxide (NO) (*Prakasa Rao and Puttanna*, 2000). Equation 2.2 shows the overall denitrification process and how the nitrate is converted back into nitrogen gas.

$$NO_3^- + \frac{5}{4}CH_2O + H^+ \rightarrow \frac{1}{2}N_2 + \frac{5}{4}CO_2 + \frac{7}{4}H_2O \tag{2.2}$$

Some studies have indicated that loss of nitrates via denitrification or biologic assimilation may be more active near the water table or in a riparian zone that is beneath a forested or wetland area (*Böhlke et al.*, 2002). Denitrification was thought to be a negligible sink for nitrate loss in the natural environment, however some studies have shown that denitrification can be a significant loss of nitrates in deeper fertile soils (*Byre et al.*, 2001). Denitrification is limited to soil where oxygen is limited and both nitrates and carbon are in abundance. *Byre et al.* (2001) suggest that if conditions are right in the soil subsurface then denitrification can eliminate larger quantities of nitrates than first hypothesized.

Nitrates have been linked to some potentially serious diseases in humans. Both nitrates and nitrites in food have been linked to a fatal affliction in babies. Methemoglobinemia reduces the oxygen-carrying capacity of the red blood cells. Lowered oxygen in the blood can eventually become fatal to new born babies (*Prakasa Rao and Puttanna*, 2000). There have been other health issues related to nitrate toxicity. Some of these include oral and colon cancer (*Prakasa Rao and Puttanna*, 2000), Alzheimer's disease (*Toghi et al.*, 1998), multiple sclerosis (*Irvine et al.*, 1993), and non-Hodgkin's lymphoma (*Prakasa Rao and Puttanna*, 2000). Nitrate contamination can also lead to hypoxia, which has been known to lead to massive fish kills in coastal regions (*Sklar and Browder*, 1998). This is discussed in detail in section 2.4.3.1.

Because of the severity of possible nitrate toxicity, some methods to remove nitrates in solution have been developed. There are chemical methods such as abiotic degradation using zero valent iron (*Prakasa Rao and Puttanna*, 2000), and reduction of nitrate to ammonia and nitrogen gas using aluminum (*Murphy*, 1991). Additional methods of nitrate removal include using vegetable oil for denitrification (*Hunter*, 2001), using engineered wetlands to reduce the nitrate loadings (*Prakasa Rao and Puttanna*, 2000), using sulfur and limestone

to encourage the denitrification process (*Flere and Zhang*, 2001), and using nanofiltration and reverse osmosis (*Bohdziewicz et al.*, 1999). These methods of nitrate removal can be costly and predicting where and when the nitrates will show up in the drinking water source is difficult. Using best management practices and an optimized fertilization schedule can reduce the need for nitrate remediation in drinking water. Using an optimized schedule, concentrations of the nitrates reaching drinking water sources can ultimately become negligible.

2.4.2 Nitrates in the Groundwater

A common source for nitrates in the ground water and surface water is the over fertilization of fields. Studies have shown that increasing the fertilizer rate from 100 to 250 kg of N per ha for certain crops will double the concentration of leached nitrate in the effluent from a tile drain from 20 to 40 mg/L (*Jaynes et al.*, 2001). The drinking water standard in Ontario for nitrate as nitrogen is 10 mg/L (*Ministry of the Environment (MOE)*, 2002).

Nitrates that migrate into the ground water from agricultural sources have multiple pathways. The first pathway for migration would be from percolation using the infiltrated irrigation water or precipitation. The second method for nitrates to migrate into groundwater would be for the nitrates to flow into the tile drains in the subsurface of some agricultural fields. The nitrate left in the ground is normally well distributed within the soil matrix before it is transported into the groundwater or into tile drains (*Kladivko et al.*, 2004). Unfortunately, due to preferential flow paths of aqueous solutions such as pesticides and fertilizers that are applied to a field, a higher flow in tile drains does not always equal higher concentrations moving into the groundwater or in the tile drains (*Kladivko et al.*, 1999). Water will potentially take preferential flow paths in the subsurface and will not contact all of the nitrates in the soil matrix.

2.4.3 Changes to the Nitrogen Cycle

The Nitrogen cycle has been perturbed by human activities such as agriculture and the combustion of fossil fuels. These changes have both increased the

mobility and availability of nitrogen over large areas on the Earth's surface (*Vitousek et al.*, 1997). By cultivating leguminous crops and forages (e.g. peas, alfalfa, soybean, etc.) in large quantities, the amount of nitrogen being fixed from the atmosphere has remarkably increased (*Vitousek et al.*, 1997). These types of crops support nitrogen fixing micro-organisms, which can fix nitrogen straight from the atmosphere. The other human influence on the nitrogen cycle is increasing the mobility of nitrogen to both groundwater and surface water bodies (*Vitousek et al.*, 1997). Common pathways include biomass burning, land clearing, and removing a natural nitrogen sink such as the organic soils of wetlands (*Vitousek et al.*, 1997). Organic wetland soils promote denitrification in aerobic conditions. Once the useable nitrogen has a pathway into the groundwater and surface waters, many undesirable conditions can start to occur in the environment.

2.4.3.1 Hypoxia

Nitrogen contamination of groundwater and surface waters is an on going problem throughout the world. Most of the contamination has been partially linked to the over fertilization of farmer's fields (*Burkart and James*, 1999). The current fertilization practices can lead to over fertilization, which can eventually result in contaminated ground waters and surface waters, and subsequently result in a phenomenon known as hypoxia. Hypoxia occurs in the surface water when dissolved oxygen (DO) drops below 2 mg/L (*Burkart and James*, 1999). This phenomenon has been well documented and mapped in the Gulf of Mexico where an area of hypoxia or "dead-zone" is created seasonally from approximately mid-June to the mid-August (*Rabalais et al.*, 2001).

Figure 2.4 shows the extent of the Gulf of Mexico "dead-zone" as of 2004. The red zones in Figure 2.4 show areas of low DO (in mg/L) ranging from approximately 0 to 2 mg/L. The yellow areas show DO with approximately 2 to 5 mg/L of DO, where the green areas have DO concentrations ranging from 5 to 8 mg/L. Nutrient rich fresh water flows out from the inland rivers, such as the Mississippi, and floats on the denser salt water of the ocean. Large blooms of phytoplankton grow in the nutrient rich waters (*Anderson et al.*, 2006). Eventually the phytoplankton will die and sink to the ocean floor. The bacterial decomposition of the phytoplankton strips the oxygen from the surrounding waters, which creates the "dead-zone" (*Rabalais et al.*, 2001). The

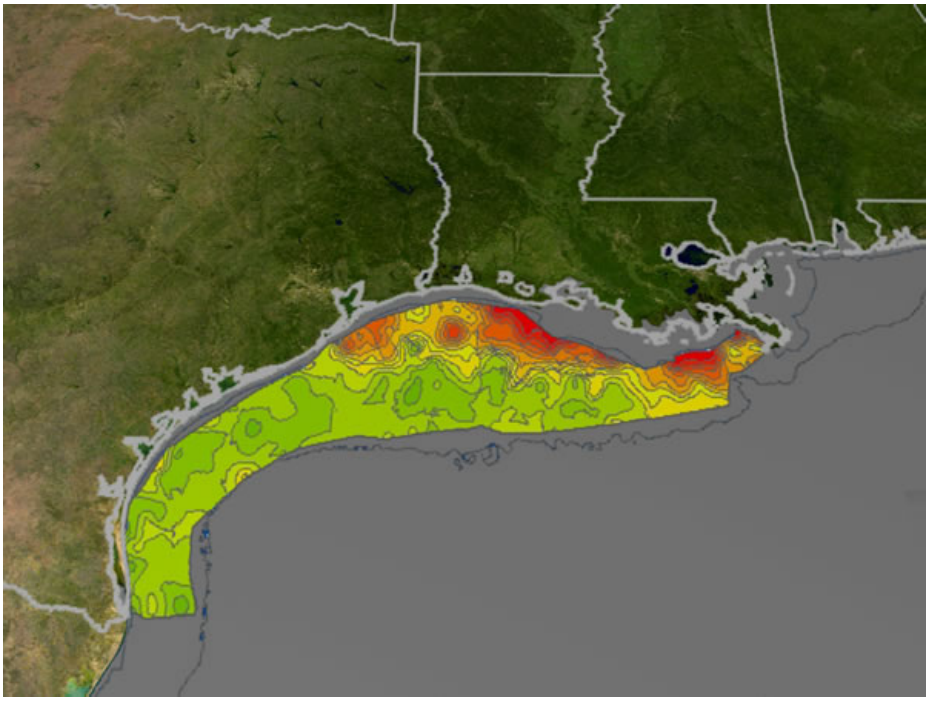

Figure 2.4: Measured DO concentrations in summer months (*National Oceanic and Atmospheric Administration (NOAA)*, 2004)

process is known as eutrophication leads to zones of hypoxia, which forces fish and other life to move away due to lack of oxygen. Figure 2.5 describes how hypoxia forms in a visual format.

The midwestern United States (US) agricultural industry is one of the main culprits for the hypoxia problems in the Gulf of Mexico. These agricultural areas drain into the Mississippi river, with a watershed area of approximately 3.2 million km^2 or 42% of the continental US (*Burkart and James*, 1999). The midwest US is where much of the country's corn is grown, a major cash crop in the US (*David et al.*, 1997). The cash crops in the midwest US use fertilizers to maximize yields. In 1991 an estimated seven million tons of fertilizer was applied within the Mississippi River basin (*Burkart and James*, 1999). Any nitrogen in the fertilizer that is not used by the crops can potentially move into the waters of the Mississippi River. The farms that are located in the midwest are known to incorporate tile drainage technology to aid in draining the fields of excess water (*Davis et al.*, 2000). Since a large portion of the midwestern States are located within the major Mississippi watershed the contaminated tile drain waters will eventually flow into the Mississippi River, which then

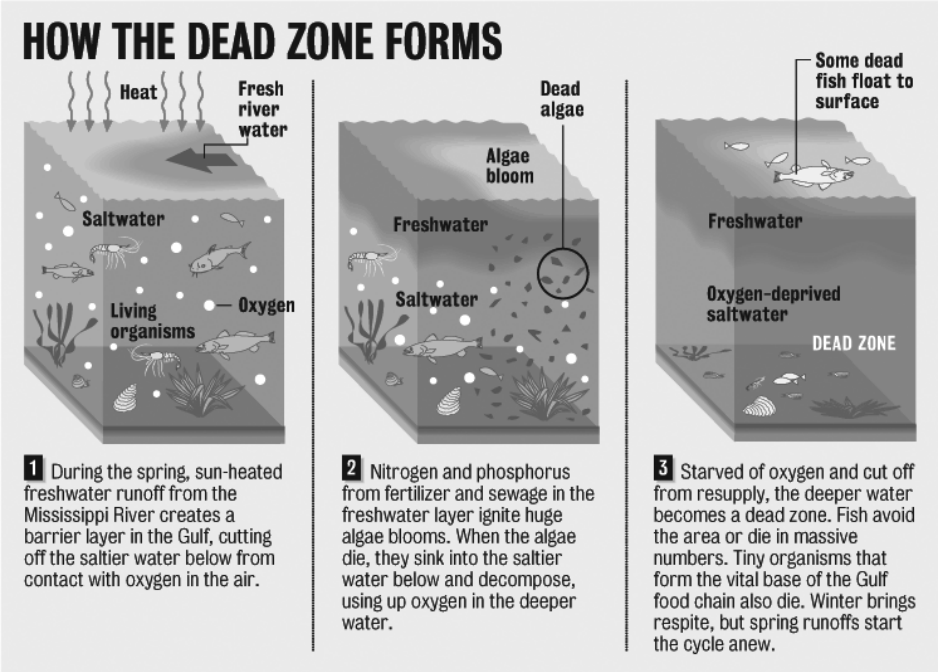

Figure 2.5: Visual representation of how hypoxia forms (*NOLA.com (NOLA)*, 2007)

discharges into the Gulf of Mexico.

2.4.4 Fertilization Loading

Fertilization is the main source of N_2 in an agricultural setting. Over fertilization has the potential of introducing nitrate contaminants into the local drinking water supply. Fertilization rates or loadings are one of the easiest variables to regulate in the field and also are one of the most important variables when examining the impact of excess nitrates from agricultural applications on drinking water sources. *Kladivko et al.* (2004) suggest that, based on their 15-yr study of tile drains and nitrate leaching into the soils and eventually into the tile drains, that the discharge nitrate decreased from 28 to 8mg/L using a combination of variables. This includes a 60% reduction in the fertilization rate from its original 38kg/ha/yr to approximately 15kg/ha/yr. The reduction of the fertilization load facilitated decreasing the discharge of nitrates into the tile drains while actually increasing the drain flow during the final stages of the study (*Kladivko et al.*, 2004). *Davis et al.* (2000) concluded that long term studies show a greater potential effect on discharge concentrations by decreas-

ing the fertilizer application loadings. The key objective for a farm is to have high crop yields that can produce enough revenue to sustain the agricultural business without excessive nitrate contamination in the local drinking water supplies.

Conventional fertilizers are placed at the beginning of the growing season. This is done to ensure that the soil has the proper amount of limiting nutrients, (i.e. nitrogen and phosphorous), when seeding occurs. Engineered or synthetic fertilizers can contain organic and inorganic nitrogen (*Tilman*, 1998). Manure is also used as a fertilizer because of its organic nitrogen content (*Tilman*, 1998). *Drinkwater et al.* (1998) additionally confirm that the conventional organic sources of nitrogen can produce just as good crop yields with less nitrogen leaching into the ground water.

Anhydrous ammonia based fertilizer is a type of fertilizer that offers a delayed release of organic nitrogen into the subsurface as opposed to using other conventional engineered fertilizers (*Kyveryga et al.*, 2004). This type of fertilization is also dependent on the type of crop, geology of the site and fertilization schedule. Anhydrous ammonia is usually used for crops, such as corn, that need more nitrogen in the soil (*Kyveryga et al.*, 2004). By using an anhydrous ammonia based fertilizer a delayed release of nitrogen into the subsurface is achieved. This type of fertilization is normally once per growing season, usually at the end of the season, so there is available nitrogen in the soil in the following spring (*Kyveryga et al.*, 2004). There are some direct health risks that are associated with using the anhydrous ammonia. These risks include eye and skin irritations but can also include chemical pneumonitis, pulmonary edema as well as asphyxia *Corporation* (2006). With the proper personal protective equipment and storage of the fertilizer, these conditions are avoidable. The biggest advantage that anhydrous fertilizer offers is that in the spring time there is less to be done before seeding, since the fertilizer will already be in the ground from the previous fall.

2.4.5 Crop Rotation

Rotating crops is a common practice on most farms due to the ease and the benefits that it offers to the land. In fact, crop rotation can have an economic benefit and potentially yield larger crops over time. This is accomplished by

planting a crop such as corn that needs more nitrogen to grow and can not uptake nitrogen very efficiently. Because corn can not readily get nitrogen from the ground, the nitrogen must be applied in the form of nitrates as fertilizer. If corn is the primary crop year after year, then fertilizer is typically applied every spring and fall season. If a crop rotation is implemented with alternating crops every second year, a more balanced nitrogen application cycle is followed. There are some crops that are used in this rotation cycle with a popular rotation crop being soybean (*Burkart and James*, 1999). This is a common choice for crop rotation due to the soybean plant being able to uptake and fix nitrogen from the ground naturally (*Vitousek et al.*, 1997). The soybean plant takes nitrogen from the atmosphere and gas in the soil. It uses symbiotic bacteria in the roots for plant growth (*Burkart and James*, 1999). When the fertilizer is applied, it is applied in a one-time fertilization before seeding of the corn crop. It is usually enough to sustain the crop until harvest. This saves the farm from applying a second fertilization in the fall to give the crop the necessary nitrogen to grow with significant yield. The crop rotation technique saves in capital cost to the farmer and it also saves the environment as it does not have to adsorb another nitrogen influx from a non-natural source.

2.5 Tile Drains

Tile drainage systems are a common subsurface structure in the American midwest and cover up to 30% of the crop land (*Davis et al.*, 2000). Tile drains are installed to decrease overland flow, increase percolation, lower the water table, and alter some of the infiltrated water to increase drainage in farm crop fields where the soil has poor subsurface drainage (*Singh and Kanwar*, 1995). However, the increased drainage in the area can also act as a transport conduit for unused nitrates and other nutrients, which end up in streams and rivers near the farm (*Davis et al.*, 2000). Originally, tile drains were made from ceramic tiles and installation was tedious and expensive. Today tile drains can be made of many different materials but perforated plastic tubing is one of the most popular choices due to its flexibility, easy installation, availability, and cost effectiveness (*ArmTec*, 2008). Most tile drainage systems currently are referred to as subsurface drainage systems since the drainage system no

longer consists of tiles but are now comprised of tubing (*Jaynes et al.*, 2001). For the purposes of this thesis, the drainage systems will also be referred to as tile drains.

The spacing and depth of the drainage system vary from farm-to-farm, which makes each drainage system unique. The diameter of the tubes for the tile drains typically range from approximately 100 to 450 mm (*Ontario Ministry of Agriculture Food & Rural Affairs (OMAFRA)*, 2008). Figure 2.6 shows a typical tile drain outlet into a ditch.

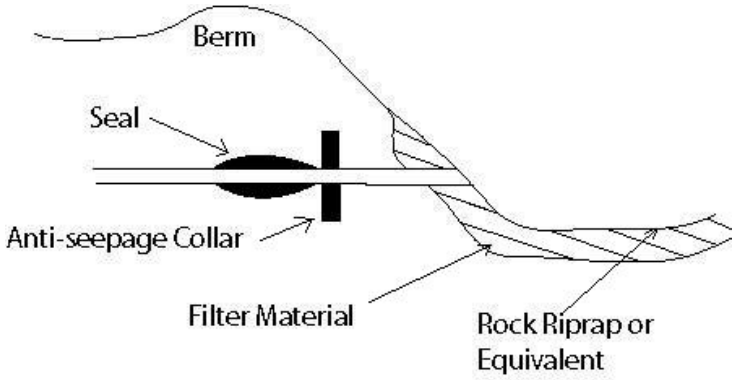

Figure 2.6: Typical tile drain outlet (*Ontario Ministry of Agriculture Food & Rural Affairs (OMAFRA)*, 2008)

The spacing of the tile drains and drain depth can be critical components to obtain optimal drainage along with maximum crop yield. Drainage spacing has been varied from 15m to upwards of 200 m depending on the farm and the crops grown on the farm (*Davis et al.*, 2000). However typical farms do not have drainage spacing larger then 100 m due to the potential negative effects on crop growth yields (*Davis et al.*, 2000). *Davis et al.* (2000) studied the effects of drainage spacing and drainage depth on the nitrate leakage out of the tile drains and subsequently into the nearest body of surface water. A result from this study shows that increasing drain spacing can decrease the amount of water and nitrates removed from the field. *Kladivko et al.* (2004) reached the same conclusions. Ideally a maximum crop yield can be obtained with proper drainage, and without adverse impact to the subsurface groundwater or the surface water.

Not only is the spacing of the drains important, but the depth at, which the drains are placed is also important. The drain depth is a site specific

variable that can vary depending on the geology of the soil as well as the intended crop(s) for the field. The depth for the drain installation can be below the root zone of the intended crop(s) as well as around the average local water table (*Oosterbaan*, 1994). The depths for the tile drains can range from approximately 0.75 to 1.2 m below ground surface (bgs) depending on the local geology and the crops intended to be grown on the land (*Kladivko et al.*, 1999).

Figure 2.7 illustrates a cross-section of a typical tile drain and how the tile drains are designed to work. The water table will mound in between the tile drains. The higher the mounding the more the drains will extract water, as the mounding decreases, less water will be extracted from the subsurface.

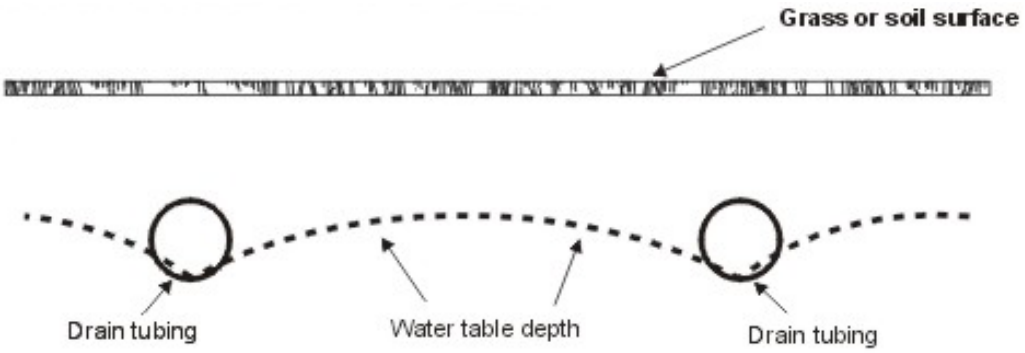

Figure 2.7: Tile drain cross section (*Badiella*, 2008)

2.6 Spatial Variability

Spatial variability in the landscape can cause a large amount of uncertainty in any modelling if it is not recognized and dealt with appropriately. One common variable that is over looked when modelling a large land surface area is the spatial variability of the soil. This variability can have a large impact on groundwater recharge. When the glaciers retreated in the last ice age, the soil in North America's landscape was mixed to such a large extent that the soil type and characteristics can change within a few metres (*Presant and Wicklund*, 1971). This spatial variability can ultimately lead to inaccurate modelling if using a traditional grid pattern with a large fixed length and width for each cell of the grid. A grid will have a set orientation and dimensions where

the soil profile of the natural landscape can have a random size and orientation. Figure 2.8 shows a soil survey of the GRW with over 700 unique soil types. This figure shows how the orientations and sizes of the soil type regions do not always align with a cartesian oriented model grid. One way to deal with this problem is to create a grid with smaller grid blocks. This enables more detail and more information to be stored. However when smaller grid blocks are used to cover the same area of interest, then the computing power needed to process the grid is greater.

Spatial variability can become much more complicated when land use is over-laid on the natural land cover of the area. There can be multiple types of LULC cells in a small area. An area might be zoned for agricultural land but the soils that are in that zoning can be highly variable. The property would be divided up into many different LULC sections depending on how many different soils are present on the property. Figure 2.9 shows that within the Grand River Watershed there are many different combinations of LULC cells.

The LULC map can become even more complex once the soil properties are added to the cells of the LULC map. This creates a complex map that divides properties of also into soil types as well. Figure 2.10 shows the complexity of the watershed map when the soils information is added to the LULC data.

There are some other complications that arise from spatial variability. For example, when land is cleared of its natural vegetation to make room for farming. The farms replace the vegetation with shallow-rooted crops, which can increase recharge rates and lead to water logging (*Peck*, 1978; *Walker et al.*, 2002). *Finch* (2001) examined the spatial variability of the land cover and land use. Some studies have suggested that the catchment patterns will be altered but the overall catchments groundwater recharge total will be the same as expected. When analyzing the spatial variability of a study site, the impact on the groundwater recharge water quality and quantity must be considered. Depending on the changes to the native land, groundwater recharge may be increased or decreased. An example of changes to the groundwater recharge is when a farm is developed into a residential area.

As suggested in the preceding paragraphs, vegetation can be a form of spatial variability. Changing the natural vegetation to something foreign can introduce more uncertainty into a model trying to simulate transportation

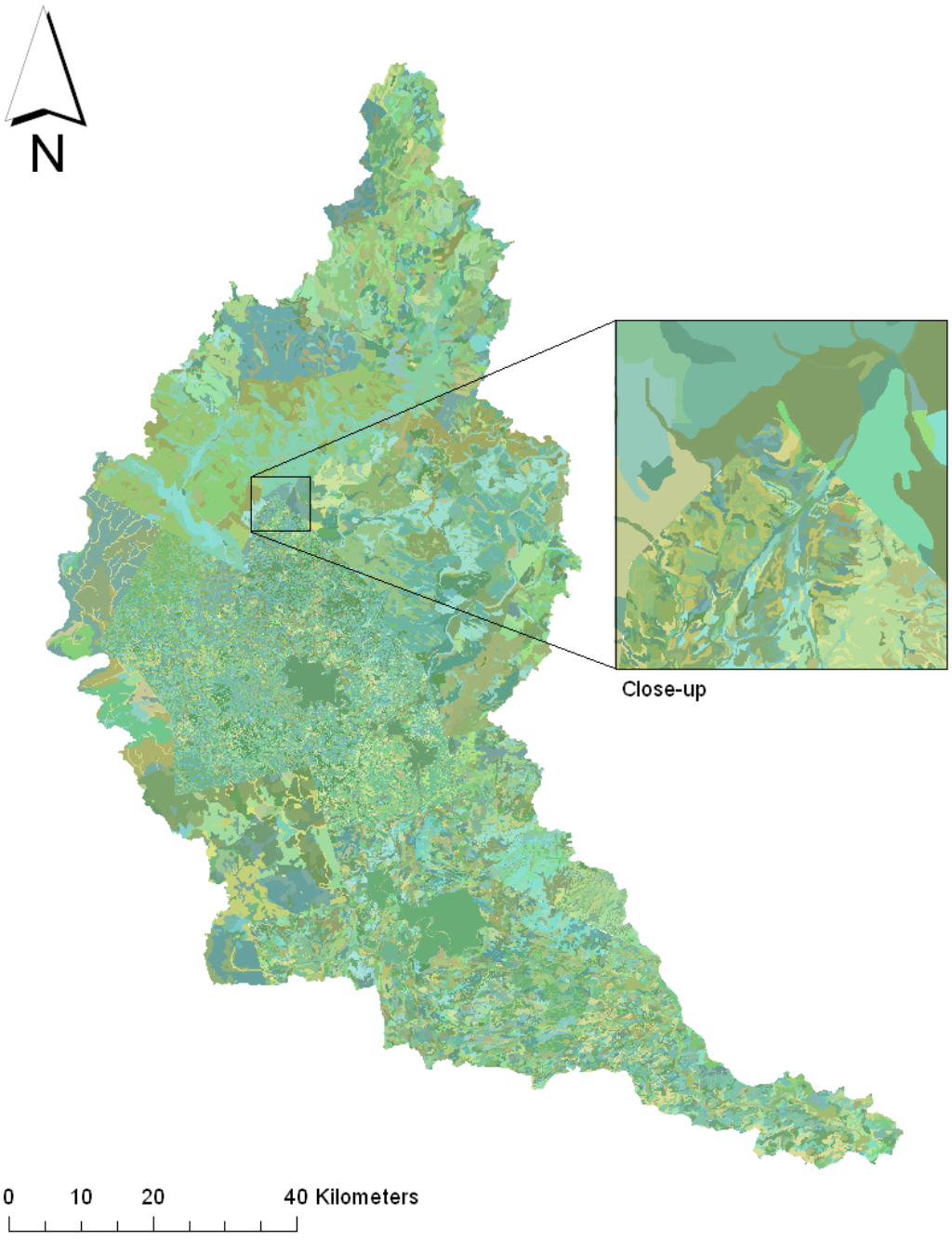

Figure 2.8: Soil survey of the Grand River Watershed with over 700 unique soil types

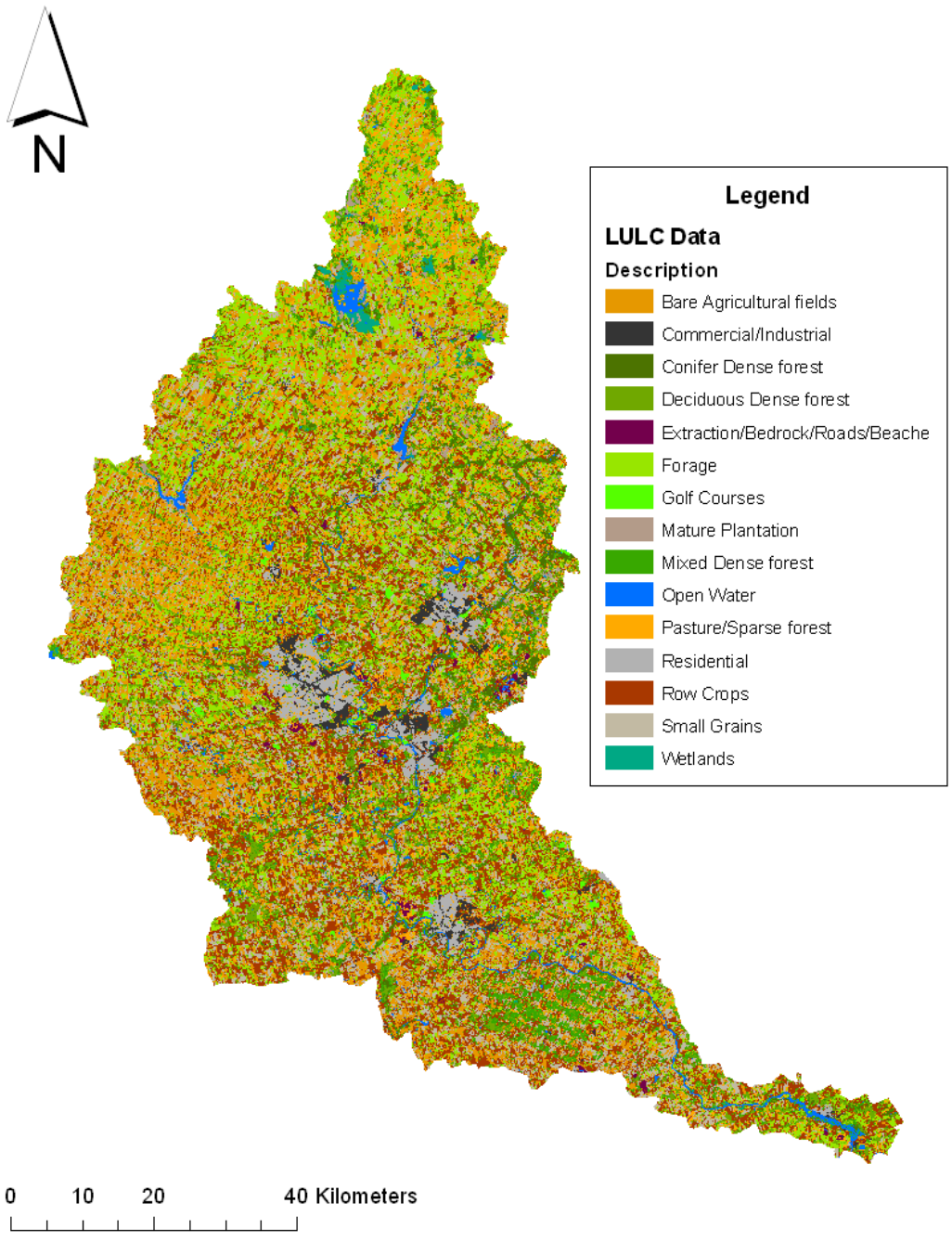

Figure 2.9: Land use/land class map of the Grand River Watershed

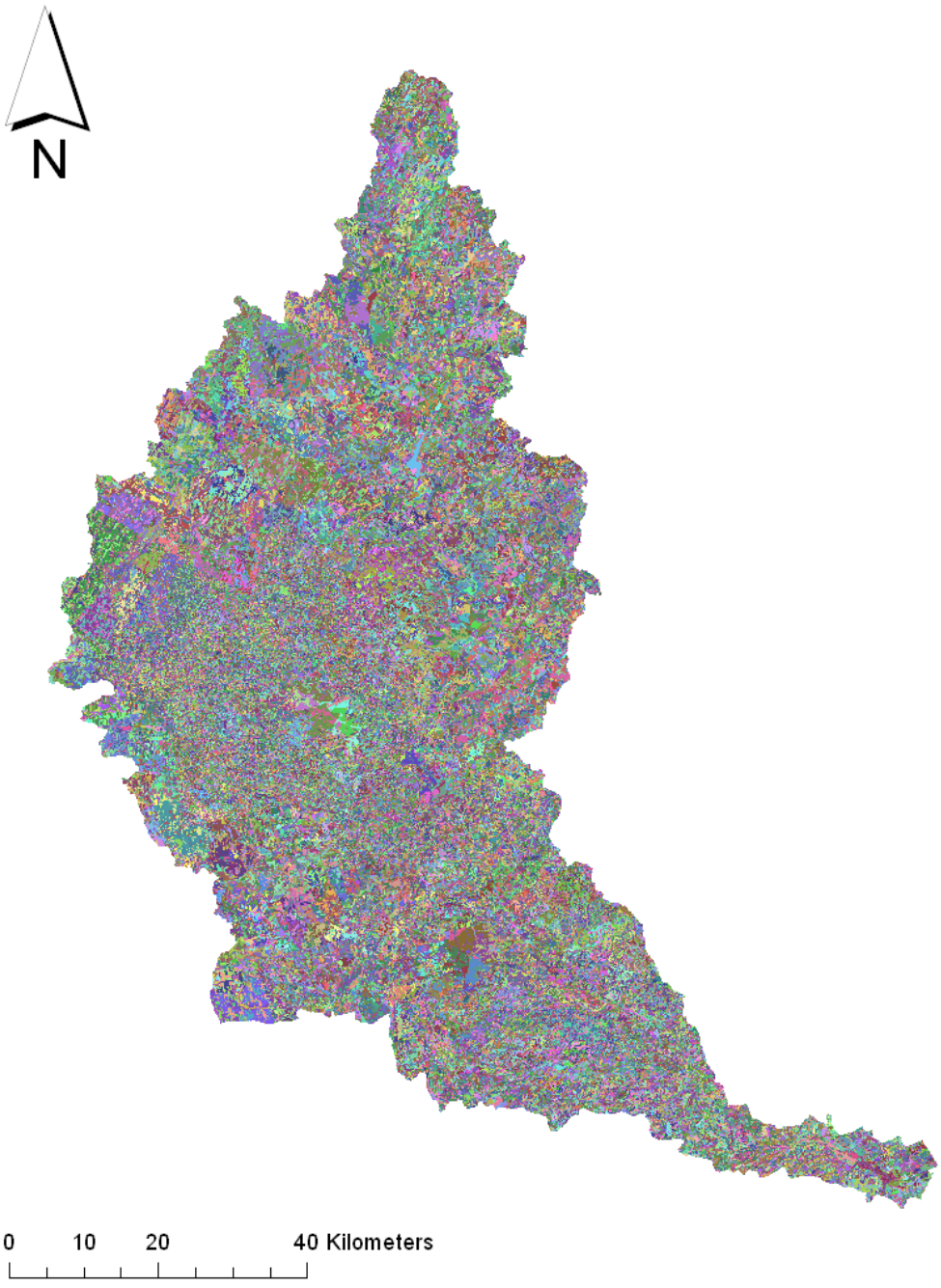

Figure 2.10: Land use/land class map with soil variability of the Grand River Watershed showing over 280,000 unique cells

(water, chemical, etc.) for that particular area. Vegetation may reduce the recharge rate by directly interfering with the passage of precipitation into the soil. Quantifying the amount of water intercepted by the vegetation canopy can be very difficult, as it is dependent on many variables such as precipitation intensity, wind speed, temperature, vegetation leaf area, and density of vegetation (*Jyrkama and Sykes*, 2007). However, this interception of the precipitation can be a significant factor with respect to the recharge in an area (*Finch*, 2001). The greatest loss of precipitation on recharge is evapotranspiration, which incorporates the processes of transpiration and evaporation. Evapotranspiration is the loss due to direct soil evaporation as well as plant transpiration. This loss of precipitation can be attributed to between 40 to 60% of the annual rainfall in humid climates (*Knutssen*, 1988). Various methods have been developed to estimate the evapotranspiration of a given area. However, most require many inputs and are normally calibrated for specific conditions, which can vary between methods.

However, vegetation is not completely a deterrent regarding the groundwater recharge. Plant root systems can potentially provide preferential flow paths for precipitation that reaches the ground (*Le Maitre et al.*, 1999). This additionally helps with reducing potentially contaminated overland flow. To summarize, in terms of groundwater recharge, vegetation can have both positive and negative effects. Vegetation intercepts precipitation and transpires water taken from the soil within the root system, as well as creating flow paths for any precipitation to reach the subsurface more quickly.

Spatial variability does not just include vegetation but urbanization as well. Urban areas are being developed rapidly in the Grand River watershed and it is not uncommon to have new residential and commercial developments being constructed next to farm fields or small forested areas. Not only will the recharge rate of the immediate surrounding area be impacted, but larger urban areas can cause effects that can alter the surrounding climate (*Lerner et al.*, 1990). Normally, with an urban area being constructed, the percent impervious area is increased due to the amount of asphalt and concrete that is placed in a modern urban environment. With an increase of impervious area, the groundwater recharge in the immediate area can be impacted by altering the recharge configuration (*Finch*, 2001).

2.7 Soil Properties

Every type of soil combination has a set of properties that dictate flow within the soil matrix. These properties include hydraulic conductivity, porosity, and field capacity. The physical properties of the soil matrix can be difficult to apply in modelling when preferred pathways such as plant root systems, cracks and fissures, and even a homogenous material like an exposed gravel aquifer can have effects on the recharge of the surrounding soil. However, the properties that control how a fluid moves through a homogenous matrix can be estimated and used in a model. Soils with a higher hydraulic conductivity can act as a preferred flow path since the resistance to flow will be less and a fluid will generally follow the path of least resistance.

The soil properties are variable not only in a spatial sense but in a temporal sense as well. The antecedent conditions of the soil moisture are critical to the conductivity of the soil. A small change in water content within the soil can change the effective hydraulic conductivity by two orders-of-magnitude (*Rushton*, 1988). For example, if a soil is saturated and a precipitation event occurs the precipitation water will move across the ground as overland flow. If the soil was not saturated and the same precipitation event occurred some of the water would still move across the ground as overland flow but some of the water would move into the ground as infiltration.

The organic carbon content of the soil is a property that can affect the amount of nitrates that can leach out of the soil and into the groundwater. *Byre et al.* (2001) discusses how the organic carbon content of the soil can be a potential limiting factor in the denitrification process. Under certain soil conditions and when there are enough nitrates leaching into the potential denitrification zone, then it is possible to remove large quantities of nitrates before they reach the groundwater and downgradient surface water supplies.

2.8 Seasonal and Climate Variability

The growing period for crops can vary depending on the geographic location of the farm. For instance the normal growing period within the Grand River watershed will vary by a couple of days from the northern edges to the southern tip of the watershed due to the seasonal temperature differences over the entire

watershed (*Muttiah and Wurbs*, 2002). Spatial variability is also emphasized when comparing farms located where the soil does not freeze in the winter months and farms where winter frost and snow are part of the regular annual cycle. Places where the soil never freezes and the temperature is warm enough to sustain healthy plant growth for longer periods of time will have different fertilization requirements than those where the ground freezes in the winter months and thaws again in the spring months.

Precipitation data along with other climatic data is used for modelling contaminant transport as well as other forms of modelling, such as regional and global climate modelling (*McGregor*, 1997). This data must be accumulated over years of observation and recording. Using seasonally varying climatic data for the analysis of a tile drainage system is an essential component of modelling. The precipitation input can be in the form of anything from rain to snow or hail. Because of this variability in precipitation type, more climatic data must be collected and interpreted. For example, *Singh and Kanwar* (1995) concluded that the actual rainfall intensity can be a critical component in predicting tile drain flows due to the macropore flow and its relationship to the observed flow in the drains. However, some consideration should also be given to the spatial variability within the soil properties (*Singh and Kanwar*, 1995) when dealing with colder climates or climates that experience a winter freeze and snow fall. The model should account for the spring runoff and lack of actual water percolating into the subsurface.

2.9 Climate Change Modelling

Climatic variations in the earth can occur due to natural causes such as changes in volcanic activity, solar output from the sun as well as unnatural causes such as the release of green house gases (*Jyrkama and Sykes*, 2007). These variations can occur from a range of temporal and spatial scales making prediction and modelling highly variable and uncertain (*Goddard et al.*, 2001). There are many predictions on the impact of climate change, however, there are some general predictions that the Intergovernmental Panel on Climate Change (IPCC) have made that may occur during this century include (*Intergovernmental Panel on Climate Change (IPCC)*, 2001):

- Average global surface air temperature predicted to increase by 1.5 to 5.4 °C.
- Global average water vapour, evaporation and precipitation are expected to increase, however, both increases and decreases in precipitation will be seen on a regional scale.
- Extreme weather is projected to increase in both intensity and frequency.
- The ice caps and glaciers are expected to continue the widespread retreat.
- The global average sea level is also expected to rise.

Modelling the climate and predicting what the climate will do on a daily basis can be a tricky task without the proper data. Human impacts on the earth and its water resources are being felt over the entire globe. Factors such as greenhouse gas releases into the atmosphere and deforestation to increase urbanization and agricultural land all have climate changing impacts (*Jyrkama and Sykes*, 2007). Climate change scenarios have been presented and some modelling has been done on a global scale as well as regional scale (*McGregor*, 1997).

Using GIS based modelling, *Rosenburg et al.* (1999) performed some hydrologic simulations using three different general circulation models (GCM) using the anticipated changes by the IPCC to temperature and atmospheric CO_2 concentrations. This modelling predicted similar results with all three models, showing a reduction in recharge to the aquifer as high as 77% (*Jyrkama and Sykes*, 2007). Many other simulations have been done on climate change modelling. Depending on the area and type of model used, different conclusions were obtained. Most simulations performed use multiple climate models to ensure that the data being used as input and the analysis results are robust. However, a common trend in the results seems to be a warmer winter for northern climates, coupled with more precipitation as rain instead of snow during the winter months (*Jyrkama and Sykes*, 2007). The IPCC has predicted an increase in precipitation for the northern climates (i.e. Alaska, Yukon Territory) during the winter months of as much as 56% from present day precipitation rates (*IPCC*, 2007b). However, this increase in precipitation is coupled with an increase in temperatures with a potential maximum of approximately 11°C (*IPCC*, 2007b). With less snow falling in the northern climates and more rain

falling, the spring melt and groundwater recharge potentially have severe impacts on the hydrologic cycle for the local environment. This type of dramatic change in the climate can present some challenges to farmers who plant and fertilize using their experience of past growing seasons.

2.9.1 Climate Change Scenarios

The IPCC has some future scenario's that have been considered. The modelling scenarios that were chosen for this thesis were the A2, A1B and the B1 scenarios. The A1B scenario assumes that there will be very rapid economic growth, a global population that peaks sometime in mid-century and a rapid introduction of new and more efficient technologies. The A2 scenario is described by *IPCC* (2007c) as a very heterogeneous world with a higher population growth, slow economic development and slow technological change. The A1 scenario is divided into three groups that describe alternative directions of technological change: fossil intensive (A1FI), non-fossil energy resources (A1T) and a balance across all sources (A1B) (*IPCC*, 2007c). These scenario's were chosen because they potentially have the most adverse impacts on the climate. The B1 scenario describes a convergent world, with the same global population as the A1 scenarios, but with a more rapid change in economic structure moving toward a service and information economy (*IPCC*, 2007c). The B1 scenario is on the other end of the spectrum with a more optimistic outlook to the climate change problem that the world is potentially facing.

The A2 scenario is considered worse then the A1B scenario with increasing annual air temperatures ranging from 2.0 to 5.4 °C over a 100 year period. This range yields a maximum of 0.054 °C/year. If this is linearly extrapolated over the 40 year period that will be simulated in this project, an overall increase of approximately 2.16 °Cwill be observed over the 40 year simulated time period. The precipitation is also expected to increase approximately 8.19% over a 100 year period. Precipitation is expected to increase in the winter but decrease in the summer months for the GRW and surrounding area.

Scenario A1B has a range of potential temperatures and precipitation that have an intermediate impact on the GRW. The air temperature for scenario A1B has a likely increase of approximately 1.7 to 4.4 °C over a 100 year period. This is a maximum increase of 0.044 °C/year with an overall temperature

increase of 1.76 °C over a 40 year period. The precipitation for the A1B scenario is expected to increase as well. This annual increase ranges from approximately -3% to 15%. Precipitation is expected to increase in the winter but decrease in the summer months for the GRW and surrounding area.

The B1 scenario is considered to be less adverse than the A1B scenario with increasing annual air temperatures ranging from 1.1 to 2.9 °C over a 100 year period. This range yields a maximum of 0.029°C/year with an overall increase of approximately 1.16 °Cover a 40 year period. The precipitation is also expected to increase approximately 4.83% over a 100 year period. The precipitation pattern is likely to follow the same pattern as the A2 and A1B scenarios with an increase in precipitation the winter months but a decrease in the summer months.

Climate change will have an important impact on precipitation and overall air temperature, as well as groundwater recharge. However, given the number of uncertainties with prediction modelling, the ability to quantify the overall outcome is difficult. This is inherit due to the mixed results that are given from the multiple global climate models.

2.10 Data Uncertainty

GIS modelling, as well as any type of modelling, is sensitive to the data input. The overall analysis can only be as good as the data that are being used. Data for GIS use has a level of uncertainty associated with it, which comes from multiple sources such as; aerial photography, remote sensing and surveying. All three of these data sources can have a level of uncertainty associated with how data is collected and eventually input and interpreted in the GIS database.

Aerial photography can provide an excellent perspective of the land surface. Examining spatial data such as land use over a specified time period can be done using this type of data. However aerial photos can have inherited radial distortions (*Akbari et al.*, 2003). With these coming from the terrain and the angle of the camera when the pictures are taken. Most GIS software can correct for these radial distortions, which can make aerial photos a powerful tool when dealing with spatial data (*Akbari et al.*, 2003). One advantage of taking aerial photos is that the flights that carry the camera apparatus can

be scheduled at ideal times. Taking pictures at solar noon can reduce errors introduced with shadows (*Akbari et al.*, 2003).

Remote sensing is the ability to gather information about the earth without having actual contact with the environment. In most remote sensing, the process involves an interaction between incident radiation and the target(s) of interest. This is exemplified by the use of imaging systems from satellites (*North American Space Agency (NASA)*). Figure 2.11 shows a visual representation of how a remote sensing system works. A common remote sensing raw data receptor are satellites in orbit, however other receptors can be used such as a tower, an airplane or even underground remote sensors (*North American Space Agency (NASA)*; *Campbell*, 2006). Some of the problems that can cause remote sensing data to be less than ideal come from interactions with the atmosphere. Remote sensing is dependent on a signal traveling through the atmosphere, which can cause the signal to scatter and/or absorb (*Campbell*, 2006). Scattering can occur when there are particles in the air such as dust, water vapour and pollution (*Campbell*, 2006). Absorption occurs when the electromagnetic signal travels through the ozone, water vapour and carbon dioxide (*Campbell*, 2006). These problems can affect the data collected and must always be considered in analysis.

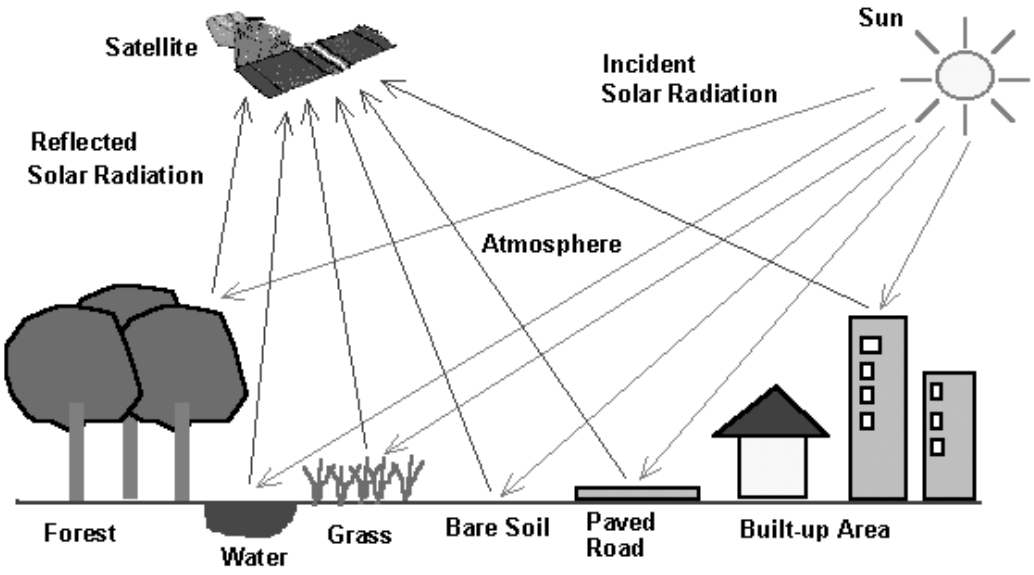

Figure 2.11: How remote sensing works (*Kovar and Jorgensen*, 2004)

When dealing with problems on a large scale (such as watershed modelling)

attempting to include many details in the modelling process can become very complex because of the scale of the project. It is a very arduous task to create a detailed model that can account for such variables as every soil type within the watershed and every vegetation type configuration in the watershed. That kind of detail would require many more complexities in the modelling process, which may not affect the regional scale. Those details would have more of an effect on the local scale.

2.11 The HELP3 Model

The hydrologic evaluation of landfill performance model (HELP3) is a quasi-two-dimensional hydrologic model. HELP3 was originally designed for conducting water balance analyses of landfills, cover systems, and other solid waste containment facilities (*Schroeder et al.*, 1994). HELP3 has been adapted and being used for groundwater modelling as seen in *Jyrkama et al.* (2002) work. The HELP3 code is written in ANSI FORTRAN 77 using Ryan- McFarland Fortran Version 2.44 (*Schroeder et al.*, 1994).

The hydrologic processes that HELP3 models can be divided into two categories: surface processes and subsurface processes. The HELP3 surface processes are snowmelt, interception of rainfall by vegetation, surface runoff, and surface evaporation. The HELP3 subsurface processes are evaporation from soil profile, plant transpiration, unsaturated vertical percolation, barrier soil liner percolation, geomembrane leakage and saturated lateral drainage (*Schroeder et al.*, 1994).

The first subsurface processes considered are soil evaporation and plant transpiration from the evaporative zone depths of the sub surface. A vegetative growth model accounts for the daily growth and decay of the surface vegetation (*Schroeder et al.*, 1994). The other subsurface processes are modelled one soil type at a time, from top to bottom, using a design-dependent range of time steps. A storage-routing procedure is used to redistribute the soil water among the modelling segments, which accounts for infiltration or percolation into the subsurface and evapotranspiration from the evaporative zone (*Schroeder et al.*, 1994). The head on the barrier soil is then used to compute the leakage/percolation through the barrier and, if lateral drainage

is permitted above the top of the barrier, the lateral drainage to the collection and removal system (*Schroeder et al.*, 1994).

2.11.1 HELP3 Assumptions

The modelling procedures are necessarily based on many simplifying assumptions. Generally, these assumptions are reasonable and consistent with the objectives of the program when applied to standard landfill designs (*Schroeder et al.*, 1994). For this thesis, the assumptions and limitations should allow for an accurate model for the GRW tile drains.

The major assumptions and limitations of the HELP3 program are summarized below. Runoff is computed using the Soil Conservation Service (SCS) method based on daily amounts of rainfall and snow melt. HELP3 assumes that cells adjacent to the target cell do not drain onto the target cell that is being modelled. There is no time distribution for rainfall intensity. This means that HELP3 cannot give accurate estimates of runoff volumes for individual storm events on the basis of daily rainfall data (*Schroeder et al.*, 1994). However, because the SCS rainfall-runoff relation is based on daily field data, the long-term estimates for runoff should be acceptable. The SCS method does not explicitly consider the length and slope of the surface over, which overland flow occurs. This limitation has been removed by developing and implementing into the HELP3 input routine a procedure for computing curve numbers that take into consideration the effect of slope and slope length (*Schroeder et al.*, 1994). The limitation of the SCS method is considered when SCS method is used for estimating a curve number when the overland flow distance is very short or has a steep slope or if there is a short high intensity rainfall event. In these cases, the SCS probably underestimates the curve number (*Schroeder et al.*, 1994).

The HELP3 model assumes Darcian flow by gravity through homogeneous soil layers. HELP3 does not consider explicitly the preferential flow that can occur through channels such as cracks, root holes, or animal burrows but allows for vertical drainage through the evaporative zone at moisture contents below field capacity. These preferential pathways can increase vertical infiltration with this being discussed in Section 2.7. The program allows vertical drainage from a layer at moisture contents below field capacity when the in-

flow would occupy a significant fraction of the available storage capacity below field capacity (*Schroeder et al.*, 1994).

The vertical drainage rate out of a soil segment is assumed to equal the unsaturated hydraulic conductivity of the segment corresponding to its moisture content, provided that the underlying segment is not a barrier soil and is not saturated. In addition to these special cases, the drainage rate out of a segment can be limited by the saturated hydraulic conductivity of the segment below (*Schroeder et al.*, 1994). When limited, HELP3 computes an effective gradient for saturated flow through the lower segment. This permits vertical percolation or lateral drainage layers to be arranged without restrictions on their properties as long as they perform as their layer description implies and not as barrier soils (*Schroeder et al.*, 1994).

HELP3 also assumes that 1) the soil moisture retention properties and unsaturated hydraulic conductivity can be calculated from the saturated hydraulic conductivity and limited soil moisture retention parameters (porosity, field capacity and wilting point) and 2) the soil moisture retention properties fit a Brooks-Corey relation (*Brooks and Corey*, 1964) defined by the three soil moisture retention parameters. Upon obtaining the Brooks-Corey parameters for the soil, HELP3 assumes that the unsaturated hydraulic conductivity relation with soil moisture is well described by the Campbell equation (*Schroeder et al.*, 1994).

HELP3 does not explicitly compute flow by differences in soil suction (soil suction gradient) and, as such, it does not model the draw of water upward by capillary drying. This upward draw of water is modelled as an extraction. With this concept, it is important that the evaporative zone depth be specified as the total depth of capillary drying (*Schroeder et al.*, 1994). Downward drainage by soil suction exerted by dry soils lower in the soil profile is modelled as Darcian flow for any soil having a relative moisture content greater than the lower soils. The drainage rate is equal to the unsaturated hydraulic conductivity computed as a function of the soil moisture content. The rate is assumed to be independent of the pressure gradient. Leakage or recharge through barrier soils is modelled as saturated Darcian flow (*Schroeder et al.*, 1994).

Recharge in HELP3 is assumed to occur only as long as there is head greater then zero on the surface of the barrier soil. HELP3 does not consider

drying of the barrier soils and, therefore, the saturated hydraulic conductivity of the barrier soil does not vary as a function of time (*Schroeder et al.*, 1994). Again this is potentially not exactly what is occurring but this assumption is still expected to provide adequate results.

The tile drains that are simulated for this thesis are being modelled using the lateral drainage algorithm in HELP3. For lateral drainage, HELP3 makes the assumption that the saturated depth profile is characteristic of the steady-state profile for the given average depth of saturation. As such, HELP3 assumes that the lateral drainage rate for steady-state drainage at a given average depth of saturation is representative of the unsteady lateral drainage rate for the same average saturated depth (*Schroeder et al.*, 1994). In reality, the drainage rate would be larger for periods when the saturation depth is increasing and smaller for periods when the saturation depth is decreasing. For example, the drains would have more water draining immediately following a short intense rain fall event versus after a period of time when it has stopped raining but some water is still being drained because the saturation levels are decreasing. In a lateral drainage layer, the vertical percolation is modelled as unsaturated flow and the lateral drainage is modelled as lateral saturated flow (*Schroeder et al.*, 1994). HELP3 requires that there is a barrier soil below a lateral drainage layer. If there is no barrier soil then the lateral drainage layer is treated as vertical drainage layer and nothing will be drained laterally.

HELP3 also assumes the vegetative growth and decay can be characterized by a vegetative growth model developed for crops and perennial grasses. In addition, it is assumed that the vegetation transpires water, shades the surface, intercepts rainfall and reduces runoff in similar quantities as grasses or as an adjusted equivalence of leaf area index (LAI) (*Schroeder et al.*, 1994).

2.11.2 HELP3 Algorithms

In HELP3, the flow of water in the subsurface is modelled using both the unsaturated and saturated flow equations depending on the soil properties, soil type, profile construction and moisture content. Vertical percolation in the soil is modelled as unsaturated flow in non-barrier soils. To calculate the unsaturated flow, the effective unsaturated hydraulic conductivity must be first calculated. HELP3 calculates the unsaturated hydraulic conductivity

using the Brooks-Corey equation:

$$K_u = K_s \left(\frac{\Theta - \Theta_r}{\Phi - \Theta_r} \right)^{3+\left(\frac{2}{\lambda}\right)} \tag{2.3}$$

where K_u is the unsaturated hydraulic conductivity (cm/sec), K_s is the saturated hydraulic conductivity (cm/sec), Θ is the actual volumetric water content (vol/vol), Θ_r is the residual volumetric water content (vol/vol), Φ is the total porosity (vol/vol), and λ is the pore size distribution, which is dimensionless (*Schroeder et al.*, 1994).

The subsurface flow is then calculated using Darcy's Law:

$$q = -K \frac{dh}{dl} \tag{2.4}$$

Where q is the rate of flow (cm/day), K is the hydraulic conductivity (cm/day), h is the piezometric head (cm), and l is the length in the direction of flow (cm). For the unsaturated condition, the hydraulic conductivity (K_u) will be calculated using equation 2.3. The piezometric head will also include any suction head that may be present in the unsaturated soil. For the lateral drainage layer the drains are modelled using equation 2.4 and using K_s for the hydraulic conductivity.

The saturated hydraulic conductivity can also be modified if the soil that becomes saturated is located in the upper half of the evaporative zone. The saturated hydraulic conductivity is described by equation 2.5 (*Schroeder et al.*, 1994):

$$\begin{aligned}(K_s)_v = (1.0 + 0.5966LAI + 0.132659LAI^2 + 0.1123454LAI^3 \\ -0.04777627LAI^4 + 0.004325035LAI^5)(K_s)_{uv}\end{aligned} \tag{2.5}$$

Where $(K_s)_v$ is the saturated hydraulic conductivity of vegetated soil in the top half of the evaporative zone (cm/sec), LAI is the leaf area index (dimensionless), and $(K_s)_{uv}$ is the saturated hydraulic conductivity of unvegetated material in the top half of the evaporative zone (cm/sec) (*Schroeder et al.*, 1994).

The lateral drainage in HELP3 is modelled by the Boussinesq equation (Darcy's law coupled with the continuity equation), employing the Dupuit-Forcheimer (D-F) assumptions (*Schroeder et al.*, 1994). The D-F assumptions are that, for gravity flow to a shallow sink, the flow is parallel to the barrier

soil and the velocity is in proportion to the slope of the water table surface and independent of depth of flow (*Forchheimer*, 1930). These assumptions imply the head loss due to flow normal to the liner is negligible, which is valid for drain layers with high hydraulic conductivity and for shallow depths of flow, depths much shorter than the length of the drainage path (*Schroeder et al.*, 1994). For this thesis the tile drains are not being placed into soils with high hydraulic conductivities. This limitation of the algorithm is noted but is unlikely to adversely affect the results. The Boussinesq equation can be written as follows:

$$f\frac{\delta h}{\delta t} = K_D\frac{\delta}{\delta l}\left[(h - l\sin\alpha)\frac{\delta h}{\delta l}\right] + R \tag{2.6}$$

Where f is the drainable porosity (porosity minus field capacity) and is dimensionless, h is the elevation of the water surface above liner at edge of drain (cm), t is time (sec), K_D is the saturated hydraulic conductivity of drain layer (cm/sec), l is the distance along liner surface in the direction of drainage (cm), α is the inclination angle of liner surface and R is the net recharge (impingement minus leakage for the layer) (cm/sec) (*Schroeder et al.*, 1994). For a visual representation of the Boussineaq equation variables refer to Figure 2.12.

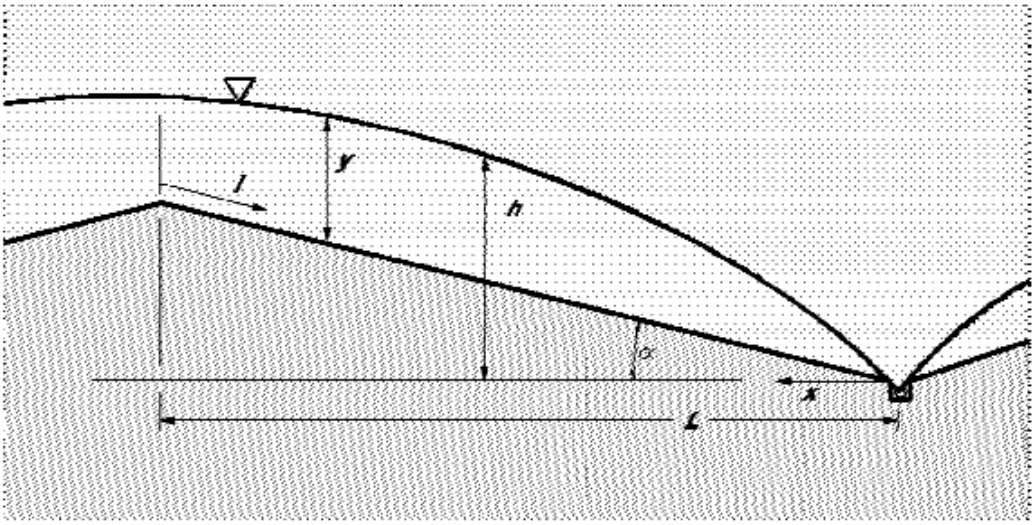

Figure 2.12: Lateral drainage definition (*Schroeder et al.*, 1994)

The lateral drainage submodel assumes that the relationship between lateral drainage rate and average saturated depth for steady flow approximates

the overall relationship for an unsteady drainage event (*Schroeder et al.*, 1994). For steady state flow, the lateral drainage rate is equal to the net recharge. The steady state lateral drainage equation is then calculated by translating the axis from l (parallel to the liner) to x (horizontal) and substituting for R:

$$R = \frac{Q_{Do}}{L} = q_D = K_D \cos^2 \alpha \frac{d}{dx}\left(y\frac{dh}{dx}\right) \tag{2.7}$$

Where Q_D (cm^2/sec) is the lateral drainage rate per unit width of drain at any x , Q_{Do} (cm^2/sec) is the lateral drainage rate into collector pipe at drain, $x = 0$, L is the length of the horizontal projection of the liner surface (maximum drainage distance) (cm), and q_D is the lateral drainage in flow per unit area (cm/sec).

2.12 Tile Drain Model Studies

2.12.1 One Dimensional Modelling

Multiple studies have been done on one-dimensional tile drain flow. *Colding* (1872) used a one-dimensional approach with Dupuit assumptions to study tile drains placed directly above an impermeable surface. The result from the study was an elliptical equation for the groundwater surface and potential. *Hooghoudt* (1940) simulated tile drains assuming a radial flow of groundwater around the tile drains. This analysis resulted in the development of the concept of equivalent depth D_e, which is defined as an imaginary water depth below the tile drains. When this concept is used in the elliptical equation from *Colding* (1872), it provides the value of maximum water table height above the drains, d_m. *Moody* (1966) then used Hooghoudt's approach to define an equivalent depth, D_e, that does not involve an infinite series:

$$D_e = \frac{D}{\left[1 + \frac{D}{L}\left(2.55 \ln \frac{D}{r_d} - c\right)\right]} \tag{2.8}$$

$$D_e = \frac{L}{2.55\left(\ln \frac{L}{r_d} - 1.15\right)} \tag{2.9}$$

Where D is the elevation of the centre-line of the drain above the base of the aquifer (m), L is the spacing between the drains (m), r_d is the radius of the

drain (m) and c is a constant (unitless) equal to:

$$c = 3.55 - 1.6\frac{D}{L} + 2\left(\frac{D}{L}\right)^2 \tag{2.10}$$

Equation 2.8 is to be used when $0 < D \leq 0.31L$ and equation 2.9 is used when $D > 0.31L$.

Sloan and Moore (1984) used a one dimensional finite element model based on Richard's equation (derived from Darcy's equation and the continuity equation) for flow in saturated and unsaturated porous media. This study focused on subsurface flow parallel to steep hill slopes during stormflow. The resulting equation for the one-dimensional approach is as follows:

$$DC(h)\frac{\delta h}{\delta t} = \frac{\delta}{\delta x}\left[K(h)D\cos^2\alpha\frac{\delta H}{\delta x}\right] + i \tag{2.11}$$

where D is the vertical soil depth (m), α is the angle of the impermeable bed to the horizontal, $K(h)$ is the unsaturated hydraulic conductivity (m/min), $C(h)$ is the specific water capacity (m^{-1}), h is the soil water pressure head (m), H is the total hydraulic head (m), x is the horizontal distance parallel to the hill slope (m), and i is the rate of water input to the saturated zone from the unsaturated zone normal to the surface of the slope (m/min). Results from the study showed that simpler physically based models were able to predict the stormflow response for the subsurface steep hillside (*Sloan and Moore*, 1984).

2.12.2 Watershed Scale Modelling

Modelling on a large watershed scale has been done in the past, but rarely have tile drains been included in the modelling process. *Singh et al.* (2005) used two separate models to simulate hydrological processes in the Iroquois watershed. Both HSPF and SWAT were used to simulate nine years of hydrology for the 5,660km^2 tiled drained watershed. The results were verified using 15 years of daily, monthly, and annual streamflow observations. Hydrological Simulation Program–Fortran (HSPF) is a comprehensive, conceptual, continuous simulation watershed scale model. HSPF simulates nonpoint source hydrology and water quality. It combines point source contributions and performs flow and water quality routing in the watershed (*Singh et al.*, 2005). Soil and Water Assessment Tool (SWAT) is a continuous simulation conceptual model with

spatially explicit parametrization (*Singh et al.*, 2005). SWAT can predict the impact of land management practices on water, sediment, and agricultural chemical loads. SWAT was designed to be used on large complex watersheds with varying soils, land uses, and management conditions (*Singh et al.*, 2005). The tile drains were not directly modelled in HSPF. To simulate tile drains in HSPF, parameters were adjusted to account for fast subsurface flow. SWAT has a tile drainage component built into the model. SWAT simulates the tile drains only during saturated flow (*Ahmad et al.*, 2002). Equation 2.12 illustrates how SWAT calculates how much water is flowing into the tile drains.

$$q_{tile} = (SW_{ly} - FC_{ly}) \left(1 - e^{\left[\frac{-24}{t_{drain}}\right]}\right) \tag{2.12}$$

where q_{tile} is the amount of water (mm) removed from the layer on a given day by tile drainage, SW is soil water content (mm) of the layer on a given day, FC is the soil field capacity and t_{drain} is time (hours) required to drain the soil to field capacity (*Ahmad et al.*, 2002). Water entering the tiles is treated as lateral flow. This equation is only used when the soil water content is greater then the field capacity of the soil.

Borah and Bera (2003) reviewed eleven different watershed scale models to determine their appropriate uses. The models that were reviewed included AGNPS, AnnAGNPS, ANSWERS, ANSWERS-Continuous, CASC2D, DWSM, HSPF, KINEROS, MIKE SHE, PRMS and SWAT. Out of these models; AnnAGNPS, ANSWERS-Continuous, HSPF and SWAT, are considered the continuous simulation models. These are generally useful for analyzing the long-term effects of hydrological changes and watershed management practices, especially in the areas of agriculture (*Borah and Bera*, 2003). *Borah and Bera* (2003) concluded that these continuous simulation model contained three major components (hydrology, sediment, and chemical) that are applicable to watershed-scale problems. SWAT was the most promising model for continuous simulations in predominantly agricultural watersheds. HSPF was determined to be promising for a mixed agricultural and urban watershed (*Borah and Bera*, 2003). This study did not specifically model tile drains on the watershed-scale.

Carlier et al. (2007) studied field-scale tile-drained soils. As an initial step towards incorporating tile drainage systems into large-scale hydrological models, an equivalent representation of tile drains buried in a soil profile by using a

homogeneous anisotropic porous medium without drains was proposed. *Carlier et al.* (2007) used two alternatives to the method. First, the soil profile equipped with the actual drain pipes is represented by an equivalent, horizontally layered system with no pipes. The second alternative was to replace the layered system with an equivalent homogeneous profile. The efficiency of these approaches was tested against a common representations of tile drains using the SWMS 3D code. SWMS solves the Richards equation for a typical drained plot configuration. The equivalent-medium approach appears to give adequate results for water outflow and mean water table elevation (*Carlier et al.*, 2007).

Macrae et al. (2007) studied the spatiotemporal variability (even-based, seasonal) in the contribution of drainage tiles within a basin as well as soluble reactive phosphorus and total phosphorus export over a period of 1 year. Tile drains were monitored and drainage rates were recorded for the year. The tile drain discharge was highly variable at both moderate (wet versus dry periods) and smaller (within-event) temporal scales. *Macrae et al.* (2007) was estimated that approximately 42% of the Strawberry Creek Watershed annual discharge originated from tile drains. Strawberry creek is located just west of Waterloo, Ontario. The majority of the discharge occurred during the winter and spring months.

Wang et al. (2006) evaluated the uncertainty in DRAINMOD predictions of daily, monthly, and yearly subsurface tile drain flow. Six years of tile drain data were used and the uncertainties in eight model parameters were considered to analyze how uncertainties in input parameters transmit to outputs. *Wang et al.* (2006) found that annual tile drain flow predicted by DRAINMOD fell well within the 90% confidence bounds. The model results were most sensitive to the vertical saturated hydraulic conductivity of any restrictive soil layers and the lateral hydraulic conductivity of the deepest soil layer.

Stillman et al. (2006) studied event-based transient subsurface flow of water into tile drains. Using the Boussinesq equation a sharp-front theory was used to determine the depth of the wetting front to estimate the flux to the water table. A semi-analytical model was developed and calibrated for predicting transient subsurface tile-drain flow. *Stillman et al.* (2006) concluded that the effective saturated hydraulic conductivity should be used for subsurface drainage analysis as well as the model developed was able to closely predict

for rainfall events with single burst hyetographs. The HELP3 program uses the effective hydraulic conductivity for calculating subsurface flows. HELP3 also calculates the lateral drainage based on the Boussinesq equation as discussed in Section 2.11.2.

Rosenburg et al. (1999) used a GIS-based program, HUMUS, in conjunction with SWAT to simulate the impact of climate change on the groundwater recharge and water yield of the Ogallala aquifer in the United States. Multiple GCM climate change models were used to simulate the impact of anticipated temperature increases and CO_2 concentrations. *Rosenburg et al.* (1999) found that there were reductions in the recharge with all simulations. There were no tile drains modelled in this study.

Croley II and Luukkonen (2003) simulated the impacts of climate change on groundwater recharge using MODFLOW on a regional scale. The region of study was Lansing Michigan. The study used a steady state approach, which did not account for transient groundwater level changes. *Croley II and Luukkonen* (2003) concluded that the groundwater recharge could increase or decrease depending on the General Circulation Model (GCM) that was used for the climate change simulation. There were no tile drains modelled in this study.

Eckhardt and Ulbrich (2003) used a revised version of SWAT to simulate the impact of climate change on streamflow and groundwater recharge for a catchment in Germany. Climate change was simulated by changing the stomatal conductance and leaf area in SWAT. This was done as a response to predicted increased CO_2 concentrations. Similar to *Rosenburg et al.* (1999); *Croley II and Luukkonen* (2003) multiple GCMs were employed with several climate change scenarios simulated. Results from the simulations were that more precipitation will fall as rain in the winter months and that groundwater recharge along with streamflow have potential to be reduced during the summer months for the modelled region. There were no tile drains modelled in this study.

Chapter 3

Methodology

This chapter of describes the model development and solution methodology. It includes a brief description of the model development and methodology that went into processing all of the data.

To model on a large scale, such as the GRW, large amount of data must be acquired, stored, and organized. Large database programs such as ARCView GIS and MS-Access provide a framework to store, manipulate and organize large amounts of spatial and relational data. Using the model developed by *Jyrkama et al.* (2002) for groundwater recharge in the GRW a tile drain component was developed and integrated into the code.

The tile drain component in the model starts out as spatial data in the GIS program. This data is merged with the previous LULC and soils data. This merge creates many more unique cells that are all modelled individually. After creating the unique cells needed as inputs for the model, the tile drain code was developed. This code was written in Visual Basic for Applications (VBA) with-in the MS-Access and used the unique cell database that was created with the GIS program. The model uses HELP3 to simulate the cells hydrologic process over the 40 year period. The process is repeated for each cell that contains tile drains. The results from the simulations are then imported back into GIS and displayed spatially in the GRW. Figure 3.1 briefly outlines how the process works.

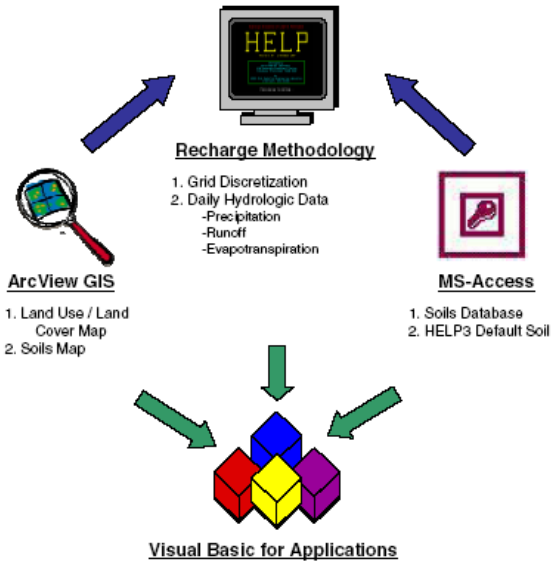

Figure 3.1: Outline of the modeling procedure

3.1 Data Gathering

One of the first steps when working with any Geographic Information System (GIS) is to gather data. Gathering data can be a long and tedious process if the data needed is obscure or records are not well kept. More data is being kept digitally and old records are being but into databases as older systems of keeping records are becoming outdated. Keeping digital records also allows for quick and easy access to the complete history of the object(s) that are of concern. This can then be transferred into GIS for a spatial representation of the data. Geographical data or meta data, includes the projection of that data in the world using co-ordinates. With all GIS files, appropriate metadata should be present so the GIS software can project and interpret the data correctly. Bad data at the beginning of the project will only lead to inaccurate results at the end of the project.

Data for this thesis were gathered from many sources. The Grand River Conservation Authority (GRCA) provided data that included the watershed boundary, and land use and land class maps created using the 1999 satellite (Landsat 7) thematic mapper. The University of Waterloo (UW) map library was able to provide tile drainage data. The tile drain data were created by the Ontario Ministry of Natural Resources in 2002. Meteorological data used in the HELP3 program were collected from the GRCA for the entire watershed.

The meteorological data were collected from observations of various locations in and around the watershed. All of the data were transferred digitally to ensure they were not modified from its original state when data manipulation began.

3.2 Data Manipulation

Projects that requires pre-existing data may have to convert the data into a useful form. For example with this thesis, one of the starting points was to clip out the actual watershed boundaries from the soils and LULC map. Using ArcMap (GIS) software, the watershed extents were used as a 'cookie' cutter to cut away any excess information. There are many other forms of data manipulation. Most of the data manipulation for this project is being performed in the GIS software, however, due to some of the GIS software constraints, some of the data manipulation must be completed using other software packages such as Microsoft Excel and Access.

3.2.1 Vector Manipulations

The vector manipulations are done using the GIS software. The spatial data has to be modified so the appropriate analysis can be performed. The following manipulations are described on how they work and how they applied to this thesis.

- LULC Merge - Combines input features from multiple input sources (of the same data type) into a single, new output feature class (ARC, 2007). The input data sources may be point, line, or polygon feature classes or tables. One caution of merging spatial data is that the coordinate projections must be the same to ensure that all of the borders and spatial data are consistent. If no coordinate system is specified in the Environment Settings, the output merged feature class will be in the coordinate system of the first feature class in the input features list. To avoid discontinuities with the data, it is best to project all the data that is to be merged in the same coordinate system. This tool was used to merge all LULC zones into one watershed shape file to be used as a base map for collecting, amalgamating and displaying data in the GIS software.

- Clip - With the clip tool, the tile drain shape files that were entirely and partially located within the GRW to be used for analysis. The clip tool takes one shape file as the input (tile drain shape file) and a "cookie cutter" shape file (watershed jurisdiction) and creates a new layer/shapefile of all of the tile drains located within the watershed (ARC, 2007). This becomes important on the boundaries of the watershed where there are partial tile drain areas.

- Union - The union tool is used to take two pieces of information (shape files) and join them into one larger shape file (ARC, 2007). With this tool the user can specify how much information from each shape file can be transferred to the new larger shape file. For this project the union tool was used to create a larger LULC data set shape file by unifying the LULC data set with the tile drainage data set. This operation increased the cell count to approximately 281247 total cells.

The union of the tile drainage layer and the LULC and soil layers has created a new master cell grid of approximately, 281247 cells. However some cells were found to have no LULC or soil profile associated with the cell. These "empty" cells were located on the edge of the watershed. The cause for this small error is most likely due to the watershed borders. The watershed borders were re-evaluated and updated constantly. The soils and LULC maps were older than the new watershed borders. Only 38 cells were found to be "empty" and were excluded from the analysis. This resulted in 281209 cells, all of, which have a specific LULC, soil profile as well as a tile drainage indicator. This method eliminates averaging across the cells and increases the level of accuracy for the GRW and the cells affected by the tile drains.

Doing a tile drainage analysis on the entire watershed is not needed because not all of the watershed has tile drains. Filtering out all of the cells that were associated with tile drains was done to create a new cell database. This new, smaller, database contained only 76639 cells, which is approximately 27% of the total number of cells in the watershed. These cells are agricultural based (i.e. Bare Agricultural Fields, Row Crops, Forage, and Small Grains). Sometimes the tile drain polygons overlap onto forested areas. However, there will be no tile drains directly placed on non-agricultural lands and the likelihood of tile drains being installed under a forested area is small. These cells are excluded from the tile drain analysis. Excluding polygons that do not apply

to tile drainage is simply done using a selection by attributes in the GIS software or using the model to filter out those polygons that will not have any tile drains. The agricultural cells are shown in Figure 3.2.

The groundwater recharge model is 1D and the results are based on a generic (1 ha) area for every cell. Therefore the new cells range in area and the results produced from the recharge model will have to be scaled with area. The area for every cell has been calculated and stored in the database of the shape files in GIS. Once the results have been produced for the cells, the results from the simulations are scaled by cell area to get an accurate estimate for the discharge and recharge volumes.

3.2.2 BIN Code Manipulations

The BIN code contains the information that indicates what type of land use the polygon is being used for as well as the soil profile and type that is located at that cell. The BIN code also contains information such as the township that it is located in as well as the sub-basin where the cell is contained. All of this information is used to determine how much precipitation occurs in that cell as well as the wind and growing period for that cell. The BIN code information is also used to for the inputs to HELP3. The BIN code has the soil profile information stored in it to be used for the HELP3 input.

The cell identification BIN code was modified to indicate that the cell had tile drains. The tile drains were added to the LULC map and increased the number of unique cells in the watershed to 281209. The BIN code was modified to include a "T" or "NT" for tiled or not tiled. This indicator is used for future coding to indicate the use of tiles in that cell.

3.3 Inputs

3.3.1 Land Use/Land Class Data

The LULC data was complied for the entire Grand River watershed. The watershed was divided into 15 specific land uses, ranging from open water to row crop land as specified in Figure 2.9. This is important when modelling

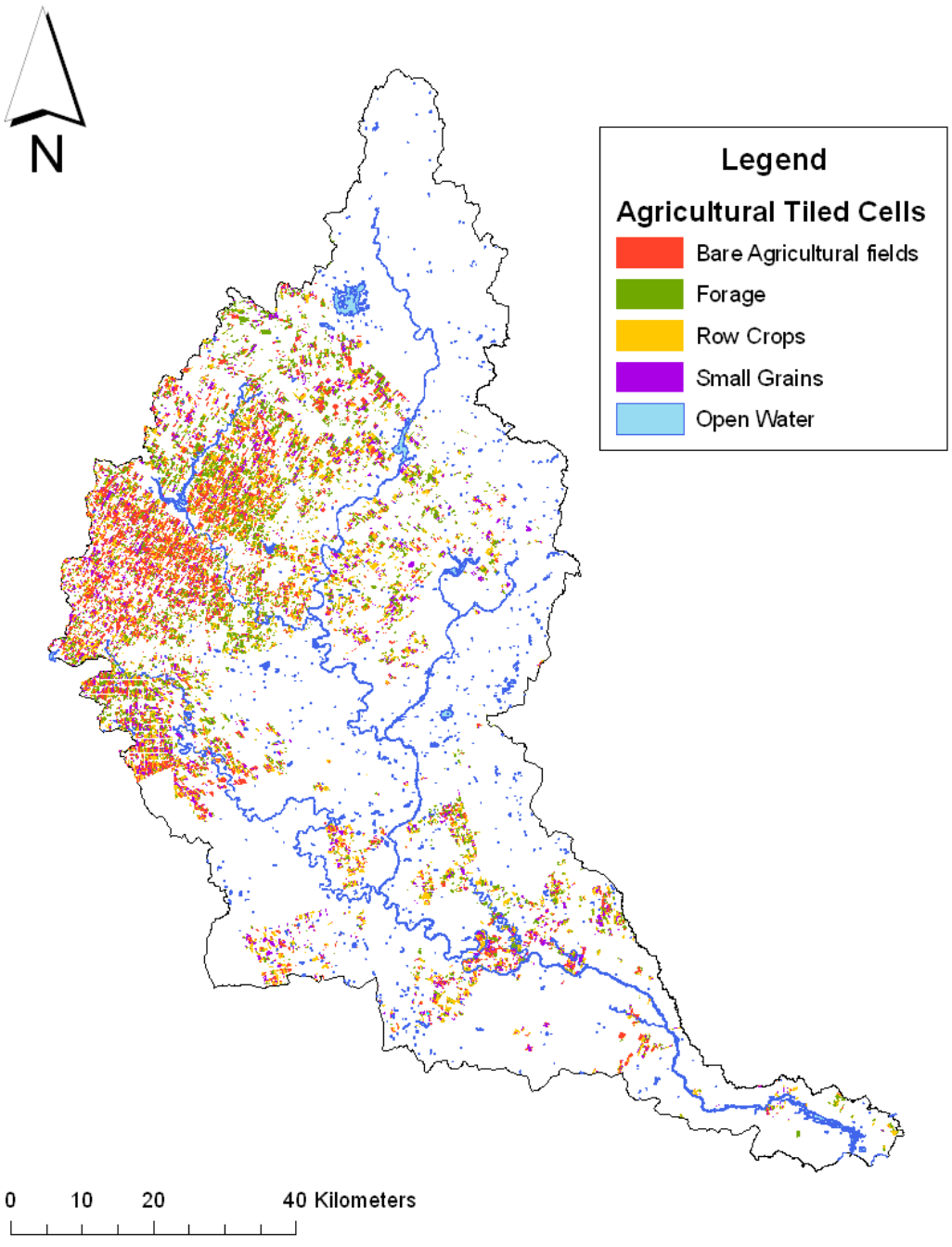

Figure 3.2: Agricultural cells with tile drains

the tile drain applications, only the appropriate cells must be targeted and modelled.

With the addition of the tile drain data to the LULC data further distinction between agricultural lands will occur. Areas that contain tile drains will affect nearby surface waters and groundwater.

Crop rotations were not included in the analysis of the 40 year period for the entire watershed. This was not included because it was assumed that the relative percentage of bare fields would be roughly the same for any given year. The only difference between the years would a spatial difference. If a crop rotation was included into the model the processing time would increase because of how the model runs through the cells and the 40 years of meteorological simulation.

3.3.2 Tile Drain Data

The tile drainage data for the Grand River watershed was obtained from the University of Waterloo (UW) map library. The tile drainage shape files were created by the Ministry of Natural Resources in 2002. The tile drain data was stored as polygons in a shape file. These polygons outlined the areas where tile drains have been installed. The tile drain data was collected for a large portion of south western Ontario. Only the drain data that was located within the GRW was used. The tile drain data was clipped to ensure only the tile drain age data located in the GRW was used for analysis. The agricultural tile drains in the GRW cover an area of approximately 99,800 ha. The reason why there are less tile drain areas in the southern portion of the GRW may be a result of lack of information. Without the proper spatial data, no analysis can be performed with any kind of accuracy.

No data was given about size of the drains, spacing, or their depth below ground surface (bgs). Because of this missing data, some assumptions were required. These assumptions include:

- Tile drain spacing was set to be 10 m;
- Depth of tile drains was set to be 0.8 m bgs;
- Tile drain slope was set to a 2% grade.

3.3.3 Soil Data

The soil data for the Grand River watershed was collected and then patched together with the GIS software. The results from this process produced a soils map containing over 700 different soil types within the watershed. Each soil type was matched to the soils in the HELP3 database. Unfortunately the HELP3 soil database is not as extensive as the variety of GRW soils. Most of the 700 soil types were matched as closely as possible to one of the HELP3 soil types that are located in the database. The soil properties are all kept the same as the native soils on-site and according to what the database indicates for each depth of the soil profile. This soil matching was done so HELP3 could simulate the hydrologic routing for each cell. The HELP3 model soil inputs were done to a depth of 3 m, to ensure that the groundwater recharge was calculated beyond the root zone. For the purposes of this thesis, the soil input was modified where tile drains are located. The HELP3 model was used to simulate the amount of water being transported by the drains. HELP3 already has this function built into it. The soil information still extends to a depth of 3m bgs, however, at approximately 80 cm bgs the layer type was changed from a vertical percolation layer to a lateral drainage layer. The lateral drainage layer was coded by selecting a depth and a layer thickness for the tile drainage layer. The tile drainage depth of 80 cm bgs was determined by inquiring with local tile drainage installation businesses as well as Prof. David Rudolph of the Earth Sciences department at UW. The soil layer thickness was selected after consulting these sources. The lateral drainage layer was determined to be 15 cm in depth. After the lateral drainage layer was incorporated into the model another soil layer type had to be integrated below the lateral drainage layer. HELP3 requires a barrier soil to be placed under a lateral drainage layer. The soil properties for all of the layers are the same as the HELP3 default properties. This means that the lateral drainage layer and barrier soil layer could be comprised of the same soil type but the layer type is different, prompting HELP3 to perform the lateral drainage analysis on the appropriate layer.

Some modifications to the recharge model were performed to incorporate the tile drains into the native soil conditions that the recharge model used. The first modification to the code was to incorporate the tile drains into the input files that would be used in the HELP3 model. The second modification

to the code was done when reading the output files for the recharge and the drainage from the output files.

Within the entire watershed there are some areas where there is little or no information on the soil type. In the database where all of the soil information is located, these soil types are still listed for completeness. Instead of removing the hundreds of potential soil types that contain little or no information, a check in the code was written to determine if the soil type was valid for analysis. If the soil passed the check then the analysis would occur, otherwise that cell would be skipped and the code would move onto the next cell in the database. These soil types were not modelled because no tile drains would be present even if the spatial tile drain data may have overlapped into these soil types. Soil types that were excluded from the tile drainage modelling include:

- Creek beds
- Stream courses
- Escarpment
- Quarries
- Potholes
- Shallow organic soils overlying limestone
- Open Water

HELP3 was designed for landfill modelling and subsequently it assumes that there is no saturated zone; that is the model only simulates the water balance processes that occur above the water table. The HELP3 model was chosen to model the cells of the watershed as it is receiving much recognition by watershed analysts (*Jyrkama and Sykes*, 2007) and its accounts for many naturally occurring events (i.e., snow pack, snow melt, amount of sunshine an area receives during the year).

3.3.4 Meteorological Data

Weather patterns change over the length of the GRW. The region was divided into 13 zones of uniform meteorology (ZUM) by the GRCA (*Jyrkama and*

Sykes, 2007). These zones were further subdivided into 293 sub basins that have unique daily precipitation, temperature and solar radiation values. Figure 3.3 shows the sub basins divided up into the respective ZUM areas. The weather data was interpolated using an inverse distance squared algorithm, equation 3.1 (*Jyrkama and Sykes*, 2007).

$$P^{SUB} = \frac{\sum_{i=1}^{13} \left(\frac{P_i^{ZUM}}{d_i^2} \right)}{\sum_{i=1}^{13} \left(\frac{1}{d_i^2} \right)} \tag{3.1}$$

where P is the daily precipitation, solar radiation, or temperature and d is the distance from the centroid of the sub basin to the centroid of the ZUM. With this weighting system, a smoother weather transition was observed across the watershed (*Jyrkama and Sykes*, 2007).

HELP3 was also used for estimating the growing seasons of each ZUM. This becomes important when dealing with an area that spans the length of the GRW. Different growing periods are associated with each ZUM. For example, ZUMs in the northern part of the watershed would potentially have a shorter growing period than those at the south of the watershed. This growing period can be influenced by climate change. If the temperature increases then the growing season will be extended.

The precipitation patterns that were discussed in this section have produced a probable precipitation map. This map shows how much precipitation would fall on the specific areas of the watershed. The map was produced using the equation 3.1 and all of the data that was gathered from various weather stations around the GRW. Figure 3.4 shows the precipitation distribution for 1999 that was produced and used during the modelling process.

3.4 Climate Change

A model for the potential climate change scenarios was developed for the GRW by *Jyrkama and Sykes* (2007). *Jyrkama et al.* (2002) presents the methodology on how this model was originally constructed. Their model was then modified in the work of the current thesis to simulate the tile drains in the watershed. The new scenario predictions for the A2, A1B, and B1 from the IPCC were included and modelled with this newly modified climate change code.

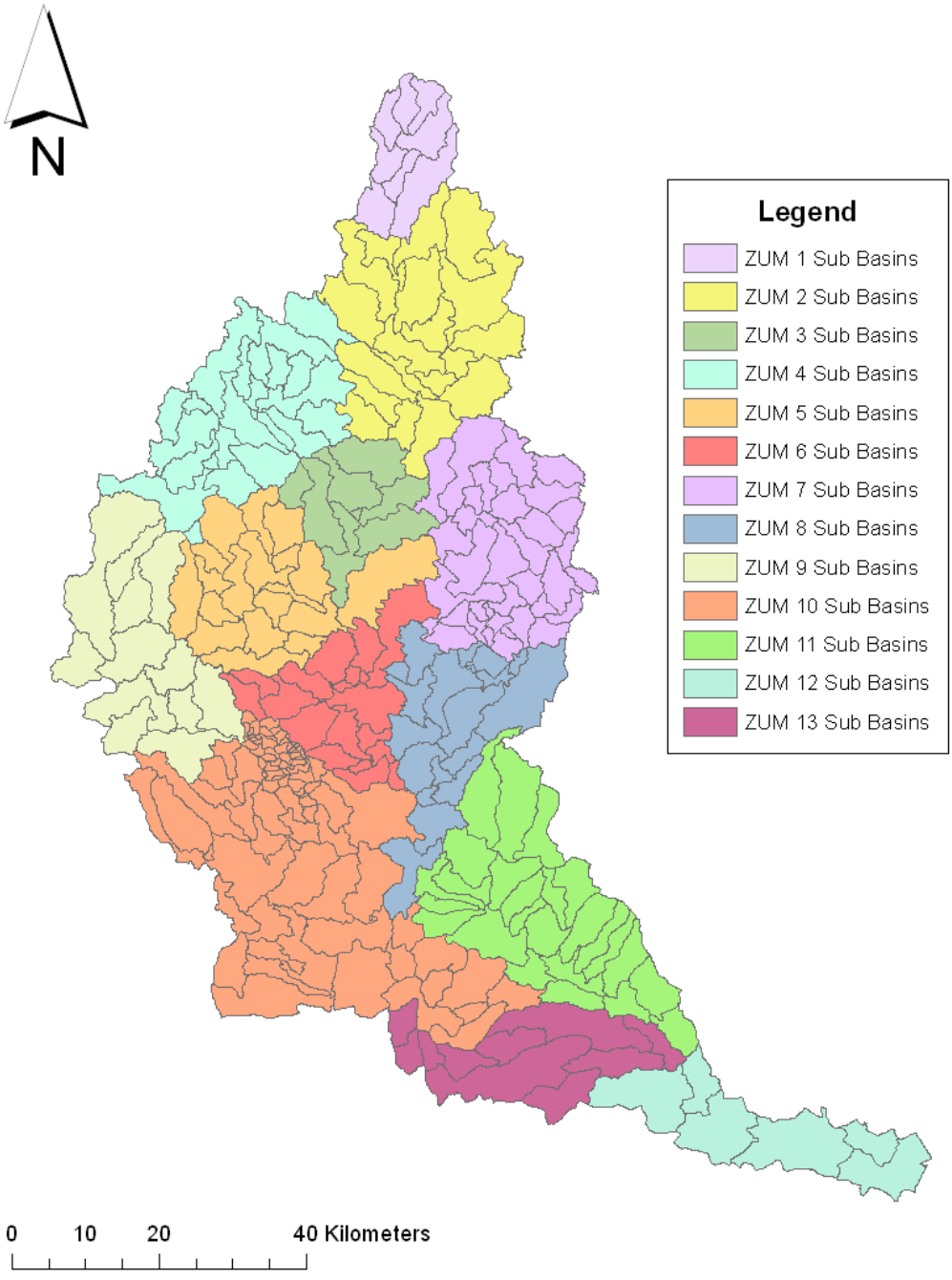

Figure 3.3: Sub-basins divided up into ZUMs for the Grand River Watershed

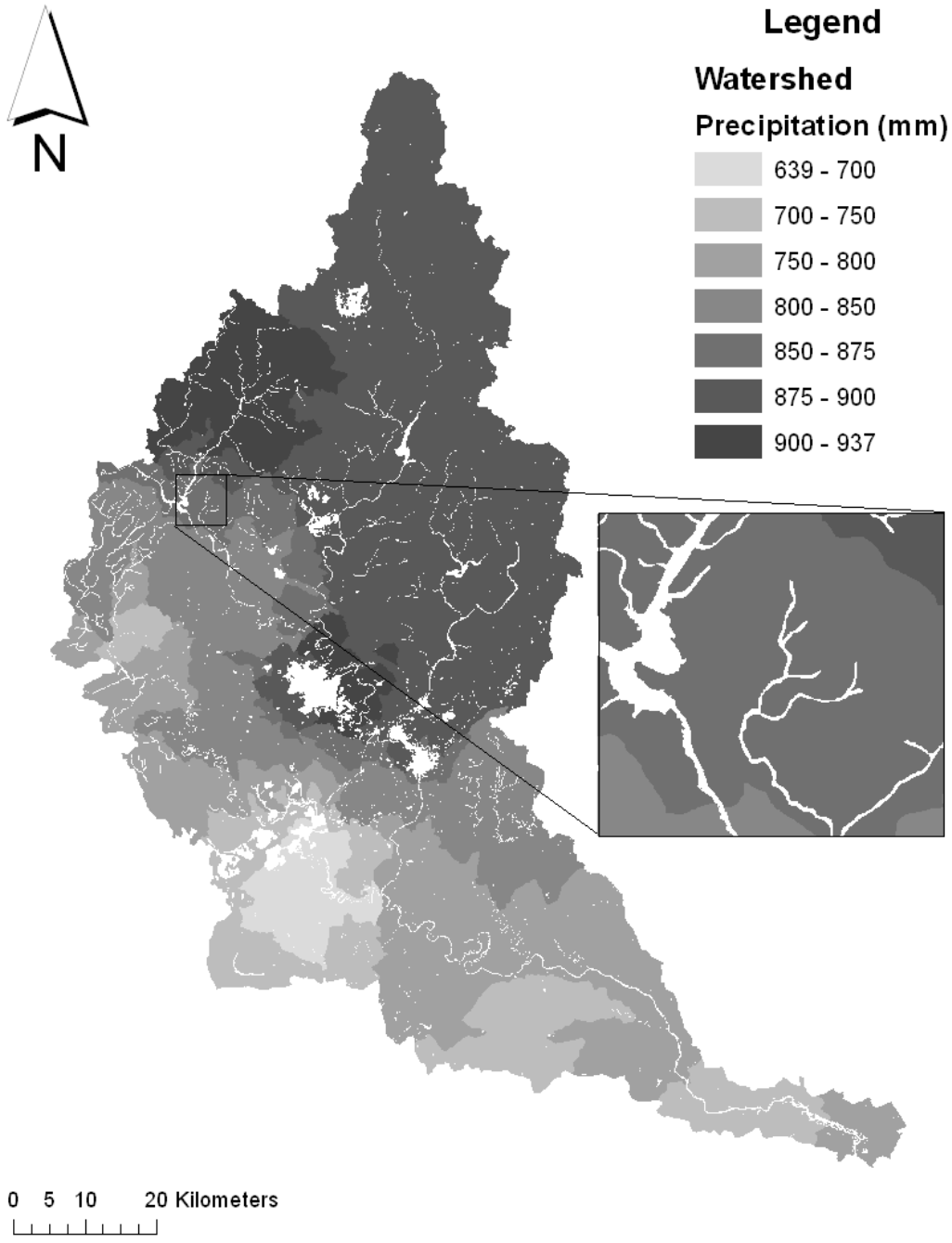

Figure 3.4: Annual precipitation distribution for 1999 for the Grand River Watershed

Each of the IPCC scenarios have a likely projected temperature range as well as a likely precipitation percentage change and a solar radiation percentage change. All of the projections from the IPCC were listed as likely to very likely (*IPCC*, 2007c). Based on the IPCC projections, a likely range of temperature and precipitation increases was chosen for modelling (*IPCC*, 2007a).

The A2 climate change scenario has the highest likely climate changes for the GRW. This scenario was chosen as the "worst case" scenario in terms of climate change. For this thesis the temperature increase of 5.4 °C was chosen, which meant that the annual temperature increase of 0.054 °C/year was modelled. The annual precipitation increase was approximated to be 0.0819%/year for the A2 scenario.

The A1B climate change scenario was chosen to model because it is a scenario with intermediate impact. For this thesis the temperature increase of 4.4 °C was chosen, which meant that the annual temperature increase of 0.044 °C/year was modelled. The annual precipitation increase was approximated to be 0.070%/year for the A1B scenario.

The B1 scenario offered the lowest increases in both precipitation and temperature. This was considered to be the least adverse of the predicted climate change scenarios. For this thesis, the smallest increase estimate of 1.1 °C was chosen. This resulted in an annual temperature increase of 0.011 °C/year. The annual increase in precipitation was approximated to be 0.0483%/year for the B1 scenario.

The original 40 year historical weather data from 1960 to 1999 was used as a base for the climate change scenarios that were used to simulate changing climate in the GRW. The temperature was modelled as a linear increase. As described in the previous paragraph, the A2 scenario the temperature was expected to increase to a maximum of 5.4°C in 100 years or 0.054°C/year. For this simulation the temperature would increase by a maximum of 2.16°C in the 40 year period. The precipitation was handled differently because this is a percentage increase in precipitation. This was calculated using the following equations

$$\Delta x = \frac{\sum_{i=1}^{N} P \cdot \delta}{\sum_{i=1}^{N} iP} \tag{3.2}$$

$$P_i^{cc} = P_i \left(1 + i\Delta x\right) \tag{3.3}$$

where P is the actual daily precipitation of the i^th day, P^{cc} is the new daily precipitation due to the climate change, Δx is the calculated change in the daily precipitation, δ is the percent change in the average precipitation (for the A2 scenario this was approximately 0.176%/yr), and N is the total number of days in the study.

The solar radiation was decreased by 0.0273%/year. This was included in the modelling, but as *Jyrkama et al.* (2002) conclude, it has little effect on the overall results of the watershed analysis.

Downscaling techniques have been used to take large GCM model outputs to help describe the local impacts of potential climate change. *Wilby and Wigley* (1997) suggest that downscaling methods perform well in simulating present observed and model-generated daily precipitation for circulation based models. However, downscaling methods are able to capture only part of the daily precipitation variability associated with model-derived changes in climate (*Wilby and Wigley*, 1997). For this thesis the downscaling that occurred was taking the average annual projected increases in both temperature and precipitation and then applying the new data on a daily time frame. The meteorological data were collected on a daily time step so the modifications must be done at this time step as well.

3.5 Output

The HELP3 model produces a unique text file for each iteration/cell that is simulated. The recharge model of this thesis reads the HELP3 text file, searches for the parameters that are of interest, stores them in an array, and finally writes the parameters to a comma separated (csv) text file for further post processing. The csv file was created because it has a relatively small size and can be used in many other programs for further processing.

For the purposes of displaying results in ArcMap, the monthly outputs were taken from months where drainage would be expected to be more active, generally the months of April and November. The annual outputs that were taken from the HELP3 files were stored in the same manner as the monthly results. The only difference between the two csv text files is the quantity of results stored in the file.

Chapter 4

Results

The tile drainage simulation for all of the tiled cells takes approximately 30 hours to complete. The model simulates every cell individually for 40 years before moving onto the next cell.

Tile drains are designed to lower the water table at the root zone of fields, thus permitting earlier crop seeding. If the drains are installed below the natural water table, they will effectively unsaturate the zone until the local water table is at the tile drain level. This is illustrated in Figure 2.7. An assumption used in the modelling and analysis process for this thesis was that if there was not sufficient water table mounding between the tile drains, then the tile drains would not collect much water. The mounding of the water between the drains is dependant on the type of soils present, the characteristics of the barrier layer that underlies the drainage layer as well as the amount of water moving through the soil. Water moving through the soil varies temporally and there are times of the year when there is more water infiltrating downwards into the groundwater than at other times of the year (e.g. spring vs summer). If there is not enough water moving through the soil near the tile drains, then there will not be sufficient mounding and the water will bypass the tile drains.

If the tiles are spread too far apart, this allows for more water to bypass the tile drains. More tiles placed closer together, in theory, would produce more water being drained. For this thesis, typical drainage spacing, depths, and slope for the area were used, as discussed in section 3.3.2. All of these variables will have some affect on the efficiency of the tile drains and, subsequently, the recharge in the local area.

4.1 Tile Drains

The variability observed in the effectiveness of tile drains stems from the parameters such as the amount of precipitation and the type of soil of the cell. As discussed in the preceding section 3.3.2, all of the tile drains that were modelled had the same depth, slope, and spacing between the drains.

As seen in Figure 4.1 the discharge/drainage from the tile drains across the entire watershed varies for the month of April 1999 from approximately 0 m^3/ha to 23.39 m^3/ha. The drainage results are shown in m^3/ha because of the area scaling that was done on the results. The total water extracted and drained from the entire watershed tile drains for April 1999 was calculated to be approximately 10500 m^3.

The tile drainage/recharge model was used to generate both monthly and annual results for the tiled cells. The annual results were able to show the annual water budget and the water balance. HELP3 calculates a mass balance for every year of simulation. There were 40 years of simulation performed on each cell. During the modelling process there were random checks on cells to examine the water balance on the cell per year. For most years, the annual water budget was balanced to within a few millimeters (+/-) per year for every cell that was checked. This indicates that the HELP3 water budget was balanced for every year, every scenario, and every cell that was examined. This is important because without a balanced water budget, water mass would be either increasing or decreasing in the model.

The drainage results from 1999 for the GRW tiled cells are shown in Figure 4.2. The annual volumes drained from the GRW tiled areas range from approximately 0 m^3/ha to 24.46 m^3/ha. The total volume of water that is extracted from the subsurface was approximately 16,100 m^3 for the year of 1999. This indicates that there is approximately 16,100 m^3 of water annually being diverted from the fields into the surface waters carrying potential contaminants. The average volume of water that is diverted from the subsurface by the drains in the GRW is approximately 0.222 m^3/ha per year. This is averaged out over all of the tiled cells.

The results show that the annual drainage collected from the tile drains can vary in a short distance. These variations show how all of the elements of spatial variability can affect the drainage of the fields. The precipitation falling

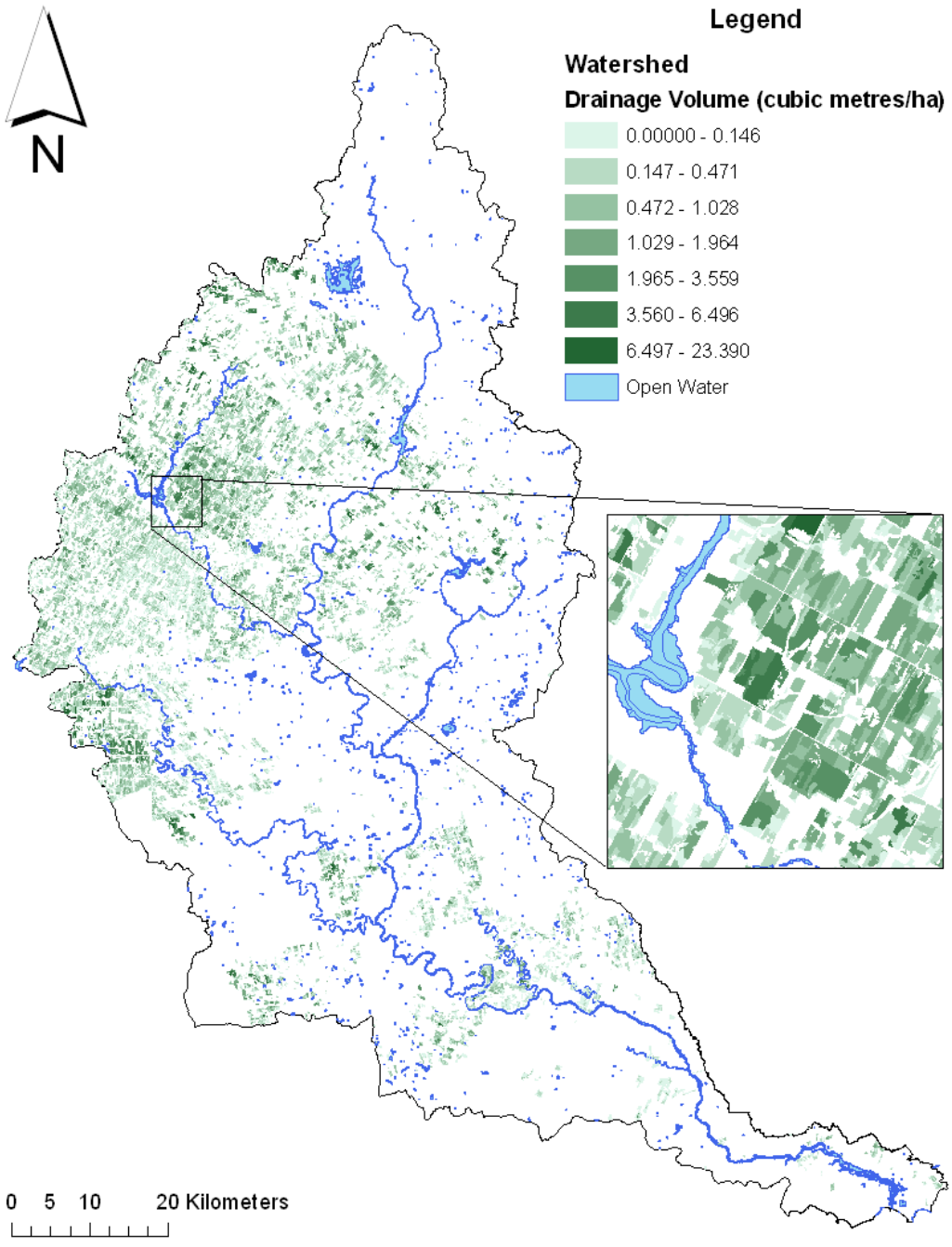

Figure 4.1: Drainage volume per hectare from tile drains for April 1999

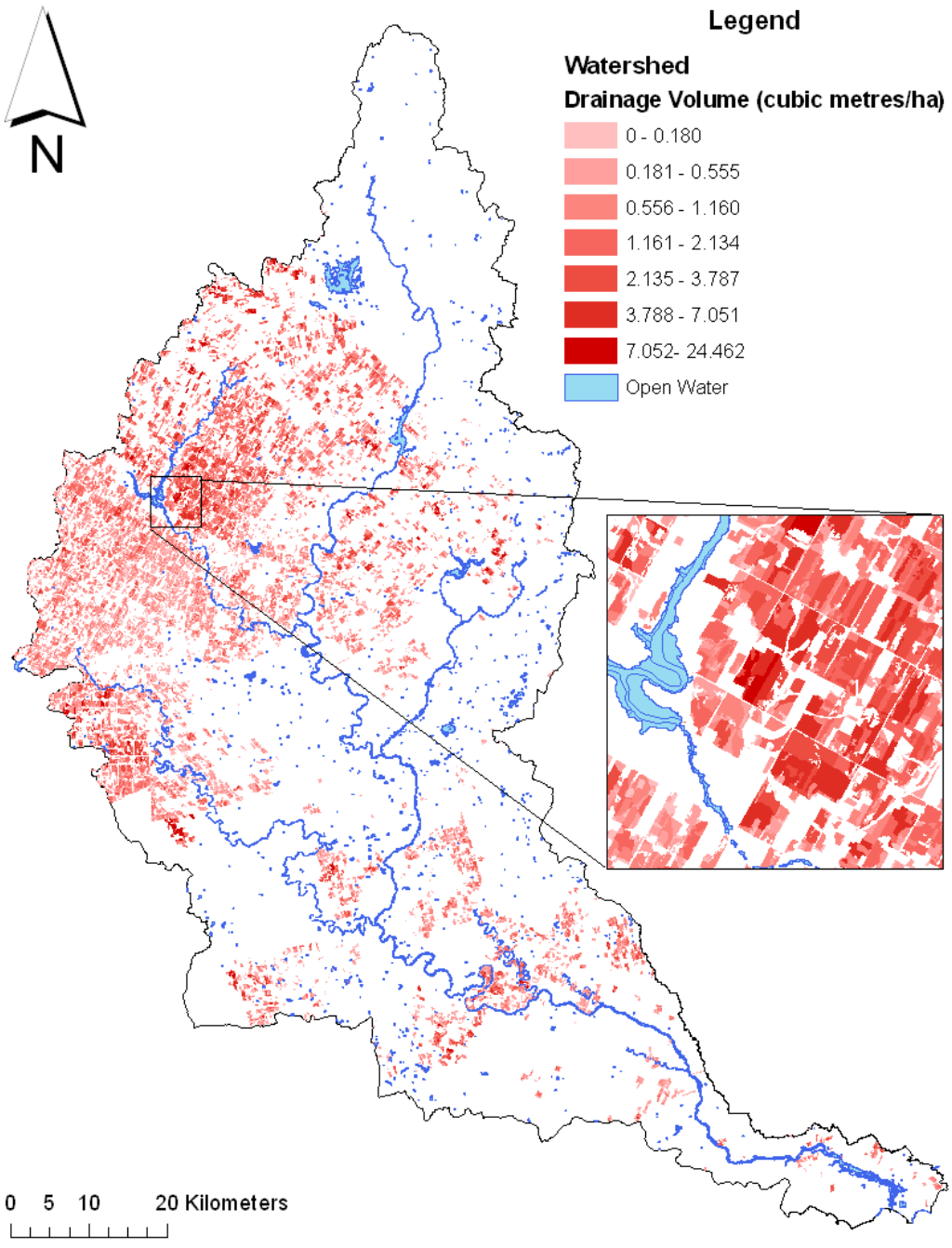

Figure 4.2: Drainage volume per hectare from tile drains for 1999

in various areas within the watershed will affect each each cell differently. The soil profiles for each cell will also affect the amount of water drained from the tile drains. If the soil profile promotes vertical percolation (such as sandy soils) and does not store a lot of water within the soil matrix then most of the water that the cell receives will move past the tile drains and move into the subsurface as recharge. If the soil is tighter and does not promote recharge (such as a silt or a clay) then more water will move into the tile drains and be moved off site into a ditch, swale, or surface body of water.

April was chosen as the month for drainage analysis because this month generally had the most drainage activity due to spring melt occurring during this month for the GRW. The difference between the annual drainage volume and melt water drainage in April may indicate how active tile drains are in April compared to the rest of the year. Figure 4.3 shows the difference between the annual drainage and the April drainage that was simulated for 1999.

It is important to note that the areas where the tile drainage was greatest pose the greatest threat to creating a short circuit in the environment. These farm fields are discharging more water from the subsurface and into the surface waters, which are also used for drinking water in certain areas. If contaminants move into the groundwater, the time taken to migrate into a drinking water capture zone may take much longer and the contaminants may have a chance to either fully or partially naturally degrade in the environment. If excessive amounts of nitrates are dumped into slow moving surface waters such as lakes and ponds, eutrophication can occur, which may lead to areas of hypoxia within the watershed as well as in Lake Erie where the GRW discharges. As discussed in Section 2.4.3.1 areas of hypoxia can put a heavy stress on the local environment.

4.1.1 Effect on Recharge in April

The recharge for the GRW is impacted in the month of April for the tiled areas. This is due to the spring melt that occurs generally in the month of April for the GRW. When the tile drains are modelled and compared to the un-tiled results the groundwater recharge shows a general increased trend. Figure 4.4 shows the change in recharge for the month of April 1999.

The green areas indicate more water moving into the subsurface as ground-

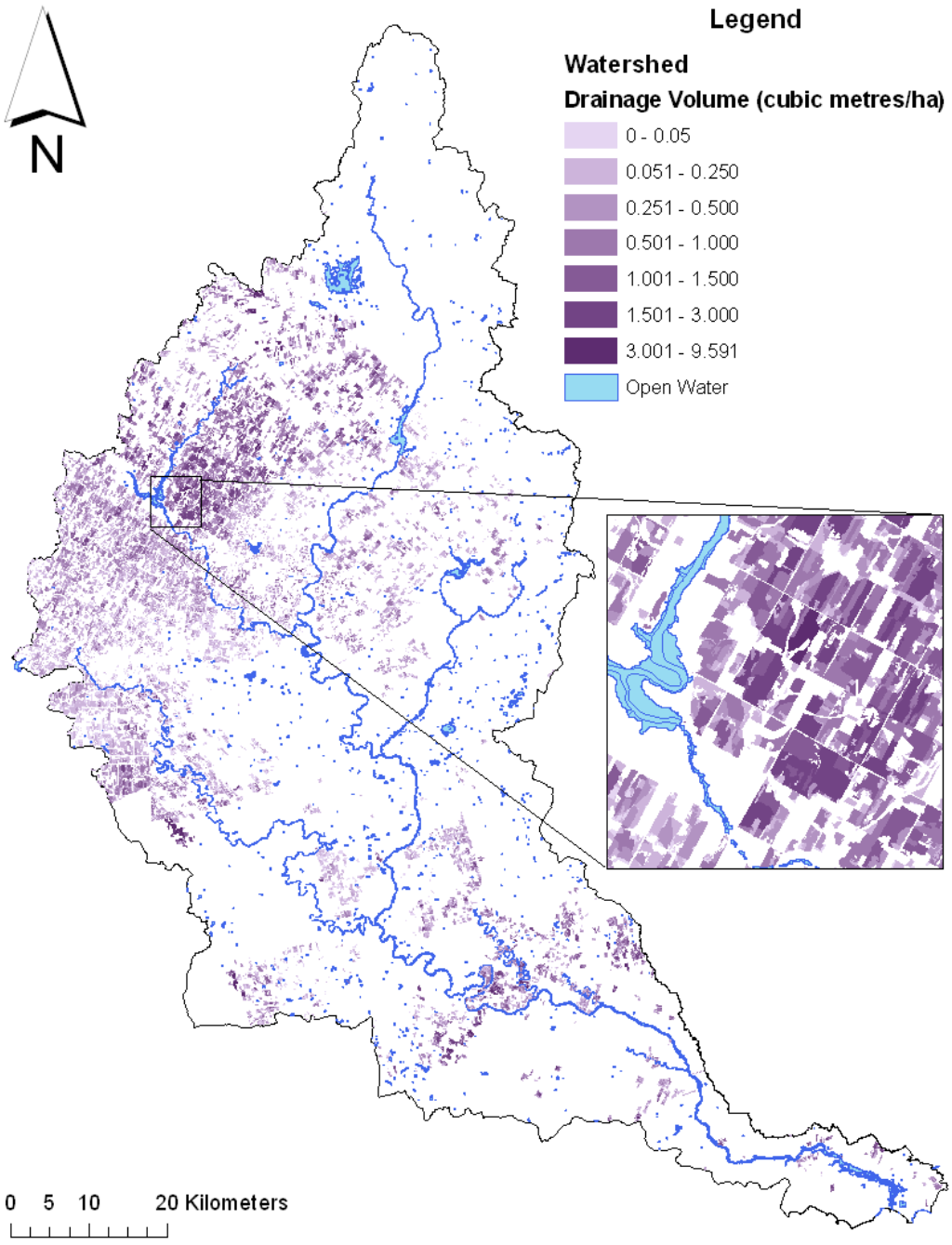

Figure 4.3: Difference in drainage (m^3/ha) between April and the rest of the year for 1999

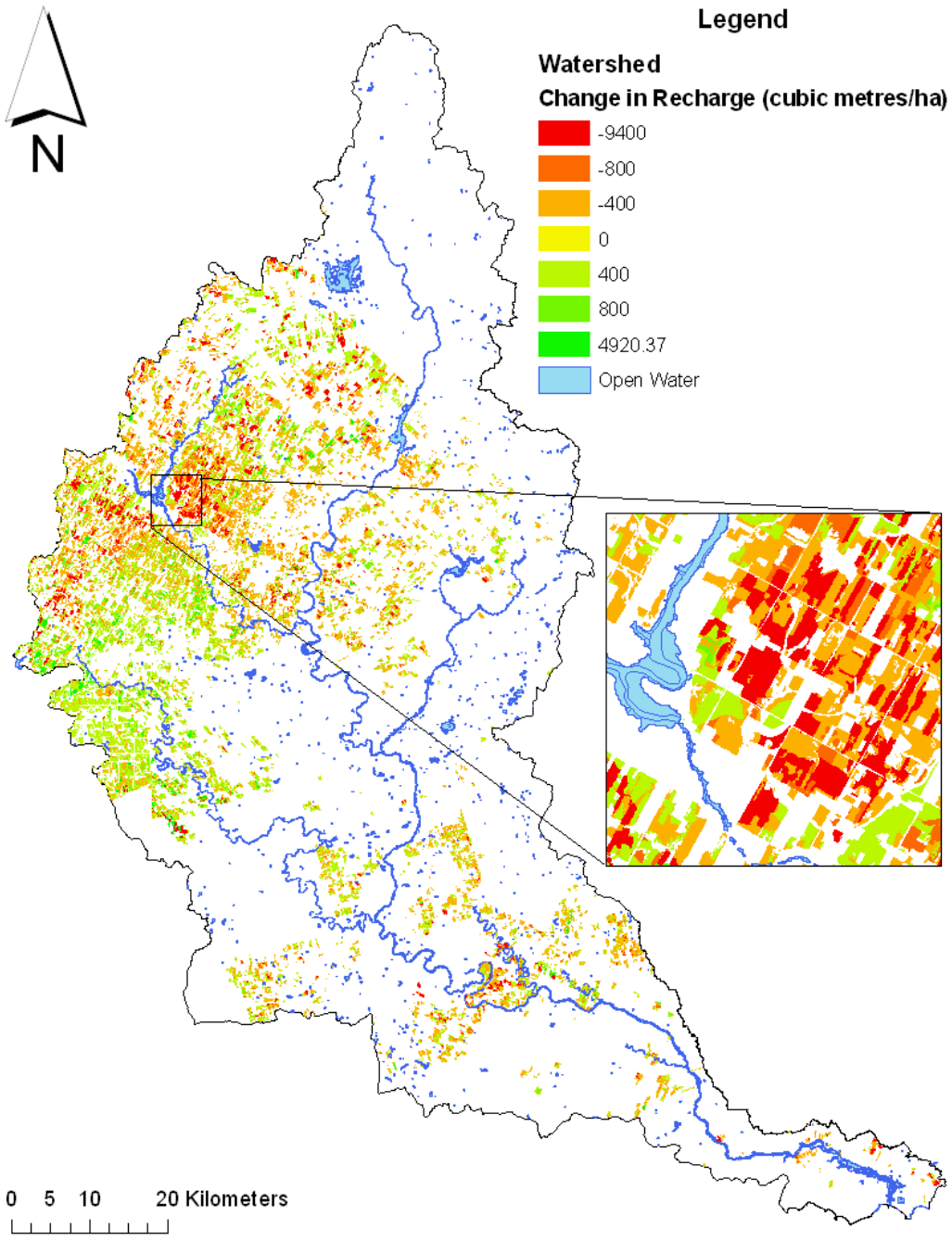

Figure 4.4: Change in recharge (m^3/ha) from un-tiled to tiled for the month of April 1999

water recharge when the tile drains are not modelled. The orange and red areas indicate less water moving into the subsurface as recharge when the tile drains are not modelled.

Figure 4.4 illustrates that there is more water entering the groundwater recharge zone when the tile drains are modelled. There is approximately 9,410 m^3 more water reaching the groundwater recharge zone in the month of April 1999 when the tile drains are present. At first it does not seem intuitive to have increased groundwater recharge when the tile drains are generally active. When the tile drains are not modelled the surface runoff and evapotranspiration for the month of April in 1999 are increased. If there is more evapotranspiration and surface runoff then there should be less water in the groundwater recharge. This can be explained by looking at the physical processes that are occurring. When the water melts from snow it will infiltrate into the subsurface, become surface runoff, or evaporate. As the subsurface becomes saturated, surface runoff should theoretically be increased. When the tile drains are modelled, more water can move into the subsurface because the tile drains are extracting water from the subsurface by providing an alternate route for the water. The water is moving vertically downward through the subsurface instead of across the surface. Figure 4.5 illustrates this trend in the GRW.

The green areas indicate more surface runoff when the tile drains are not modelled. The orange and red areas indicate less surface runoff when the tile drains are not modelled.

There was approximately 17,000 m^3 more surface runoff for the tiled areas in the GRW when the tile drains are not modelled. The trend is similar for the evapotranspiration and is discussed in section 4.1.5.

4.1.2 Effect on Annual Recharge

Not only is the drainage affected by the tile drains but the recharge that the cells generate will also change. Both scenarios were run for the areas where tile drains were present. The annual difference, for 1999, between the two scenarios was calculated and can be seen in Figure 4.6. The tiled areas were modelled without the tile drains to understand how the tile drains are affecting the local recharge, surface runoff, and evapotranspiration. The green areas show more

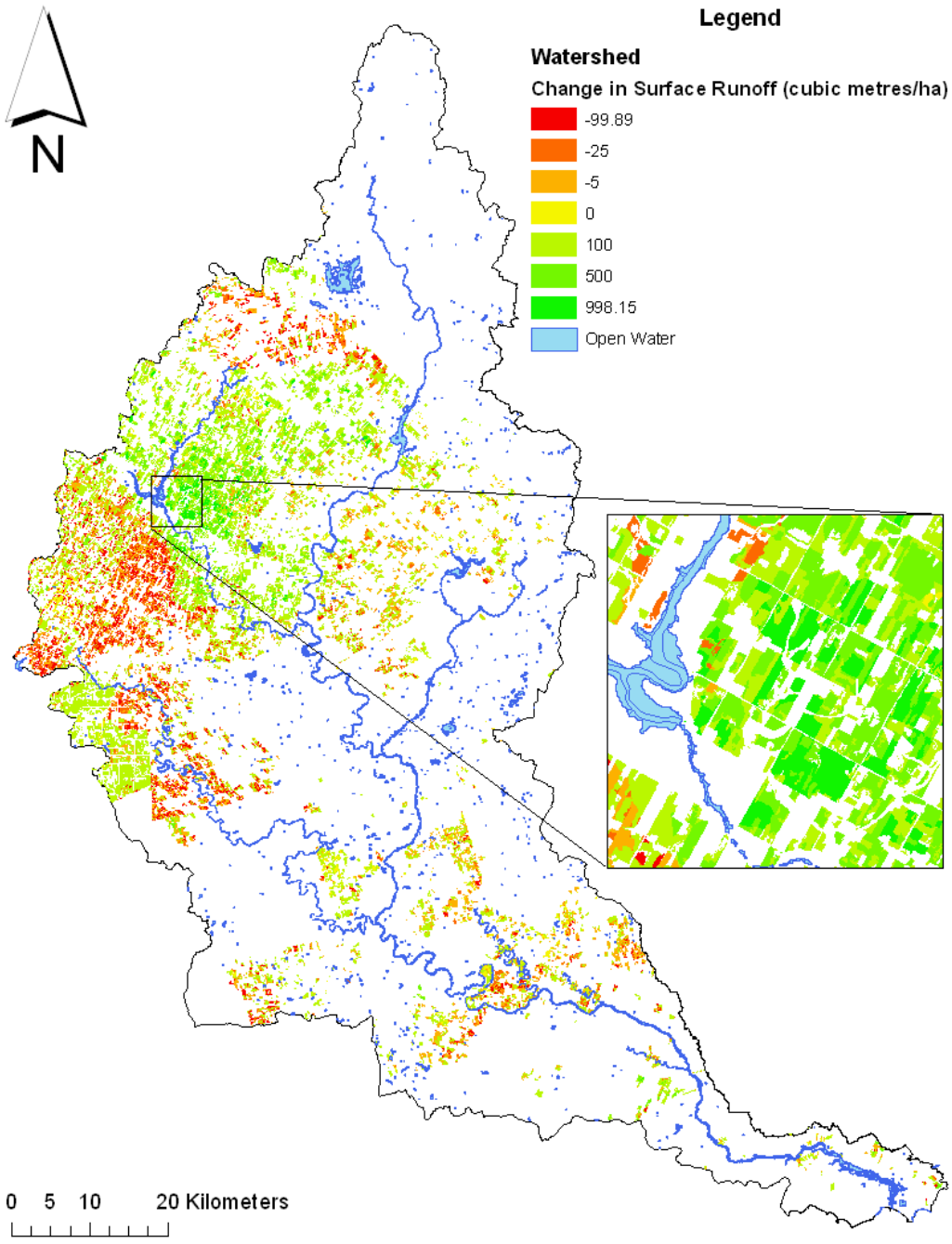

Figure 4.5: Change in surface runoff (m^3/ha) from un-tiled to tiled for the month of April in 1999

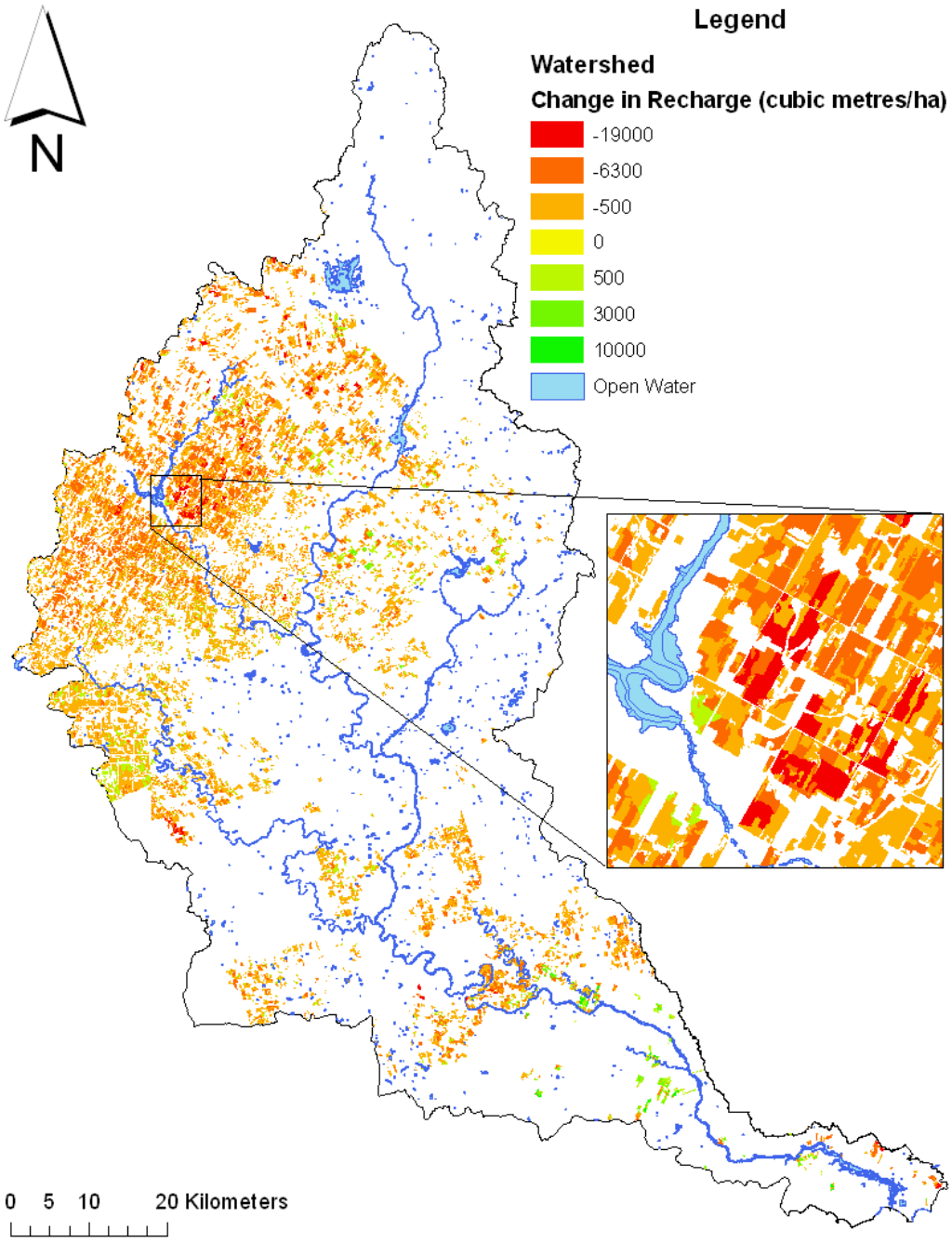

Figure 4.6: Annual change in recharge (m^3/ha) for 1999 with and without the tile drains

groundwater recharge when the tile drains are not included in the model. The orange and red areas indicate less water is reaching the groundwater recharge zone when the tile drains are not included in the model. For the analysis, areas were modelled with the same soil conditions and weather conditions with and without the tile drains. All of the tile drains were simulated at the same depth and the same slope. As seen in Figure 4.6, the tile drains are affecting the local recharge. When the tile drains are not simulated there is approximately 177,000,000 m^3 of water reaching the groundwater zone for the tiled cells in 1999. The total annual groundwater recharge (1999) for the tiled areas was calculated to be approximately 185,000,000 m^3 when the tile drains are included. The change in groundwater recharge when the tile drains are included in the simulation is approximately 7,500,000 m^3 for 1999. Figure 4.7 illustrates the recharge (mm/yr) when the tile drains are included in the model. The surface runoff distribution is similar however it has increased for

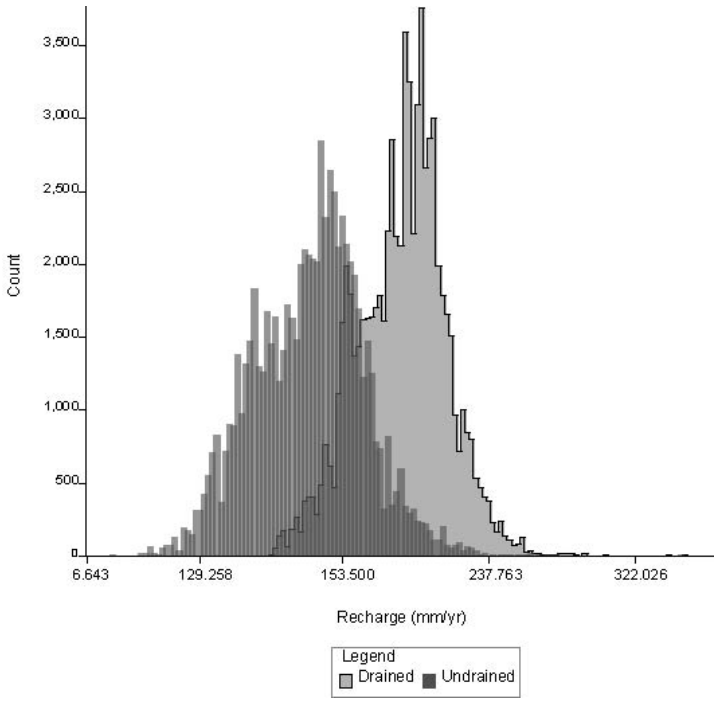

Figure 4.7: Annual groundwater recharge (mm/yr) for 1999 with and without the tile drains

the majority of the tiled cells. The darker grey indicates the recharge rates when the tile drains are not modelled whereas the lighter grey indicates the recharge rates when the tiles are simulated.

This increase in annual groundwater recharge when the tile drains are included in the model might be explained by increased volumes of water moving into the subsurface. The tile drains are removing water during the spring melt and in some case during the fall months. During the times when the tile drains are draining water from the subsurface, more water can move into the subsurface. If the tile drains do not capture the increased infiltration it will move into the groundwater recharge zone.

4.1.3 Effect on Surface Runoff in April

As seen in Section 4.1.1 the surface runoff in the month of April is impacted when the tile drains are included in the simulation. Figure 4.5 illustrates the overall increase in surface runoff when the tile drains are not modelled for the month of April 1999. When the spring melt starts in April there can be a lot of water stored as snow and ice that is lying on top of and just below the ground surface. As the melting process starts the snow and ice lying on top of the ground will find its way into the subsurface, as a liquid, if the ground is not frozen. This is not very likely to happen until later in the spring melt for the GRW. At the beginning of the melt it is more likely that the water will move overland as opposed to infiltration.

Once the subsurface is unfrozen and the subsurface becomes saturated, then this will also promote surface water runoff as opposed to infiltration. Along with an increased surface runoff when the tile drains are not modelled, there is potential for an increase in evapotranspiration because of the water being evaporated while in the shallow soils and on the surface of the ground.

4.1.4 Effect on Annual Surface Runoff

The surface runoff from the tile drained cells show an annual trend of decreasing when the tile drains are added to the model. The overall change in surface runoff for the year (1999) when the tile drains are added into the model was calculated to be approximately 3,060,000 m^3. Figure 4.8 shows the annual change in surface runoff for the tiled areas of the watershed for 1999. When the tile drains are modelled the water in the subsurface will be extracted and allow more water to infiltrate. When the tile drains are not installed the sur-

face soils become saturated quicker and more water will then move as surface runoff.

The green areas show where more water is being removed through surface runoff when the tile drains are not modelled. The red and orange areas show areas where there is less water being removed through surface runoff when the tile drains are not modelled.

Figure 4.9 illustrates the surface runoff (mm/yr) when the tile drains are included in the model. The surface runoff distribution is similar however it has increased for the majority of the tiled cells. The darker grey indicates the surface runoff rates when the tile drains are not modelled whereas the lighter grey indicates the surface runoff rates when the tiles are simulated.

4.1.5 Effect on Evapotranspiration in April

During the April spring melt, the suns rays begin to hit the surface for longer periods of time. Vegetation begins to grow and the snow and ice begin to melt in the GRW. As the vegetation starts to grow and the longer period of sunlight occurs, the evapotranspiration for the area will also increase. Examining the cases for the non-tiled and tiled scenarios shows that there is generally more evapotranspiration occurring in the month of April when the tile drains are not installed. There is a total of approximately 567,000 m^3 more water removed by evapotranspiration when the tile drains are not modelled for April 1999. Figure 4.10 illustrates this trend in the GRW for 1999.

The green areas indicate where the evapotranspiration is greater when the tiles are not modelled. The orange and red areas indicate where the evapotranspiration is less when the tile drains are not installed compared to when the tile drains are modelled.

This increase in evapotranspiration for April 1999 can be explained by more water infiltrating into the evaporative zone. Less water is moving away through surface runoff, which is described in Section 4.1.3. More water is infiltrating into the subsurface. Some of this water will then evaporate from shallow soils.

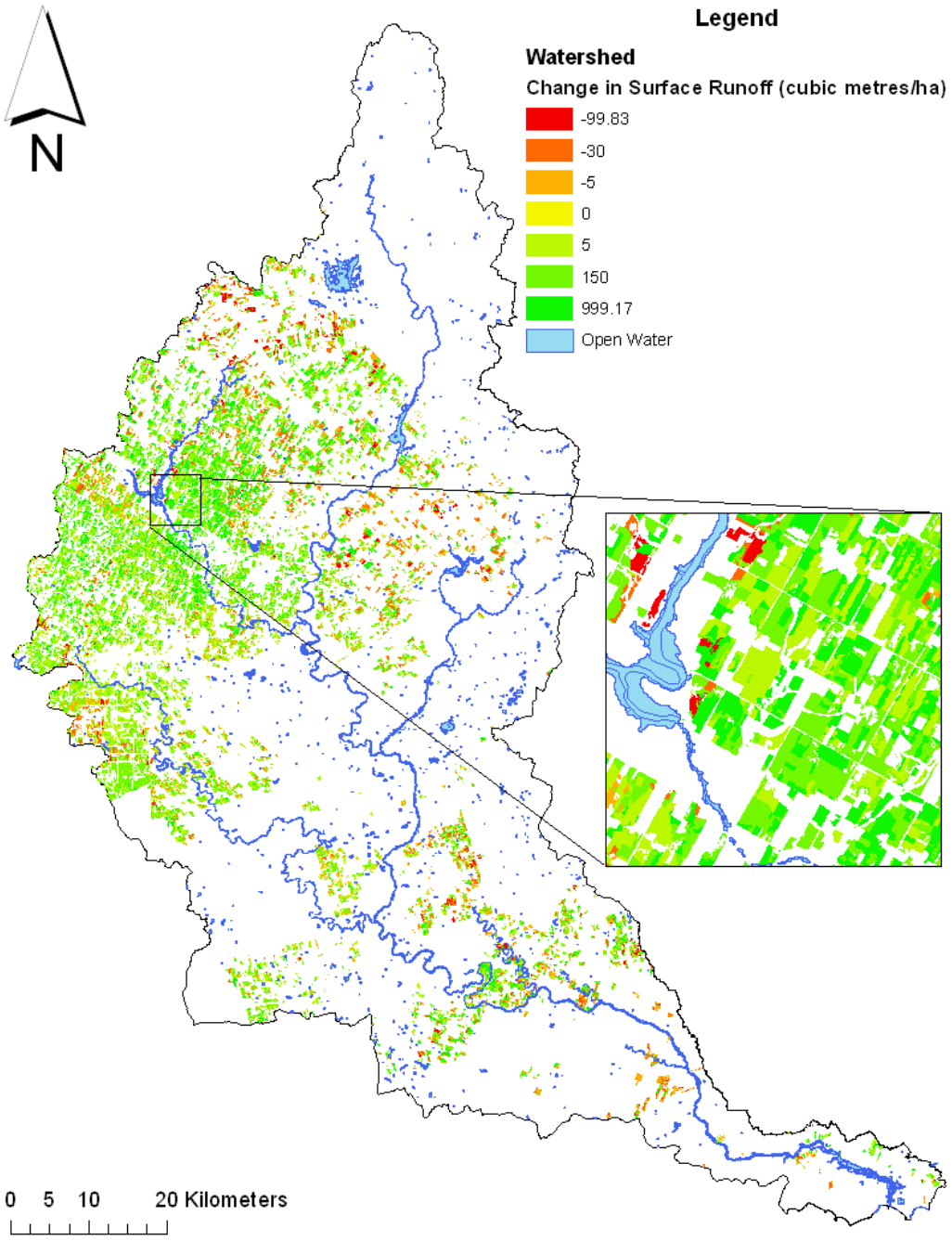

Figure 4.8: Annual change between the surface runoff (m^3/ha) with and without the tile drains modelled for 1999

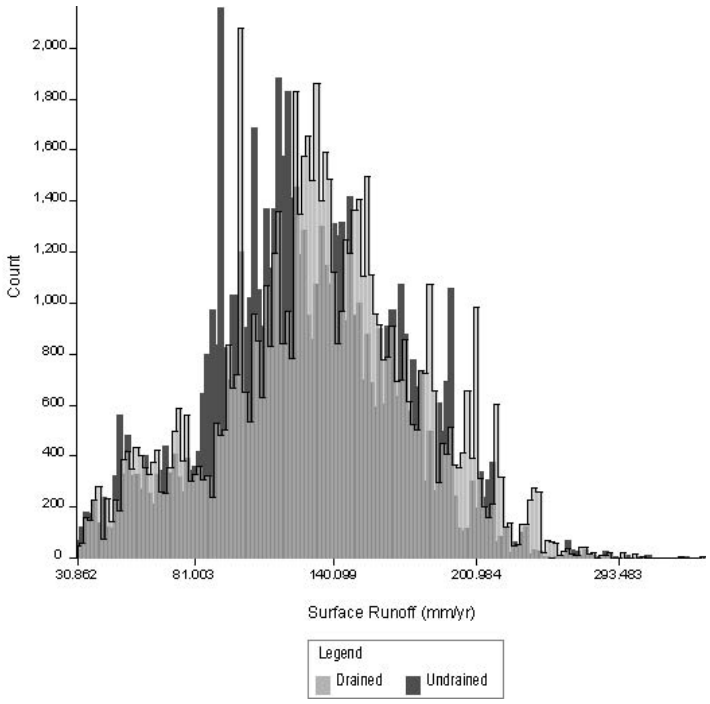

Figure 4.9: Annual surface runoff (mm/yr) for 1999 with and without the tile drains

4.1.6 Effect on Annual Evapotranspiration

The evapotranspiration for the tiled cells have a decreasing annual trend in the GRW when the tile drains are modelled. The decreased evapotranspiration was calculated to be removed between the scenarios was approximately 1,480,000 m^3. When the tile drains are modelled, the annual evapotranspiration decreases over the tiled cell areas. This could be due to more water moving into the evaporative zone in the subsurface. When the tile drains are installed there is more water moving into the subsurface and not moving away through surface runoff. The water will move slowly as it infiltrates into the subsurface and while it is still within the evaporative zone there is greater chance that the water will be removed through evapotranspiration. Figure 4.11 shows the change in evapotranspiration in (m^3/ha) of water between the non-tiled scenario and the tiled scenario for 1999.

The green areas show where more water is being removed through evapotranspiration from the watershed when the tile drains are not modelled. The red and orange areas show areas where there is less water being removed through evapotranspiration when the tile drains are not modelled.

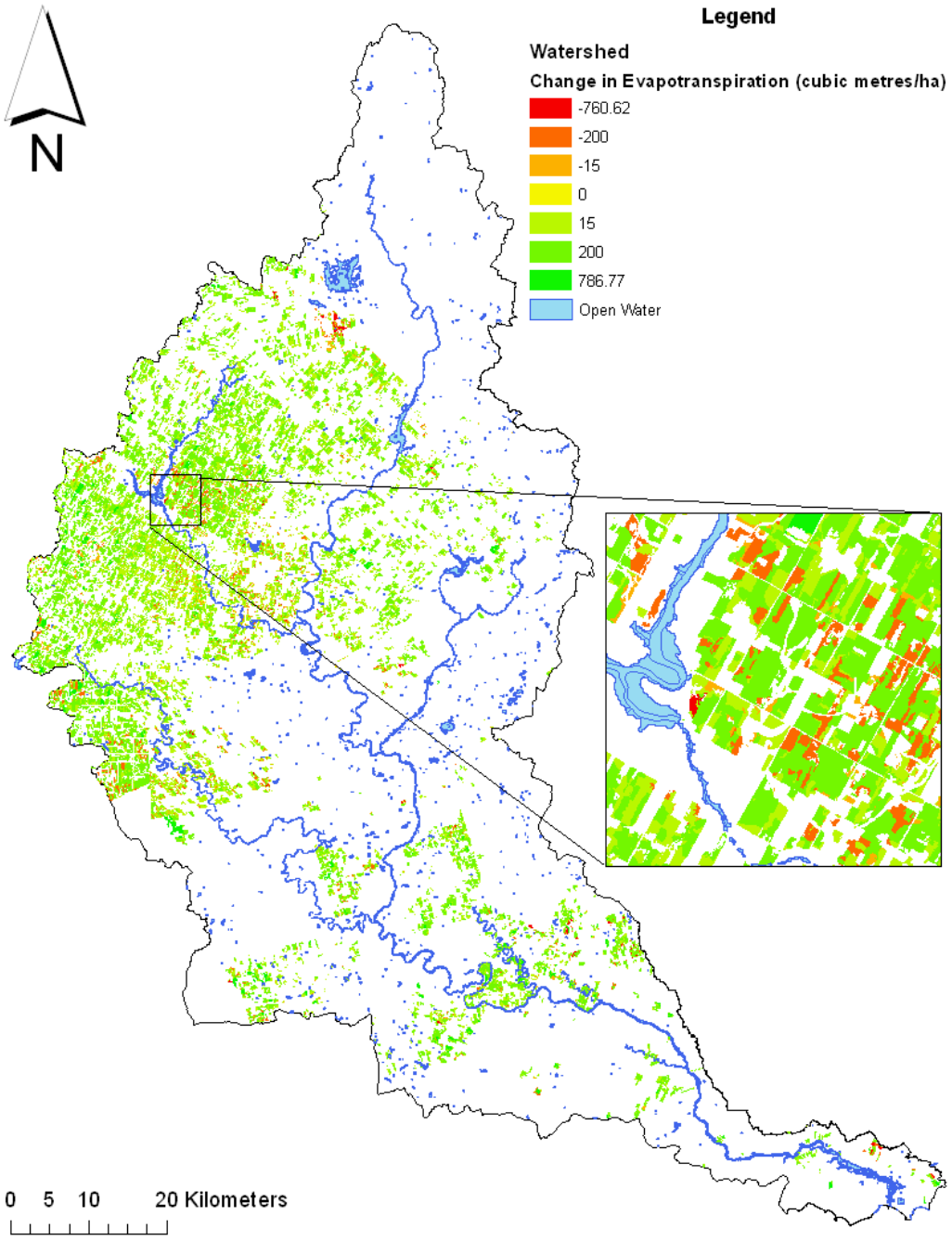

Figure 4.10: April change between the evapotranspiration (m^3/ha) with and without the tile drains modelled for 1999

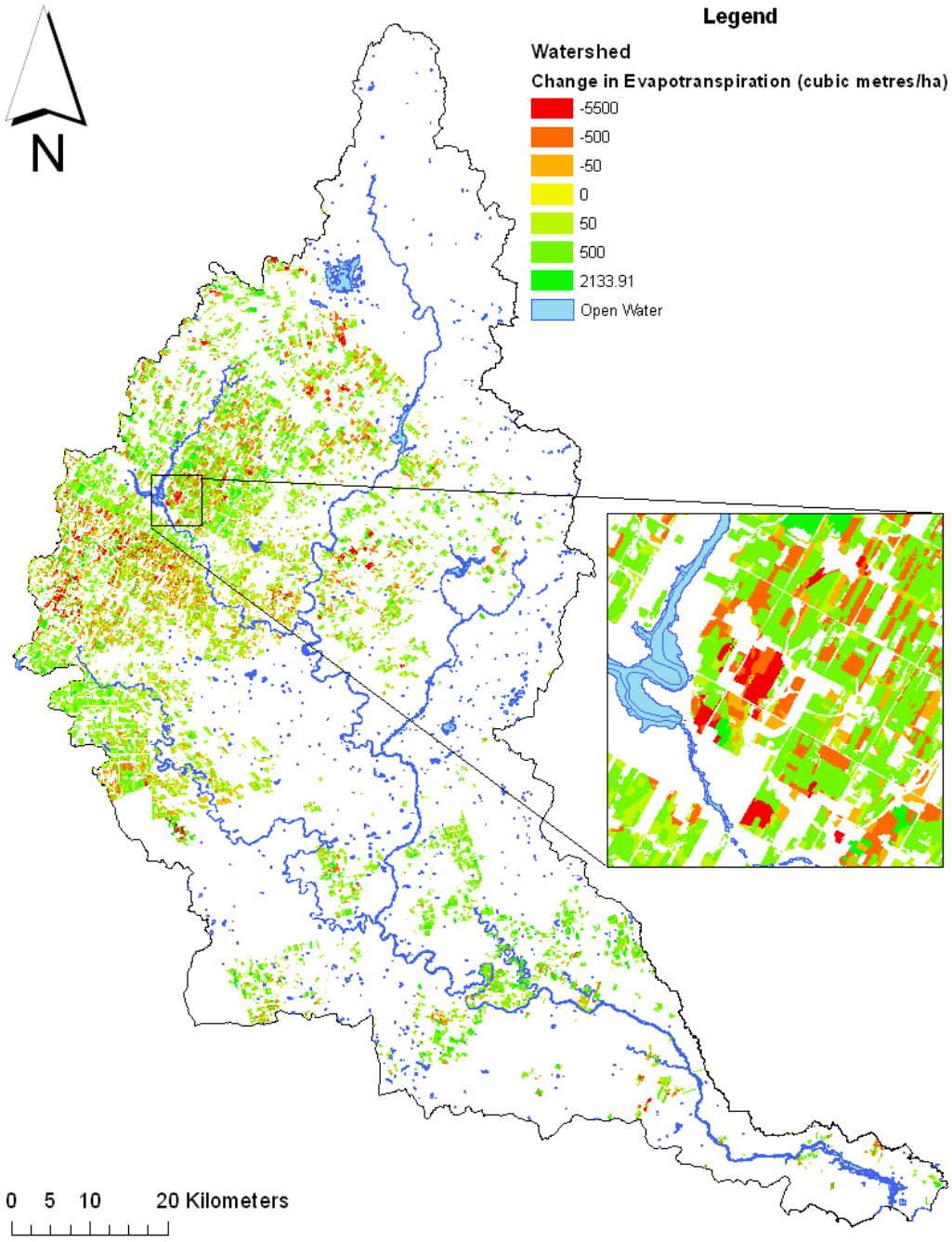

Figure 4.11: Annual change between the evapotranspiration (m^3/ha) with and without the tile drains modelled for 1999

Figure 4.12 illustrates the evapotranspiration (mm/yr) when the tile drains are included in the model. The evapotranspiration distribution is similar how-

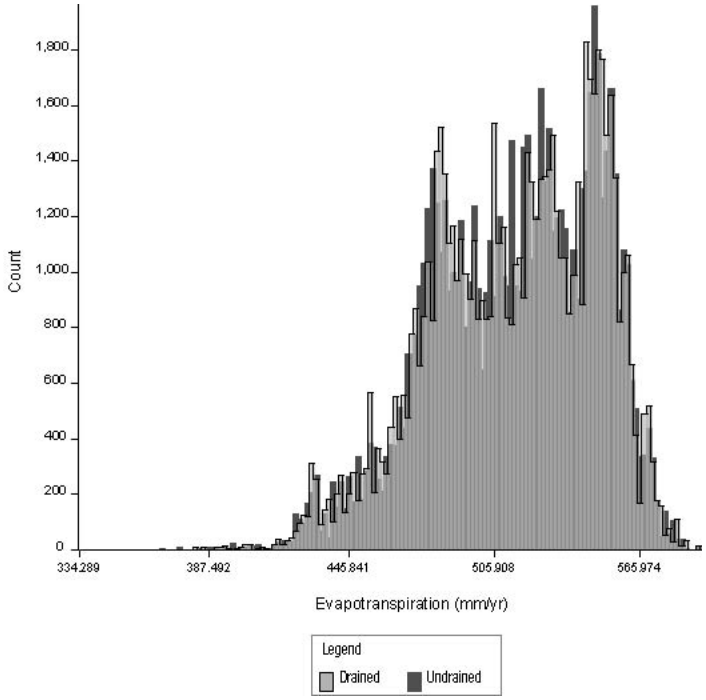

Figure 4.12: Annual evapotranspiration (mm/yr) for 1999 with and without the tile drains

ever it has slightly increased for the tiled cells. The darker grey indicates the evapotranspiration rates when the tile drains are not modelled whereas the lighter grey indicates the evapotranspiration rates when the tiles are simulated.

4.2 Cell Time Series Analysis

To understand what is occurring on an annual cycle, a time series analysis of two separate cells was conducted. The first cell is row crops located in sub basin 118 in Wellington County. The second cell is a forage area that consisted of a soil in sub basin 142 in Perth County. Row crops account for approximately 26%, by area, of the tiled cells and Forage accounts for approximately 29%, by area.

The main differences between the cells are in the properties of the surface soil. These differences in the soil properties are summarized below in table 4.1.

Cell 1 has a surface of loam where cell 2 has a surface of silty loam. The other major difference in the cells is type of vegetation cover. The vegetation will help prevent soil erosion as well as have an increased evaporative zone where the plants can extract water from the subsurface.

Table 4.1: Soil Properties

Silty Loam	Parameter	Loam
0.5010	Porosity (vol/vol)	0.4630
0.2840	Field Capacity (vol/vol)	0.2320
0.1350	Wilting Point (vol/vol)	0.1160
$0.1900*10^{-3}$	Effective Sat. Hyd. Cond. (cm/sec)	$0.3699*10^{-3}$

The HELP3 results from the cells were analyzed for a monthly basis. The monthly totals for precipitation, recharge, and drainage for three successive years were plotted. The time series analysis produced a three year time line showing the precipitation (m^3/ha), recharge (m^3/ha), and the drainage (m^3/ha) from the cell. Figures 4.13 and 4.14 illustrate the three year time line for the selected cells.

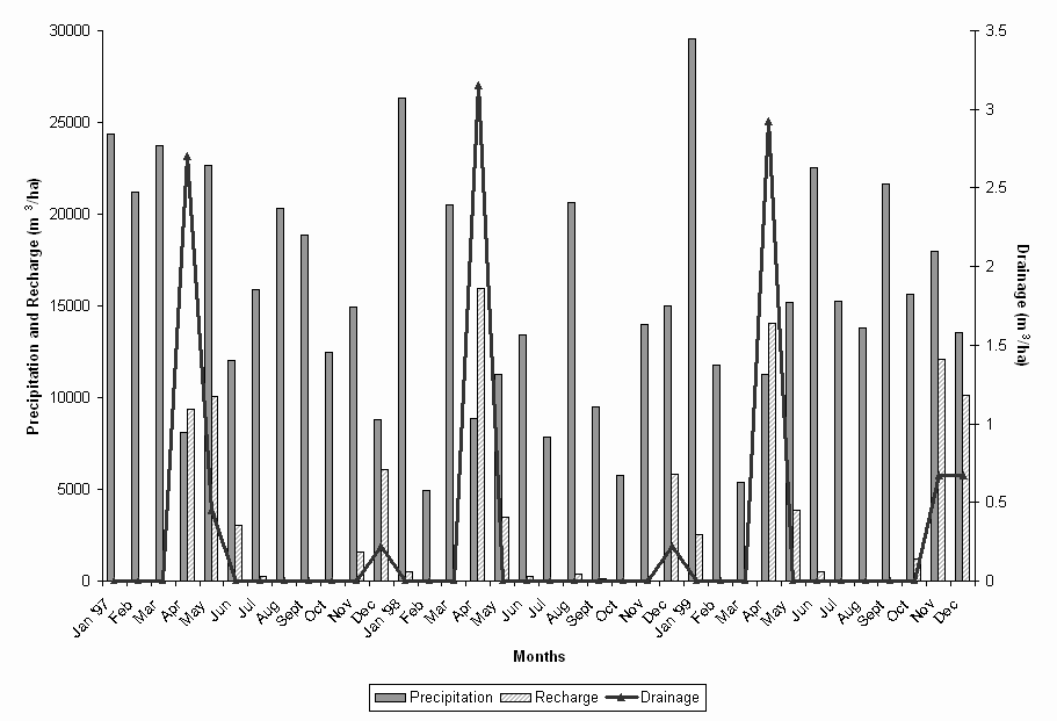

Figure 4.13: Cell 1 (row crops) three year time line analysis

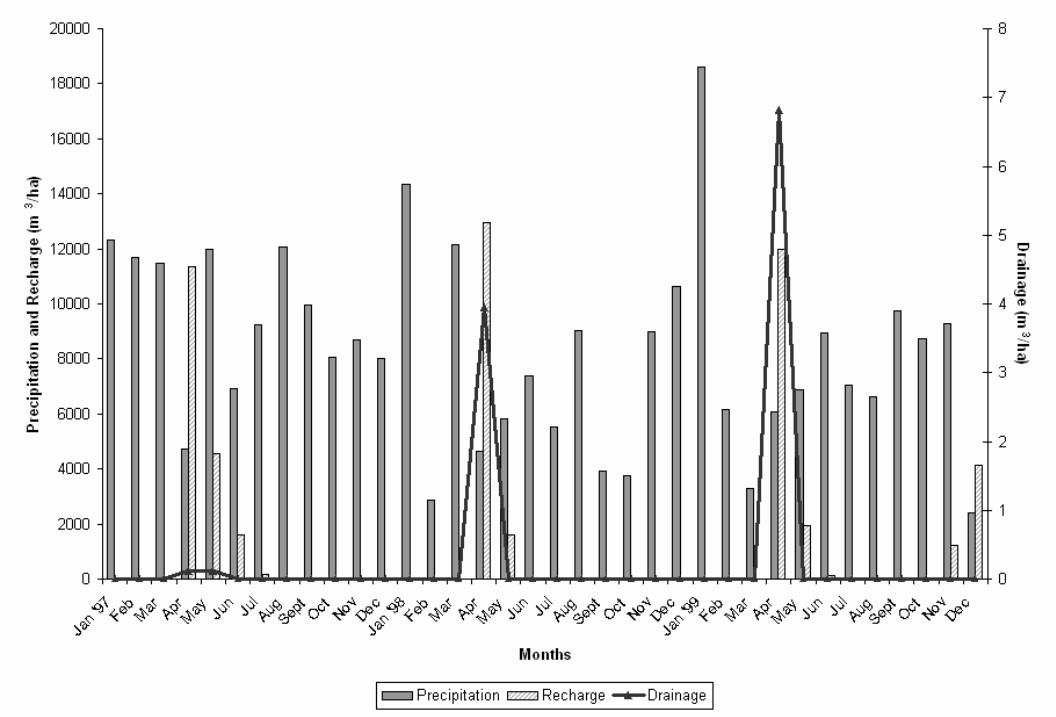

Figure 4.14: Cell 2 (forage) three year time line analysis

Both time lines show the precipitation that the cell is receiving as well as the groundwater recharge predicted for each month. The final information that is presented with Figures 4.13 and 4.14 is the drainage that tiles are extracting from the subsurface per month for the three year period. The drainage scale is on the right side of the figures and the precipitation and recharge scales are located on the left side.

It should be noted that the drainage values are reported on a monthly basis. The lines connecting the points are plotted to show a theoretical trend for the drainage between points.

To understand how the tile drains are working over the entire 40 year simulation, the drainage (m^3/ha) was plotted versus time. Figure 4.15 illustrates the drainage for the tile drains in cell 1 over the entire 40 year simulation period. Figure 4.15 shows the times when the tile drains are active and when they are not draining for cell 1. The tile drains are mainly effective during the spring melt in the months of April and May and then will drain again during the fall months of October and November with some drainage occurring into December before the ground becomes frozen again. Over the 40 year period for

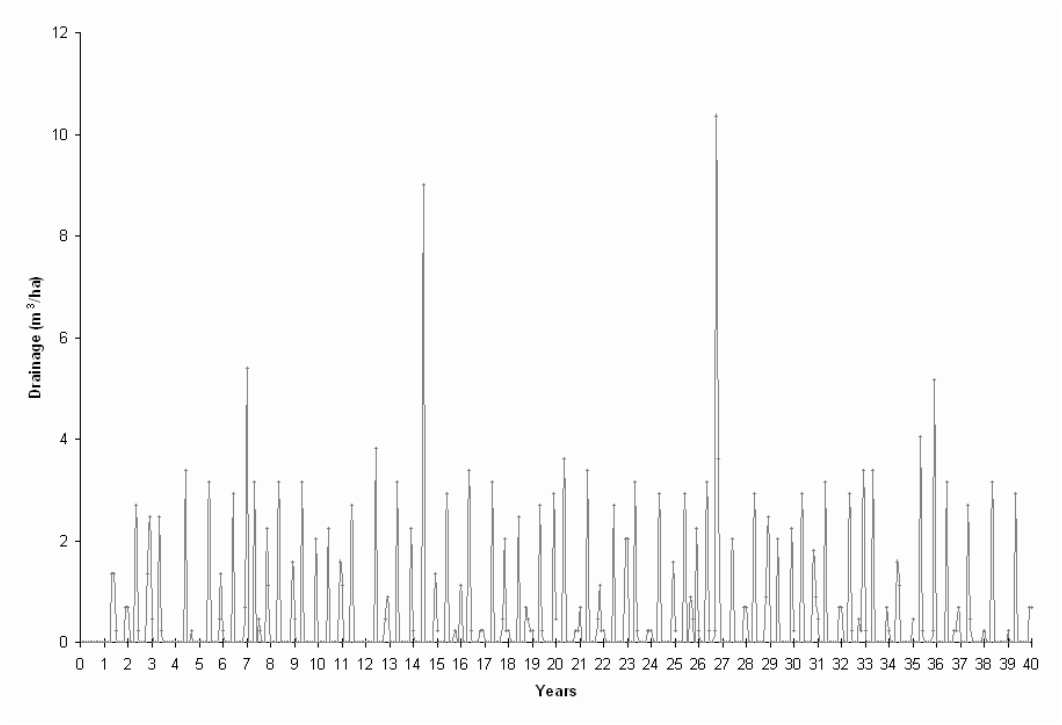

Figure 4.15: Cell 1 drainage (m^3/ha) time line for the 40 year simulation

cell 1, April saw the most drainage at approximately 76.3 m^3/ha followed by May, November, and December with 48.2 m^3/ha, 43.6 m^3/ha, and 18.5 m^3/ha respectively.

The increased activity in the fall months can be attributed to large storm systems that originate out on the Atlantic ocean. As these massive storm systems reach tropical storm and hurricane levels they first impact the southern United States. As the storm system moves northward it dissipates in strength. By the time the storm system reaches the GRW the storm still has enough water to cause very wet conditions. These storms are likely to increase in intensity and frequency as discussed in section 2.9.1.

Macrae et al. (2007) did observe that peak discharge times occurred during April during the spring melt and again in the fall. The same trend was also observed in the results from the simulations for the tiled cells.

For cell 2, the same analysis was carried out to observe how a different surface soil, LULC conditions and slightly different meteorological conditions would impact the drainage over the same 40 year period. Figure 4.16 illustrates the drainage trend for cell 2.

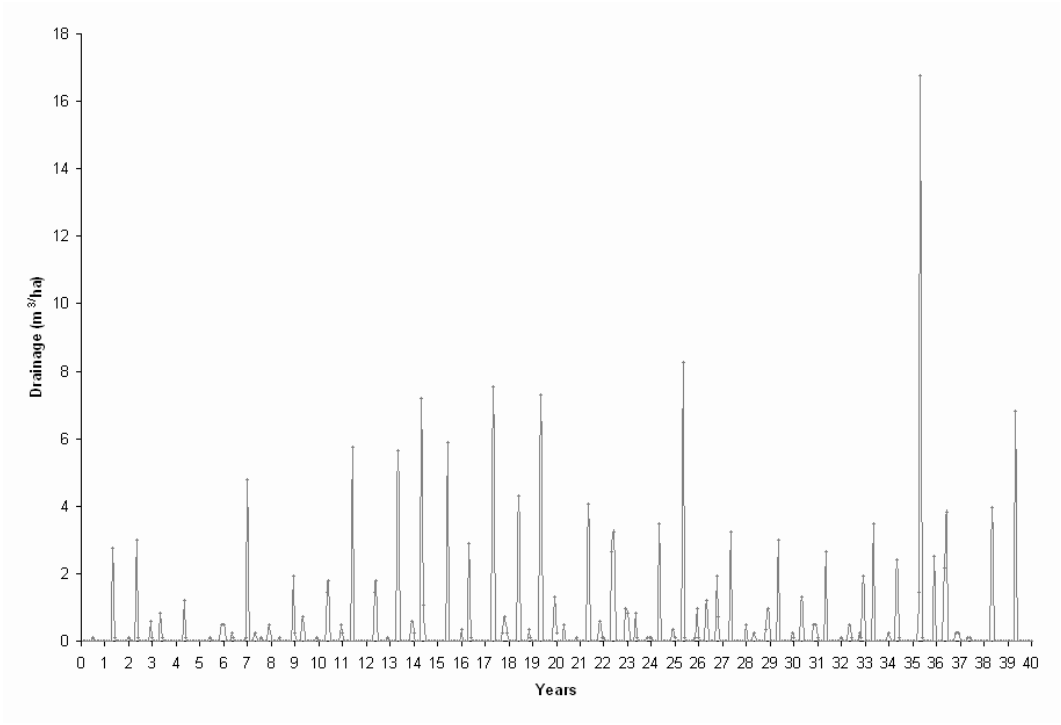

Figure 4.16: Cell 2 drainage (m^3/ha) time line for the 40 year simulation

Figure 4.16 shows the times when the tile drains are active and when they are not draining for cell 2. The tile drains are mainly effective during the spring melt in the months of April and May and then will drain again during the wetter fall months of October and November with some drainage occurring into December before the ground becomes frozen. Over the 40 year period for cell 2, April saw the most drainage at approximately 110 m^3/ha followed by May, November, and December with 29.2 m^3/ha, 15.5 m^3/ha, and 9.22 m^3/ha, respectively.

To examine the detail of when the tile drains operate the drainage and precipitation, both in m^3/ha, were plotted. Figure 4.17 illustrates the daily precipitation values along the top of the Figure, with the y-axis on the left increasing downwards. Drainage along the bottom with the y-axis on the right increasing upwards. Figure 4.17 represents the daily values simulated by HELP3 for 1999 of cell 1.

As seen in Figure 4.17 the main times when the tile drains are active are the months of April, May, September, October, and November with some drainage occurring in December and early January. These are seen as the

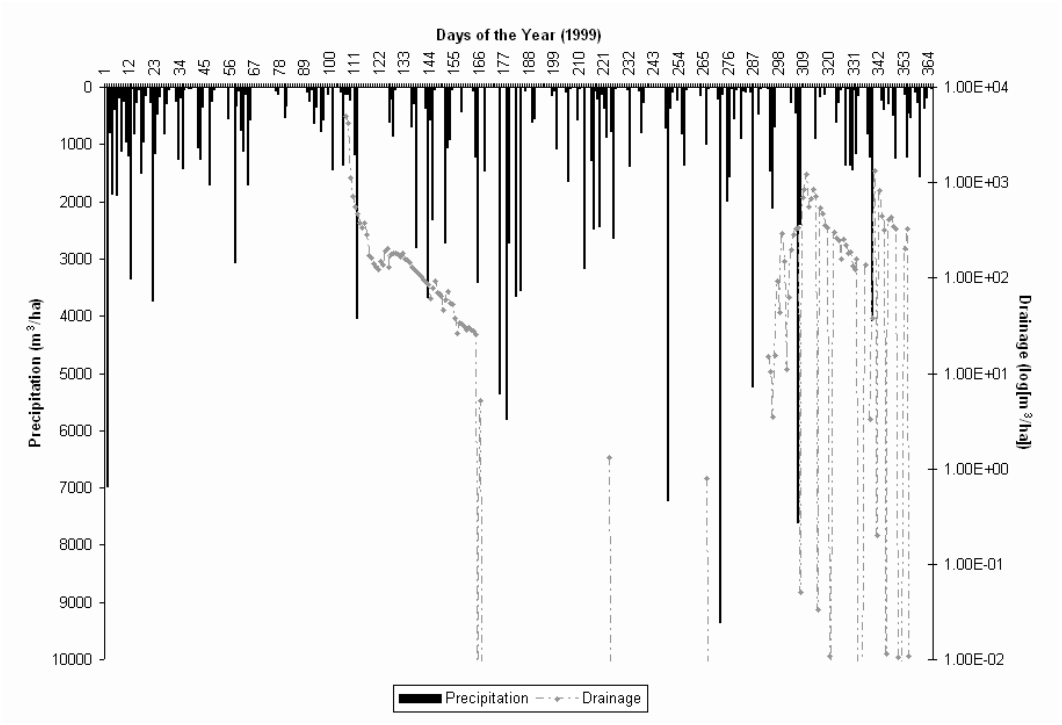

Figure 4.17: Cell 1 (row crops) drainage (m^3/ha) time line for 1999

spikes in drainage time line. For the rest of the year, cell 1 does not have much activity associated with drainage. This is a general trend for most cells in the GRW. The drainage is scaled on a log scale to show there is some drainage occurring in the later months and to observe that the drainage has a lag after the initial precipitation event.

4.3 Climate Change

Climate change scenarios were simulated using the recharge model. The climate change scenarios indicate an annual increase in overall temperature as well as precipitation for the GRW. The climate change scenarios are expected to have an impact on the tile drainage, recharge, surface runoff, and evapotranspiration for the tiled cells. As seen in *Jyrkama and Sykes* (2007), climate change can impact the hydrological processes of the GRW.

The climate change scenarios are reported as a forecast for 2039 because the climate change scenarios were simulated as if the they would instantly begin after 1999. All three scenarios A2, A1B, and B1 produced increased

precipitation as well as higher temperatures each successive year. The initial estimates for the A2 scenario indicate a 17% increase in temperature and precipitation from the A1B scenario. Initial estimates for the B1 scenario indicate an approximate 31% decrease in temperature and precipitation from the A1B scenario. Figure 4.18 shows the increase in precipitation for the final year of the A2 scenario that was simulated compared to the final year (1999) of the original base-case. Figures 4.19 and 4.20 show the precipitation increases from the 1999 base-case scenario for the A1B and B1 scenarios respectively. The A2 scenario has the largest increases in precipitation followed by the A1B, and the B1 scenarios. This is expected and follows the projected scenario increases. The specifics of each scenario and how they will be modelled are presented in section 2.9.1.

4.3.1 Effect on Tile Drains

The A2 scenario had an impact on the tile drainage. Some areas saw a decrease in annual drainage while some areas saw a substantial increase in water extracted. The results from the A2 climate change scenario can be examined in Figure 4.21. The results of this comparison are the A2 scenario to the original tiled results from the 1999 simulation. The change in the amount of water discharged ranges from approximately -17 m^3/ha to 33.44 m^3/ha. More water reaching the tile drains is expected because there is more precipitation falling in the area. The annual average amount of water that was extracted from the tile drains was approximately 0.023 m^3/ha per year and a total net gain of approximately 1,640 m^3.

For the A1B and the B1 scenarios the annual results from the climate change scenarios were compared to the 1999 base-case annual results. The A1B scenario ranged from -18 m^3/ha to 9.00 m^3/ha for the volume of water that changed in the tile drains. The B1 scenario ranged from -18 m^3/ha to 7.95 m^3/ha for the change in water in the tile drains. The tile drains averaged +0.021 m^3/ha (A1B) and -0.022 m^3/ha (B1) when compared to the 1999 base-case annually. The total change in annual volume of water collected by the tile drains was calculated to be approximately +1,491m^3 and -1,615m^3 for the A1B and the B1 scenarios respectively. Figures 4.22 and 4.23 illustrate the change in volume extracted by the tile drains.

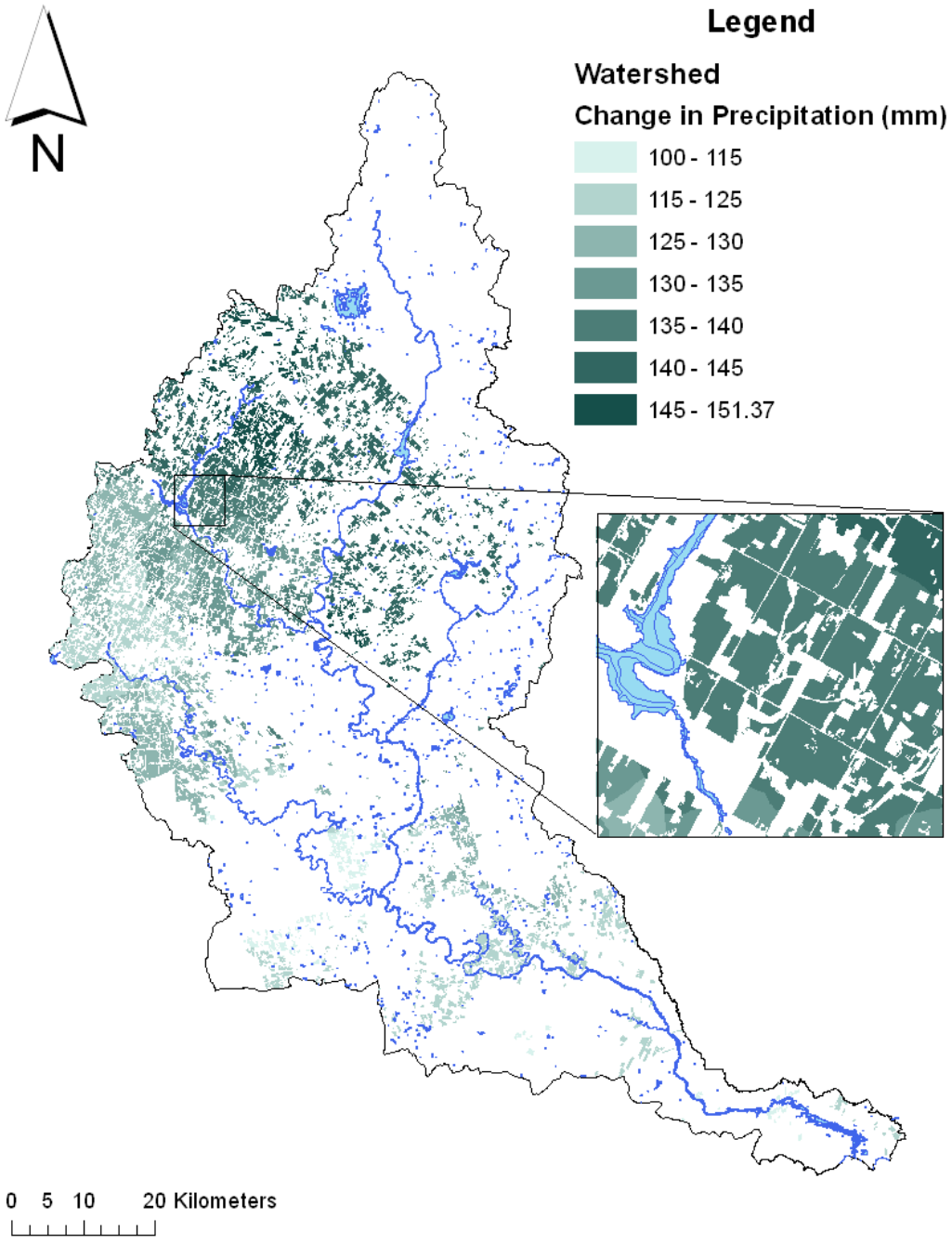

Figure 4.18: Tiled cells annual change in precipitation (mm) for the A2 scenario

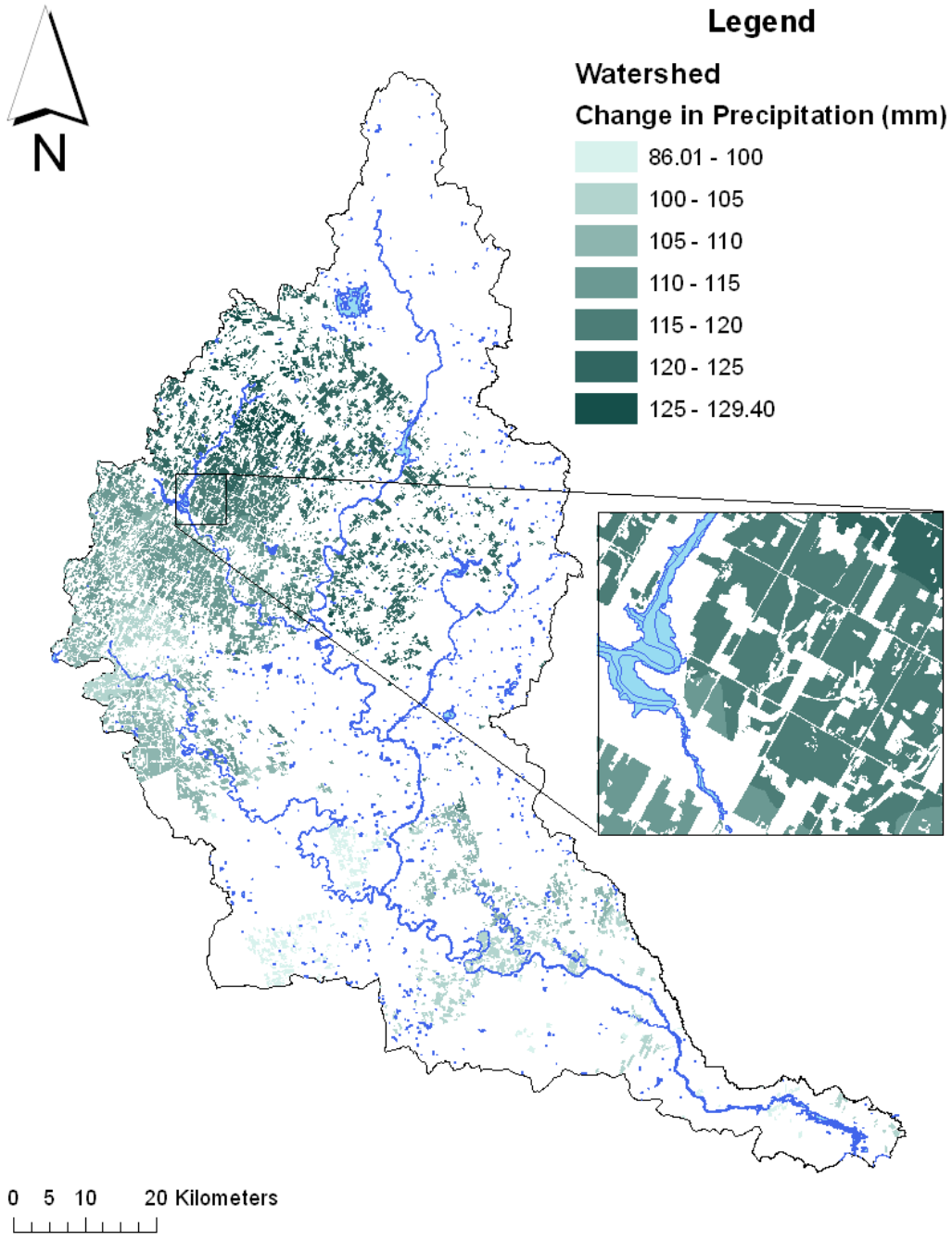

Figure 4.19: Tiled cells annual change in precipitation (mm) for the A1B scenario

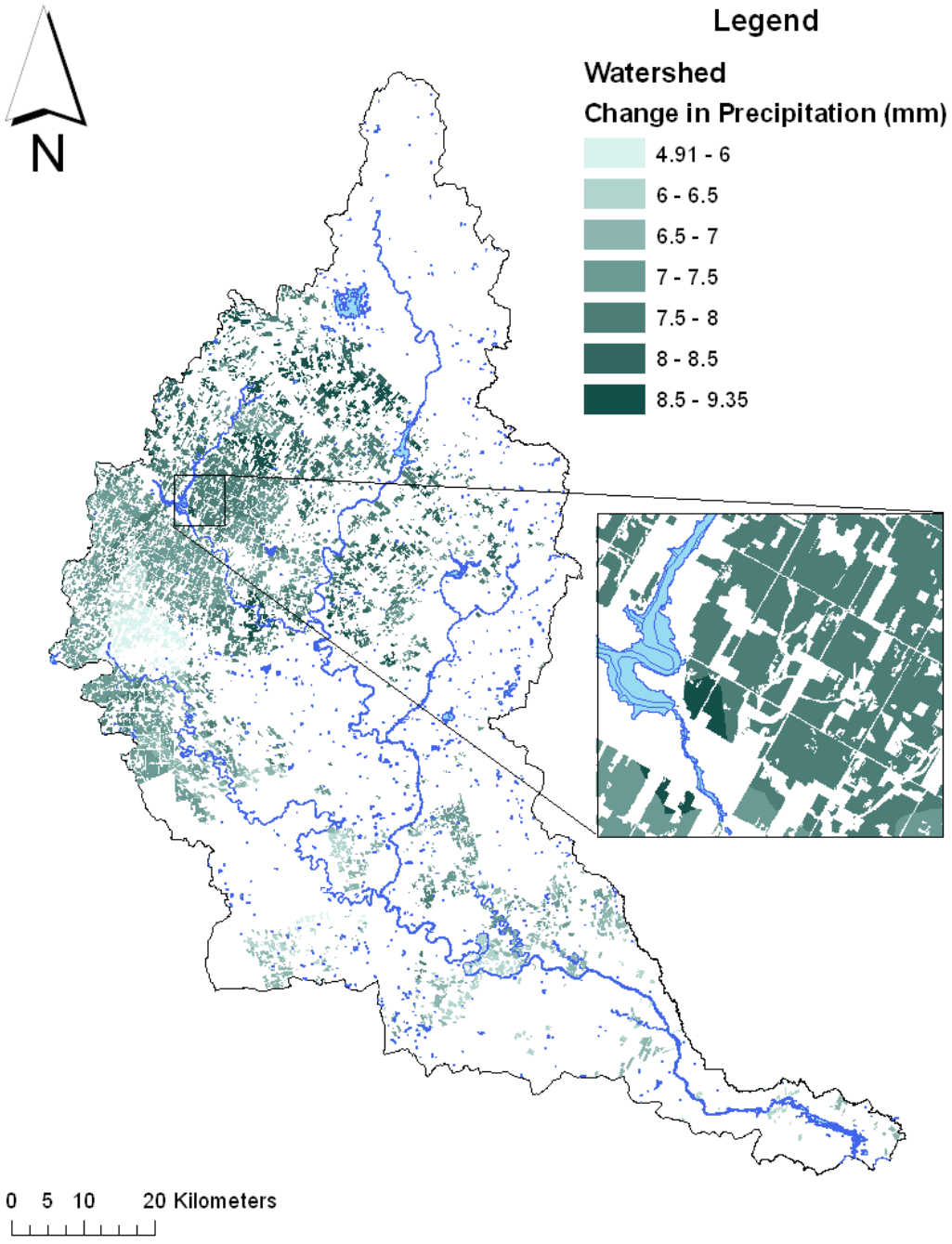

Figure 4.20: Tiled cells annual change in precipitation (mm) for the B1 scenario

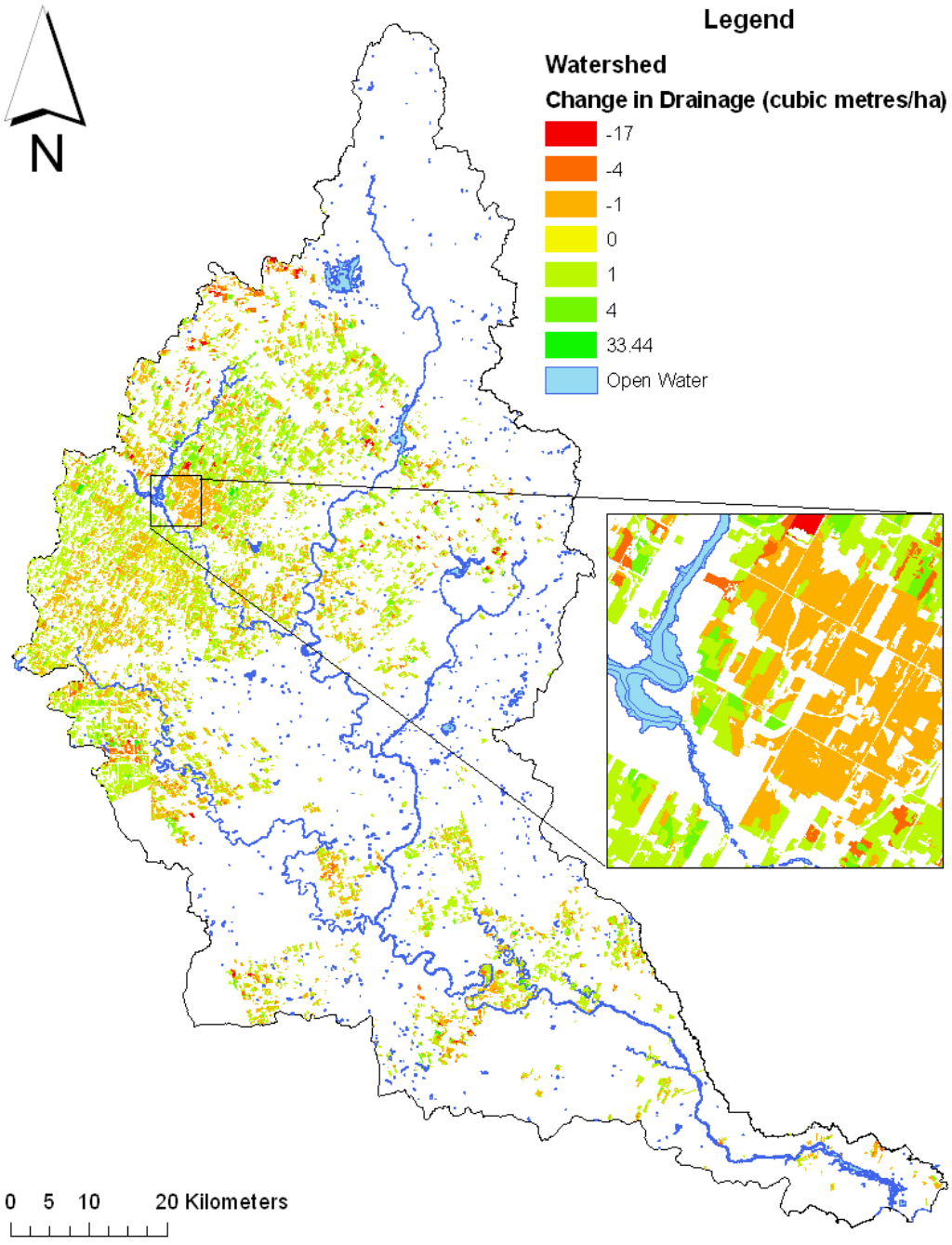

Figure 4.21: Annual change in drainage (m^3/ha) for the A2 scenario

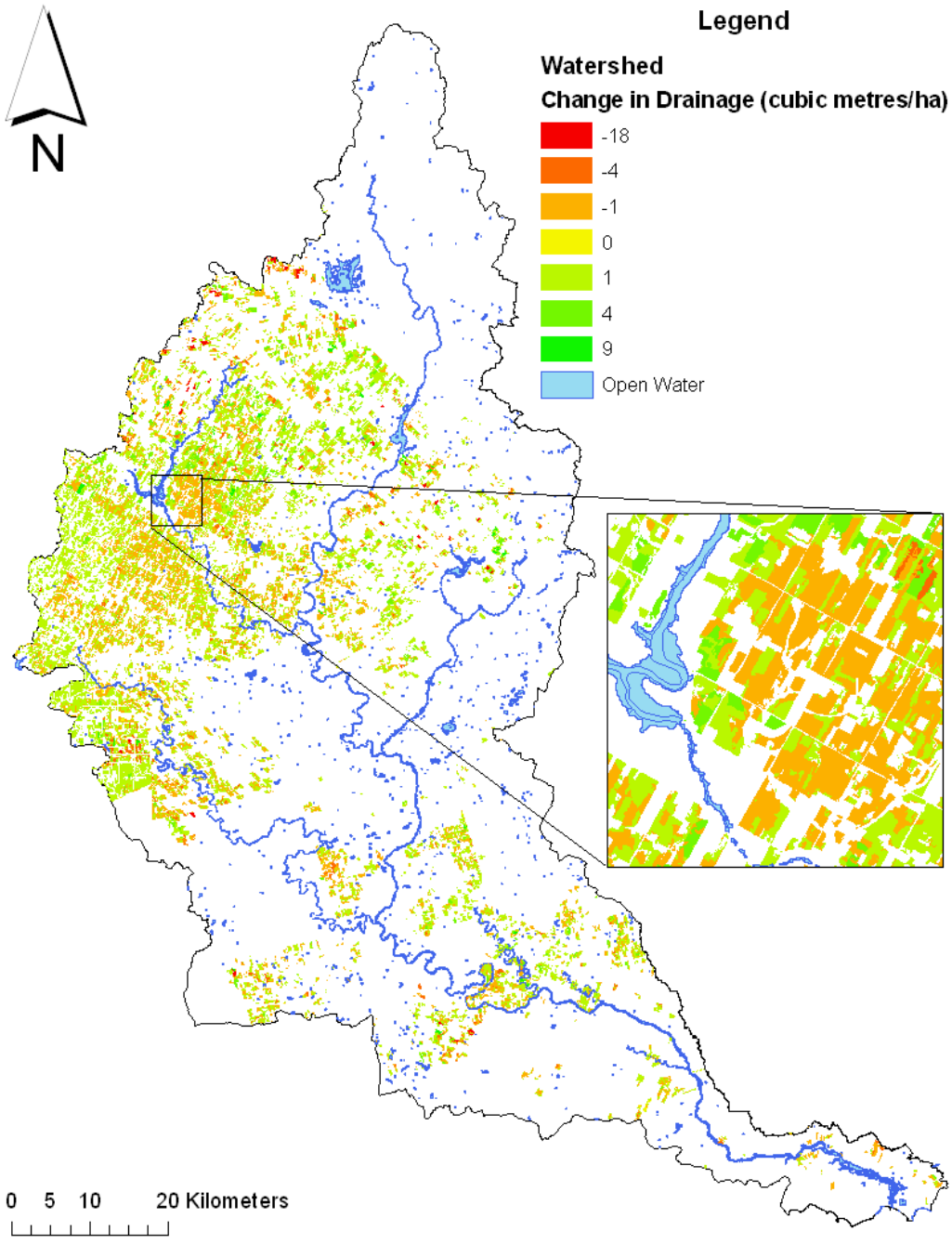

Figure 4.22: Annual change in drainage (m^3/ha) for the A1B scenario

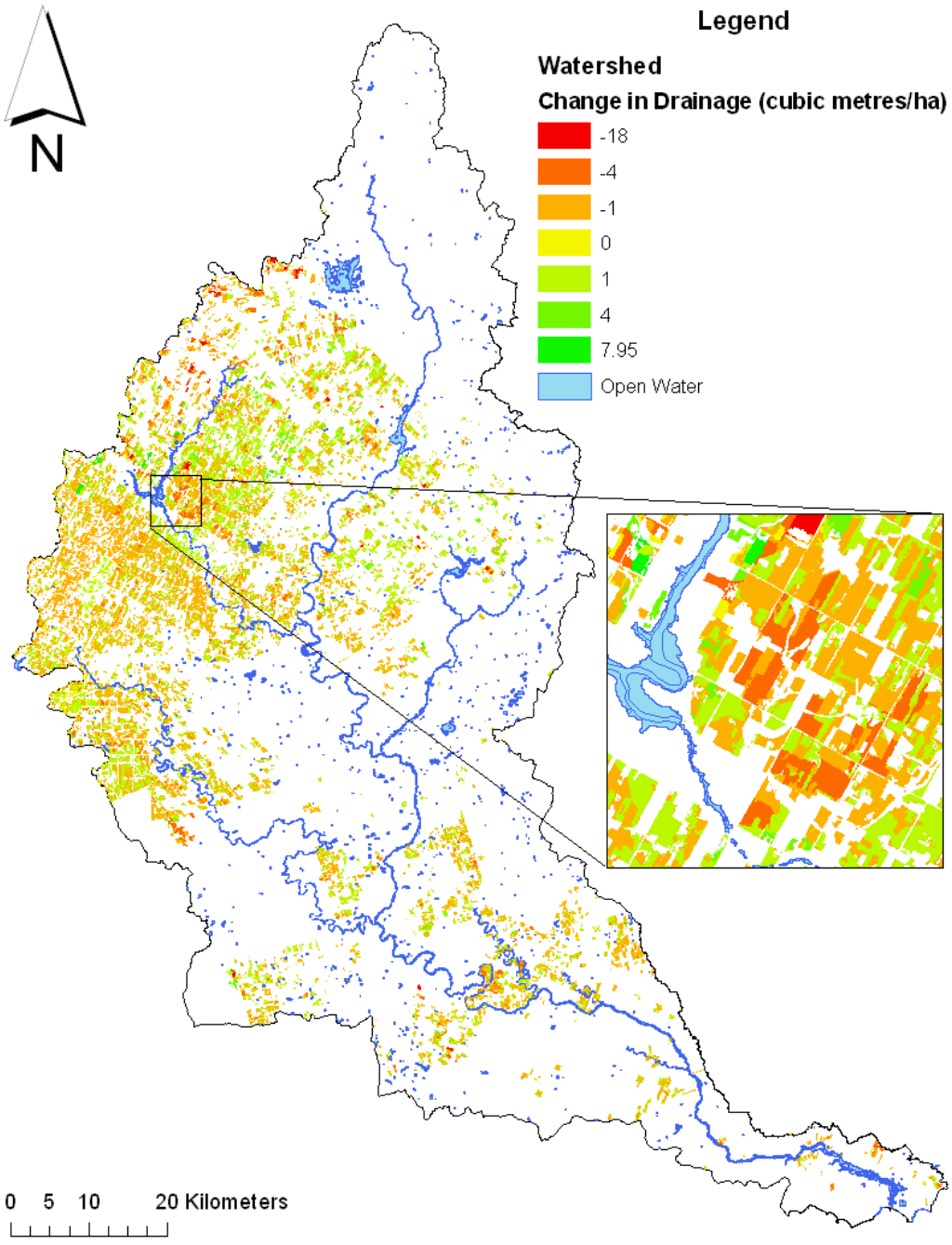

Figure 4.23: Annual change in drainage (m^3/ha) for the B1 scenario

The amount of water that is being discharged annually from the tile drains with respect to the annual precipitation for the base-case in 1999 was approximately on average 0.028% per cell with a maximum of 2.7% per cell. When the climate change scenarios were modelled the amount of water that was discharged by the tile drains was approximately on average 0.026% per cell with a maximum of 3.9% per cell, annually for the A2 scenario. The A1B scenario discharged an approximate annual average of 0.026% per cell, of the precipitation with an approximate maximum of 1.9% per cell. The B1 scenario had approximately an annual average 0.025% per cell, discharged by the tile drains with an approximate maximum of 1.7% per cell.

The increase in annual average percentage of water is consistent with the fact that there is more precipitation in the watershed. The maximum annual drainage for the A2 scenario is slightly more then the 1999 base-case scenario due to the increased precipitation that is projected to fall on the watershed. The annual volume of water was calculated to be approximately 17,700 m^3, 17,600 m^3, and 14,400 m^3 annually for the A2, A1B, and B1 scenarios, respectively. The base-case scenario total volume of water was calculated to be approximately 16,10 $0m^3$. The comparison shows that the annual tile drainage in the watershed has the potential to increase or decrease due to changes in the environmental conditions.

4.3.2 Effect on Recharge

The climate change scenarios also had an impact on the recharge in the tile drained cells. The results from the A2 scenario can be observed in Figure 4.24. The results from the A2 climate change scenario on the groundwater recharge (recharge) indicate that there are some areas where less water is going to recharge. However, there are many areas where it has increased.

The increase in recharge is expected because of the increased precipitation that is predicted by the A2 climate change scenario. The recharge ranged from -8,800 m^3/ha to 18,000 m^3/ha for the tiled cells under the A2 scenario. The average annual change in recharge was calculated to be approximately 253 m^3/ha for the tiled cells. This net increase in recharge was calculated to be approximately 18,300,000 m^3 in the final year for the A2 scenario. The same analysis was performed on the A1B and B1 scenarios. The recharge ranged

from -10,000 m^3/ha to 16,000 m^3/ha and -19,000 m^3/ha to 4,160 m^3/ha for the A1B and the B1 scenarios, respectively. The average annual recharge increase was calculated to be approximately 196 m^3/ha for the A1B scenario. The total annual increase in water entering the water through recharge was calculated to be approximately 14,200,000 m^3 in the final year of the A1B scenario. The average annual decrease for the B1 scenario was calculated to be approximately 114 m^3/ha. The total annual decrease of recharge was calculated to be approximately 8,230,000 m^3 in the final year of the B1 scenario. Figures 4.24, 4.25, and 4.26 illustrate the change in recharge under their respective climate change scenarios.

On average, approximately 22% of the annual precipitation reaches the recharge zone in 1999 for the base-case scenario in the tiled areas. A maximum of approximately 45% of the annual precipitation was groundwater recharge. When the climate change scenarios were introduced and simulated on the same areas approximately 21% of the annual precipitation was groundwater recharge for all of the climate change scenarios. The approximate maximum percentage of precipitation reaching the recharge zone was 45%, 45.1%, and 44.8% for the A2, A1B, and B1 scenarios. All three scenarios indicate less percentage of the precipitation becoming recharge.

Although there is slightly less percentage of the annual precipitation becoming recharge, there is a greater volume of water reaching this zone. With all three climate change scenarios there is an annual increase in precipitation for the GRW. Figures 4.18, 4.19, and 4.20 illustrate this trend.

4.3.3 Effect on Surface Runoff

The A2 climate change scenario impacted the surface runoff for the tiled cells of the watershed. The change in surface runoff from the A2 scenario, when compared to 1999 for the base-case scenario, ranged from approximately 0 m^3/ha to 1,000 m^3/ha. The average annual increase over the original scenario was calculated to be approximately 166 m^3/ha. The total annual surface runoff water increase in the tiled areas was calculated to be approximately 12,000,000 m^3 for the A2 scenario. Figure 4.27 shows the change in the annual surface runoff predicted by the A2 climate change scenario.

The surface runoff in the GRW was also impacted by the A1B and B1

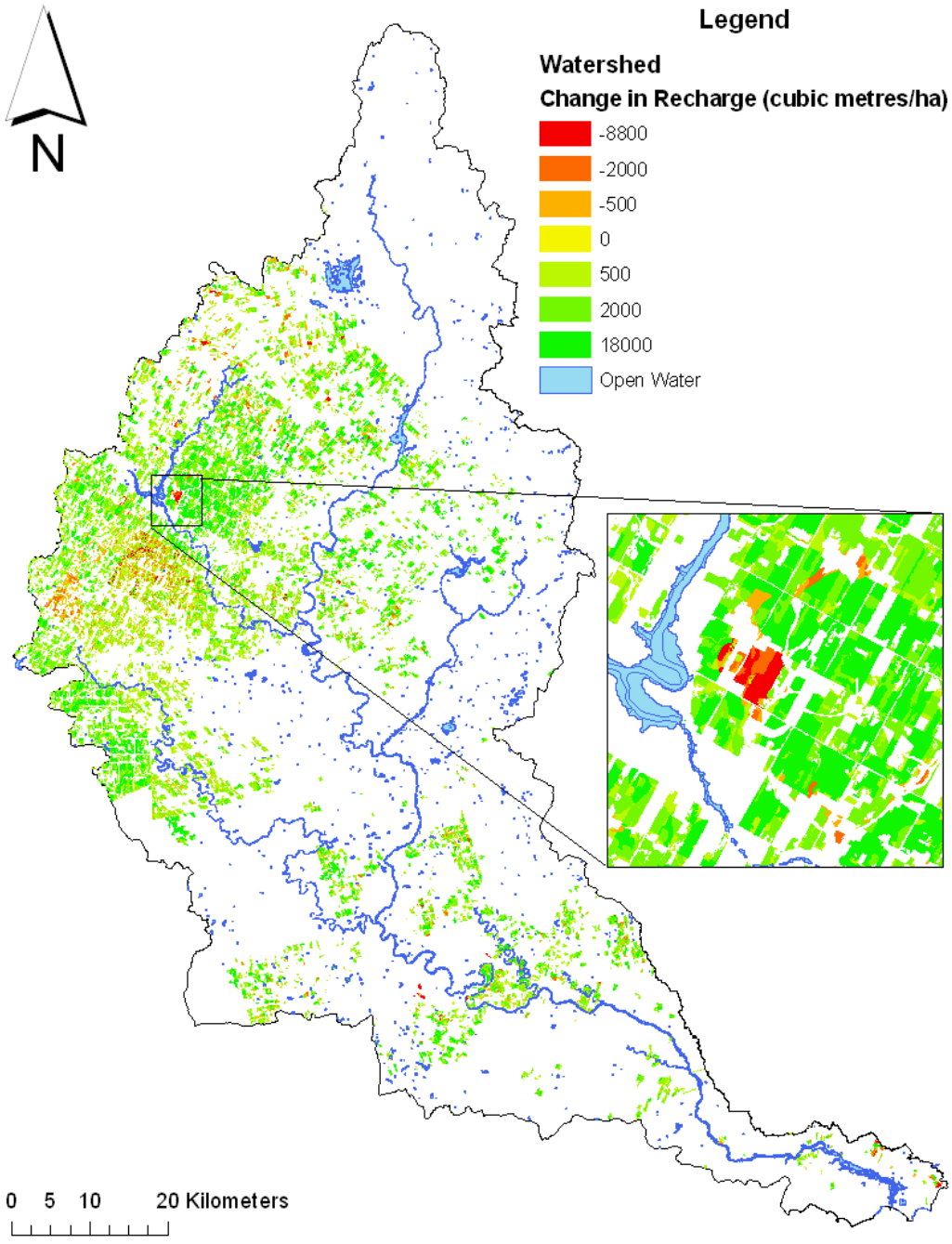

Figure 4.24: Annual change in recharge (m^3/ha) for the A2 scenario

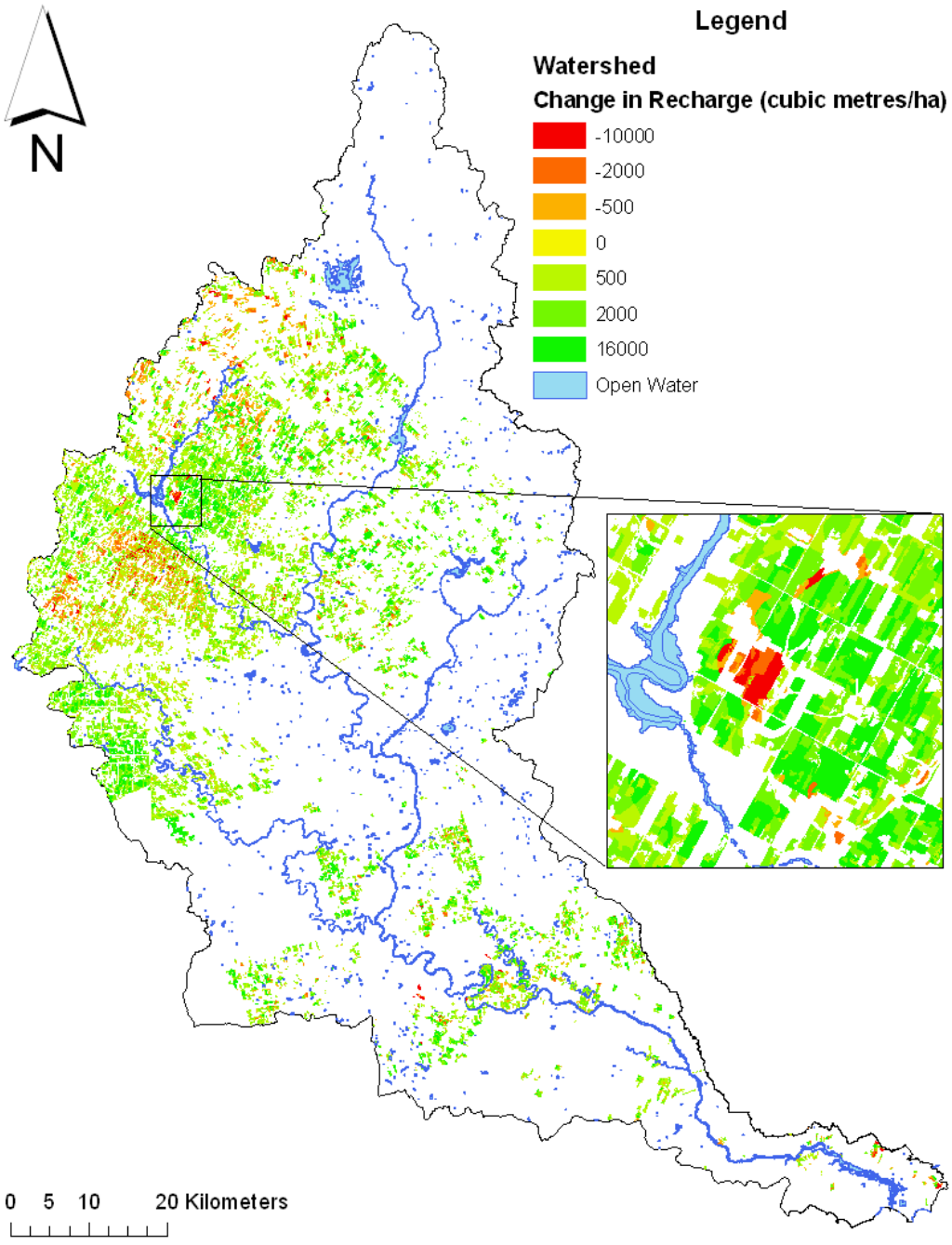

Figure 4.25: Annual change in recharge (m^3/ha) for the A1B scenario

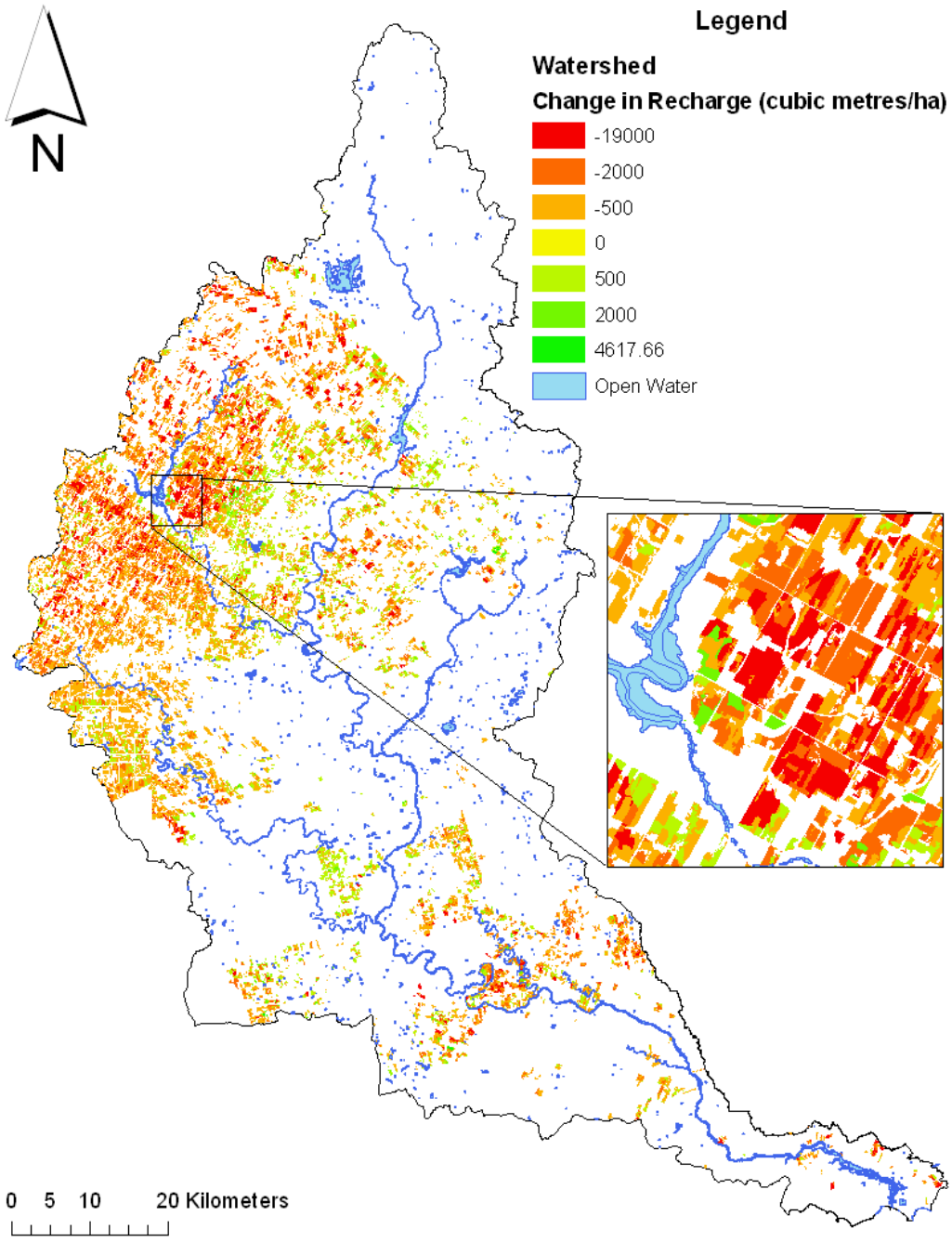

Figure 4.26: Annual change in recharge (m^3/ha) for the B1 scenario

scenarios. The change in annual surface runoff ranged from -0.35 m^3/ha to 1,000 m^3/ha and -100 m^3/ha to 1,000 m^3/ha for the A1B and the B1 scenarios respectively. The average change in surface runoff was calculated to be approximately 160 m^3/ha and 60.2 m^3/ha for the A1B and B1 scenarios respectively. The total annual surface runoff increase was calculated to be approximately 11,600,000 m^3 and 4,360,000 m^3 for the A1B and B1 scenarios respectively. Figures 4.28 and 4.29 illustrate the annual change in surface runoff for the A1B and B1 climate change scenarios.

On average, approximately 17% of the annual precipitation was removed through surface runoff in 1999 for the base-case scenario in the tiled areas. A maximum of approximately 42% of the annual precipitation was removed through surface runoff. The A2 climate change scenario was simulated and the annual surface runoff average was approximately 18% with a maximum of 44% of the annual precipitation extracted by surface runoff. The A1B and B1 scenarios produced annual averages of approximately 18% and 17% with maximums of 44% and 42% of the annual precipitation extracted by surface runoff respectively.

4.3.4 Effect on Evapotranspiration

Similar to the surface runoff the evapotranspiration generally had an increase in the volume of water that was removed from the watershed by the A2 climate change scenario. The increase in the evapotranspiration, with respect to the 1999 base-case scenario, ranged from 0 m^3/ha to 81,000 m^3/ha. The average annual evapotranspiration change was calculated to be approximately 1,100 m^3/ha. The total annual volume of water removed from the tiled cells is approximately 79,500,000 m^3 for the A2 scenario. Figure 4.30 illustrates the annual change in the evapotranspiration for the the tiled cells in the GRW.

The evapotranspiration impacted in the GRW was also estimated for the A1B and B1 scenarios. The change in evapotranspiration ranged from -0.063 m^3/ha to 61,000 m^3/ha and -2,300 m^3/ha to 13,000 m^3/ha for the A1B and the B1 scenarios respectively. The average annual change in evapotranspiration was calculated to be approximately 953 m^3/ha and 109 m^3/ha for the A1B and B1 scenarios, respectively. For the A1B and the B1 scenarios the total annual increase in evapotranspiration was calculated to be approximately

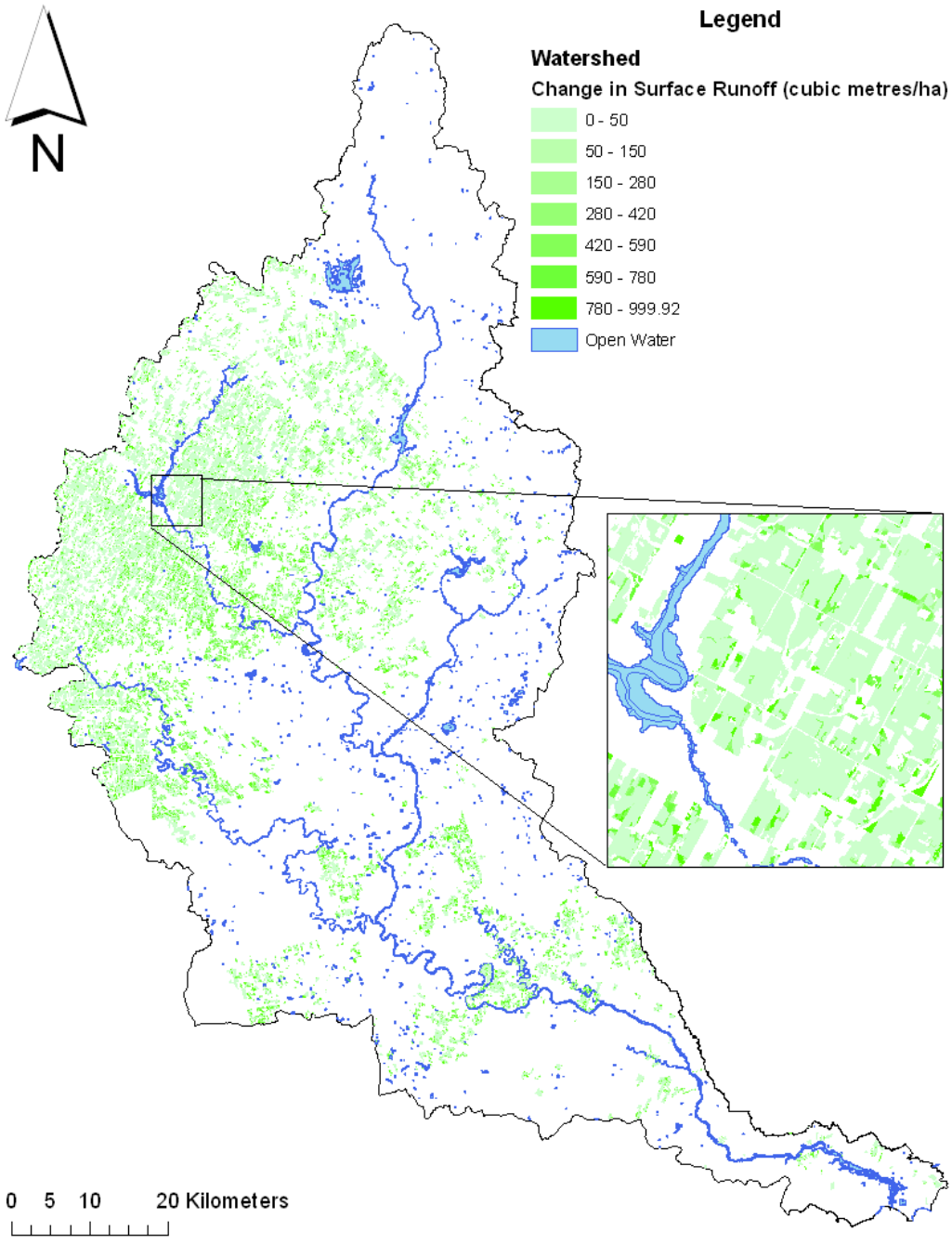

Figure 4.27: Annual change in surface runoff (m^3/ha) for the A2 scenario

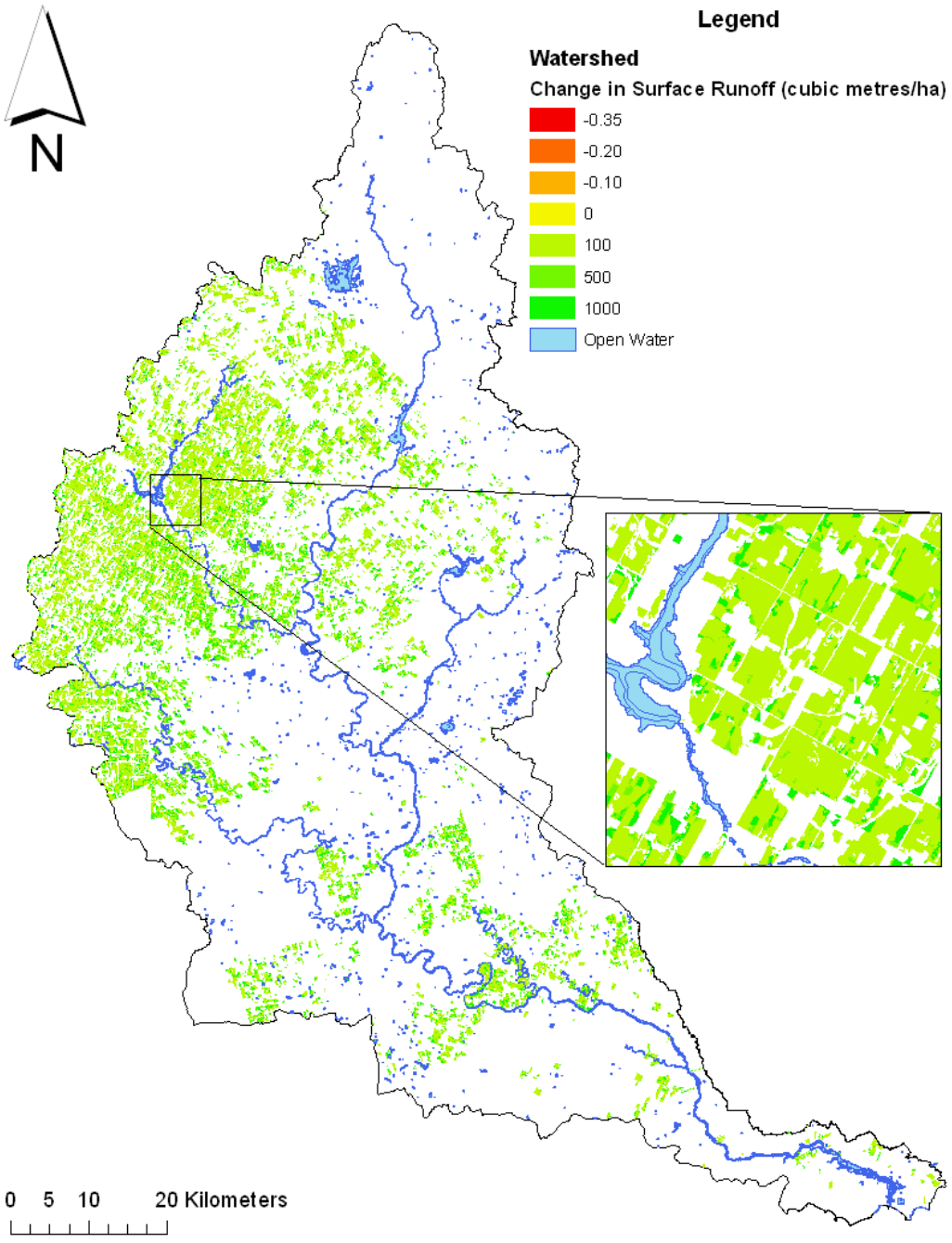

Figure 4.28: Annual change in surface runoff (m^3/ha) for the A1B scenario

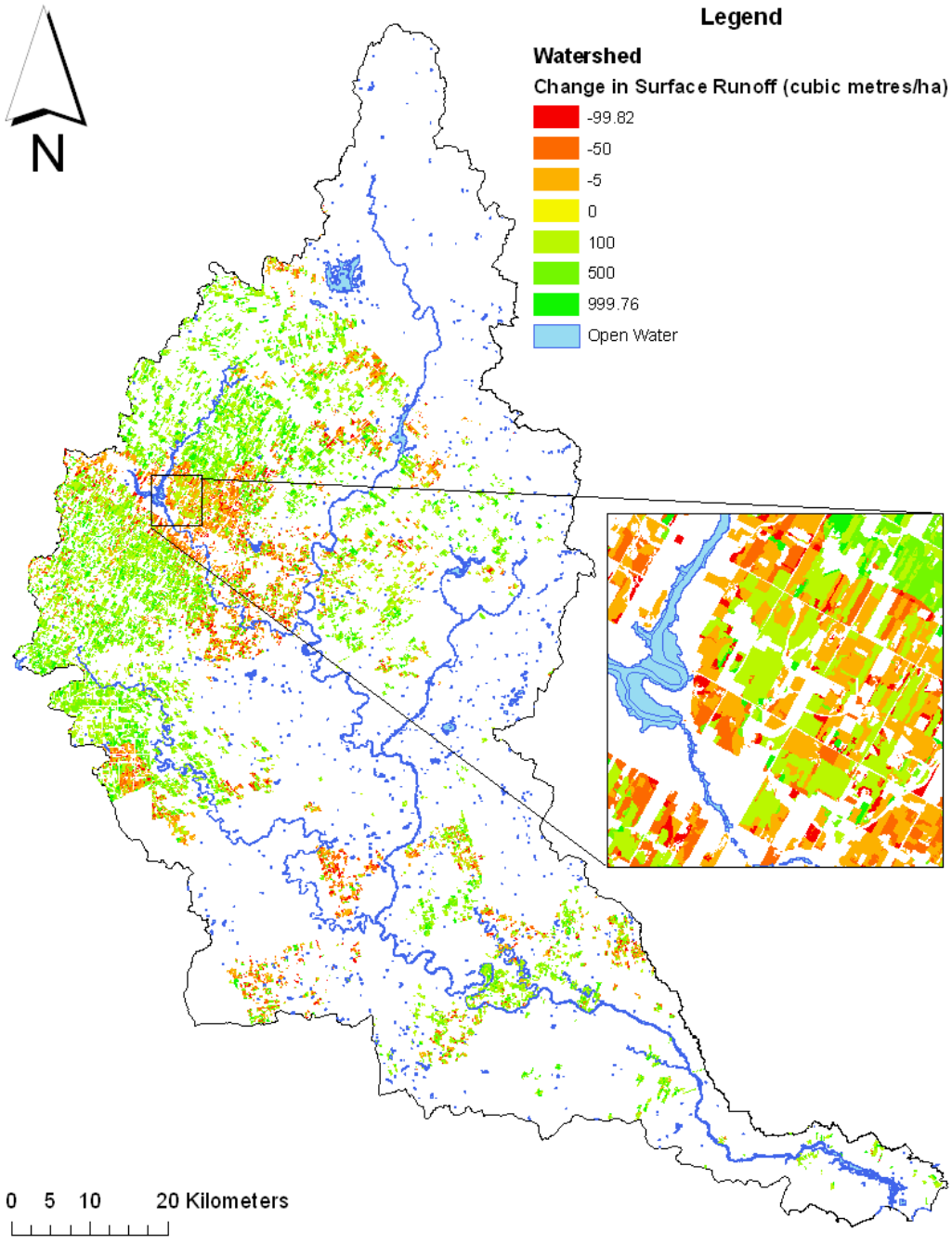

Figure 4.29: Annual change in surface runoff (m^3/ha) for the B1 scenario

69,100,000 m^3 and 7,900,000 m^3, respectively. Figures 4.31 and 4.32 illustrate the annual change in evapotranspiration for the A1B and B1 climate change scenarios.

Calculating the annual percentage of evapotranspiration with respect to the total annual precipitation for 1999 for the base-case scenario resulted in an average of 62% with a maximum of 73%. The climate change scenarios were simulated and the annual evapotranspiration average was calculated to be approximately 30% with a maximum of 73% of the annual precipitation extracted through evapotranspiration for the A2 scenario. The A1B and B1 scenarios produced an annual average of approximately 62% and 62% with maximums of 72% and 74% of the annual precipitation extracted through evapotranspiration, respectively.

4.3.5 Climate Change Annual Summary

The climate change scenarios had an impact on the hydrological processes for the tiled cells. Table 4.2 summarizes the change that each of the scenarios had on the base-case in 1999. Precipitation (Precip), surface runoff (Runoff), evapotranspiration (Evapo), tile drainage (Drainage), and groundwater recharge (Recharge) is reported as (mm/yr). The climate change scenarios are reported as a forecast for 2039 because the climate change scenarios were simulated as if the they would instantly begin after 1999.

Similar to the results found by *Croley II and Luukkonen* (2003), the groundwater recharge may increase or decrease from the base-case depending on the climate change scenario that is modelled. Unlike the results found by *Rosenburg et al.* (1999), groundwater recharge did not decrease for all climate change scenarios that were modelled.

4.3.6 Changes in April

The predicted changes to the climate were analyzed monthly time scale in addition to an annual time scale. For the base-case analysis, the month that had the most drainage was April.April was again examined in more detail to determine the impact of the climate change scenarios. Average change for the tiled cells is calculated by taking the mean of the comparisons between the

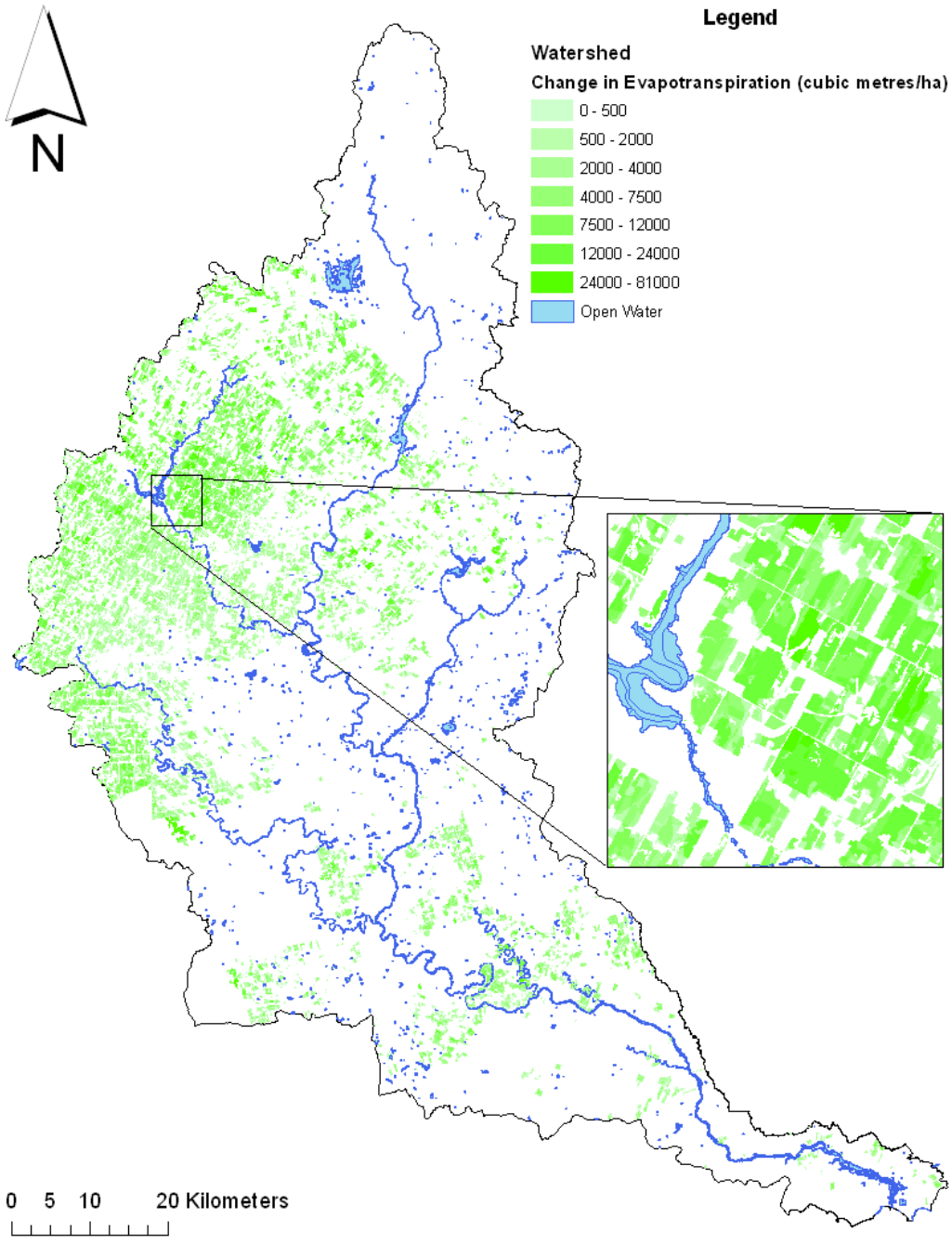

Figure 4.30: Annual change in evapotranspiration (m^3/ha) for the A2 scenario

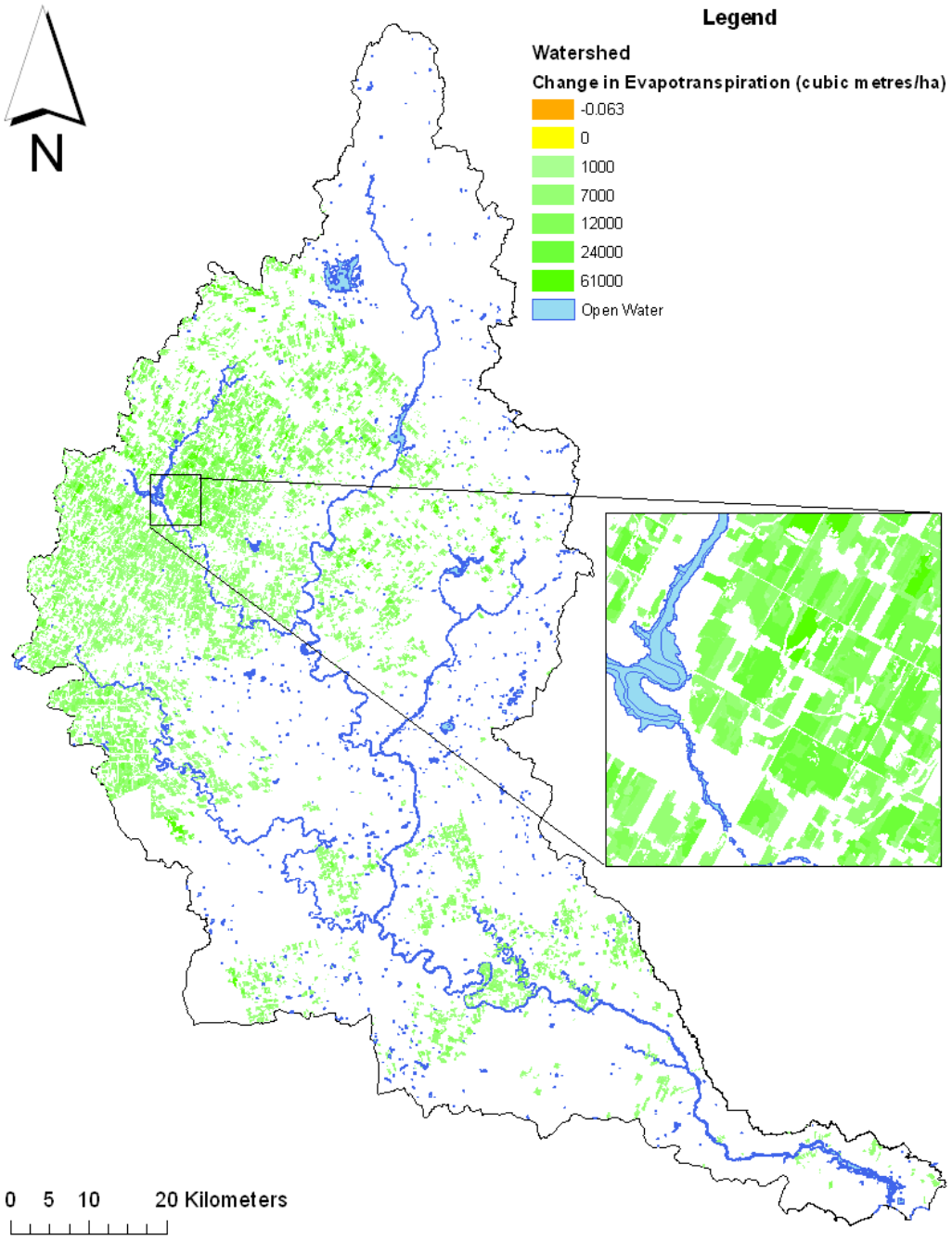

Figure 4.31: Annual change in evapotranspiration (m^3/ha) for the A1B scenario

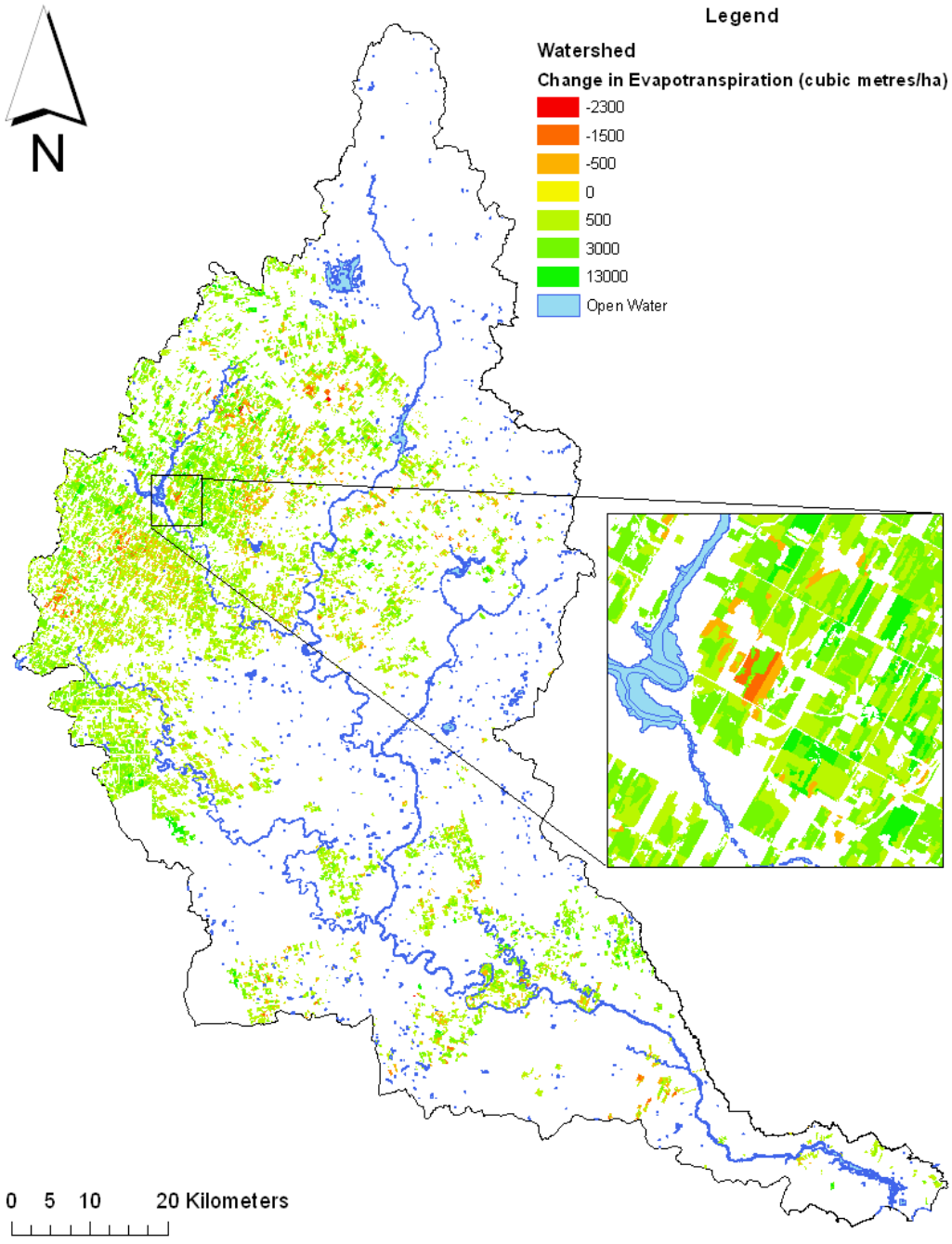

Figure 4.32: Annual change in evapotranspiration (m^3/ha) for the B1 scenario

Table 4.2: Climate Change Annual Summary

Scenario	Precip (mm/yr)	Runoff (mm/yr)	Evapo (mm/yr)	Drainage (mm/yr)	Recharge (mm/yr)
Base-case 1999					
Avg	833	134	514	0.017	188
Max	937	298	591	1.35	366
Min	639	30	333	0.0001	5.4
2039 A2					
Δ Avg	132	39	80	0.0021	18.6
Δ Max	151	194	133	1.0	118
Δ Min	100	3.2	4	-1.2	-83
2039 A1B					
Δ Avg	113	33.4	69	0.0014	14.5
Δ Max	129.4	185	124	1.0	114
Δ Min	86.01	-0.6	-0.5	-1.3	-81
2039 B1					
Δ Avg	7.44	8.2	7.8	-0.0019	-8.3
Δ Max	9.35	135	46	1.14	65
Δ Min	4.91	-25	-33	-1.3	-100

climate change results and the base-case 1999 results for all of the tiled cells in April. Total change is the net increase or decrease in the for the tiled cells in the GRW when comparing the climate change results with the base-case in April 1999.

Comparing the tile drainage volumes from the A2 scenario and the base-case scenario yielded results that show a general decrease in total drainage. The April changes in drainage ranged from -18 m^3/ha to 29.6 m^3/ha. The average change in drainage was calculated to be approximately -0.003 m^3/ha with a total decrease of approximately 209 m^3 for the month of April. Figure 4.33 shows the change in the drainage volumes.

Alternatively, the tile drainage volumes from the A1B scenario were compared to the base-case scenario and yielded results that show a general increase in total drainage. The April changes in drainage ranged from -19 m^3/ha to 8.5 m^3/ha. The average change in drainage was calculated to be approximately

0.0001 m^3/ha with a total increase of approximately 10.5 m^3 for the month of April. Figure 4.34 shows the change in drainage volumes.

Similarly to the A2 scenario, the tile drainage volumes from the B1 scenario were compared to the base-case scenario and yielded results that show a general decrease in total drainage. The April changes in drainage ranged from -18 m^3/ha to 8.3 m^3/ha. The average change in drainage volume was calculated to be approximately -0.010 m^3/ha with a total decrease in drainage of approximately 730 m^3 for the month of April. Figure 4.35 shows change in drainage volumes.

The green areas for these figures indicate where the drainage volumes have increased for the month of April. The orange and red areas indicated where the drainage volumes have decreased in the month of April due to the respective climate change scenario.

The A1B scenario indicates there is a slight increase in drainage for the month of April, likely due to the meteorological conditions that the A1B presents. The other two scenarios, A2 and B1, indicate a decrease in the overall drainage for the tiled cells. Both scenarios are on the outer limits of the predicted climate change scale. A2 has the highest increases in temperature and precipitation and B1 has the lowest increases.

The change in recharge in the month of April for the A2 scenario as compared to the base-case analysis ranged from -6,300 m^3/ha to 7,400 m^3/ha. The April recharge had an average increase in the change of recharge of approximately 71.2 m^3/ha with a total increase of approximately 5,160,000 m^3. The change in recharge in the month of April under the A1B scenario as compared to the base-case analysis ranged from -6,400 m^3/ha to 6,710 m^3/ha. The A1B scenario resulted in an average increase in the change of recharge of approximately 62 m^3/ha with a total increase of approximately 4,500,000 m^3. The change in recharge in the month of April under the B1 scenario as compared to the base-case analysis ranged from -9,700 m^3/ha to 3,300 m^3/ha. The average change in recharge for the month of April was calculated to be approximately -23 m^3/ha with a total decrease of approximately 1,680,000 m^3 for the tiled areas in the GRW. Figures 4.36, 4.37, and 4.38 illustrate the change in the recharge between the respective climate change scenario and 1999 of the base-case scenario.

The green areas indicate where recharge has increased for the month of

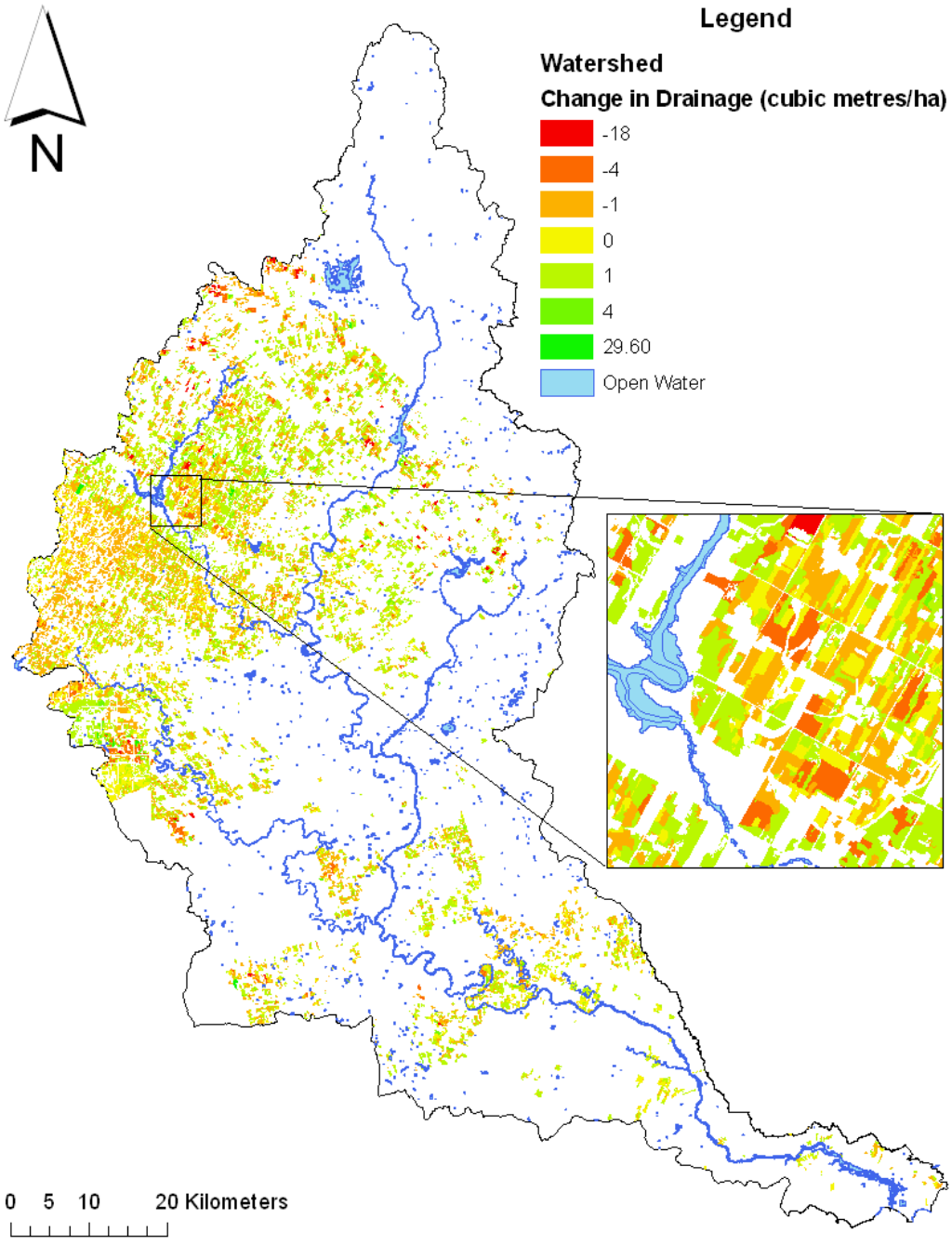

Figure 4.33: Change in drainage (m^3/ha) in April for the A2 scenario

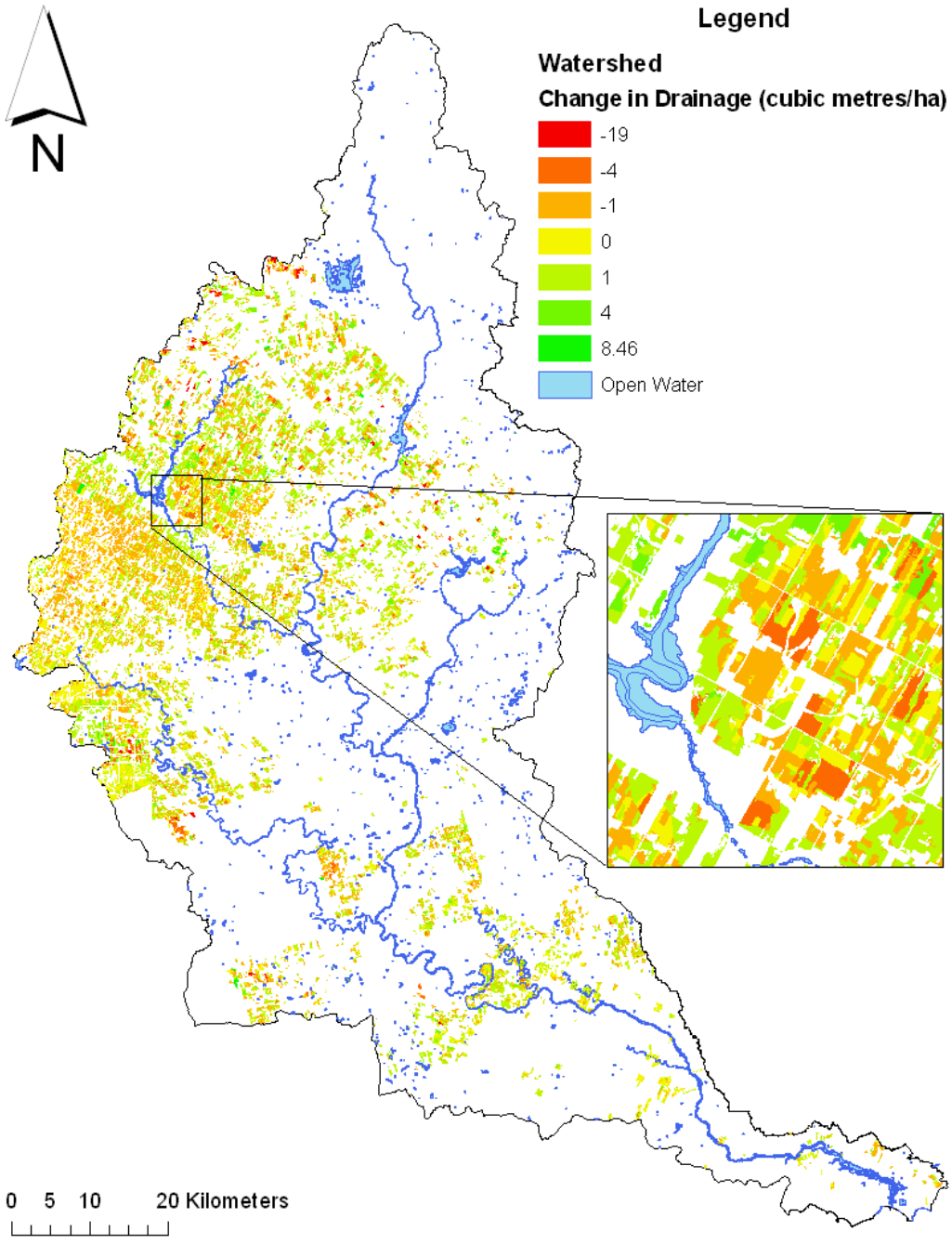

Figure 4.34: Change in drainage (m^3/ha) in April for the A1B scenario

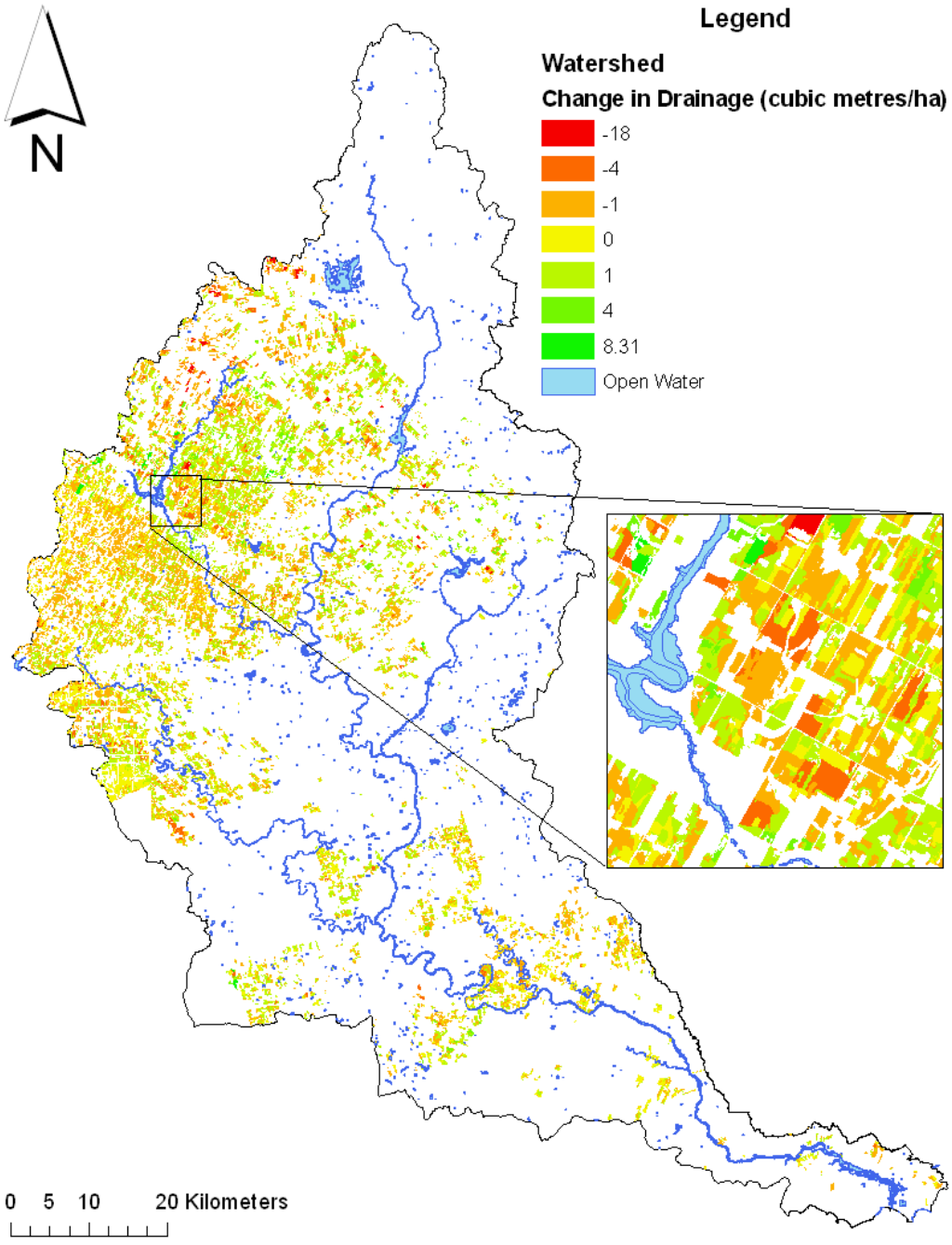

Figure 4.35: Change in drainage (m^3/ha) in April for the B1 scenario

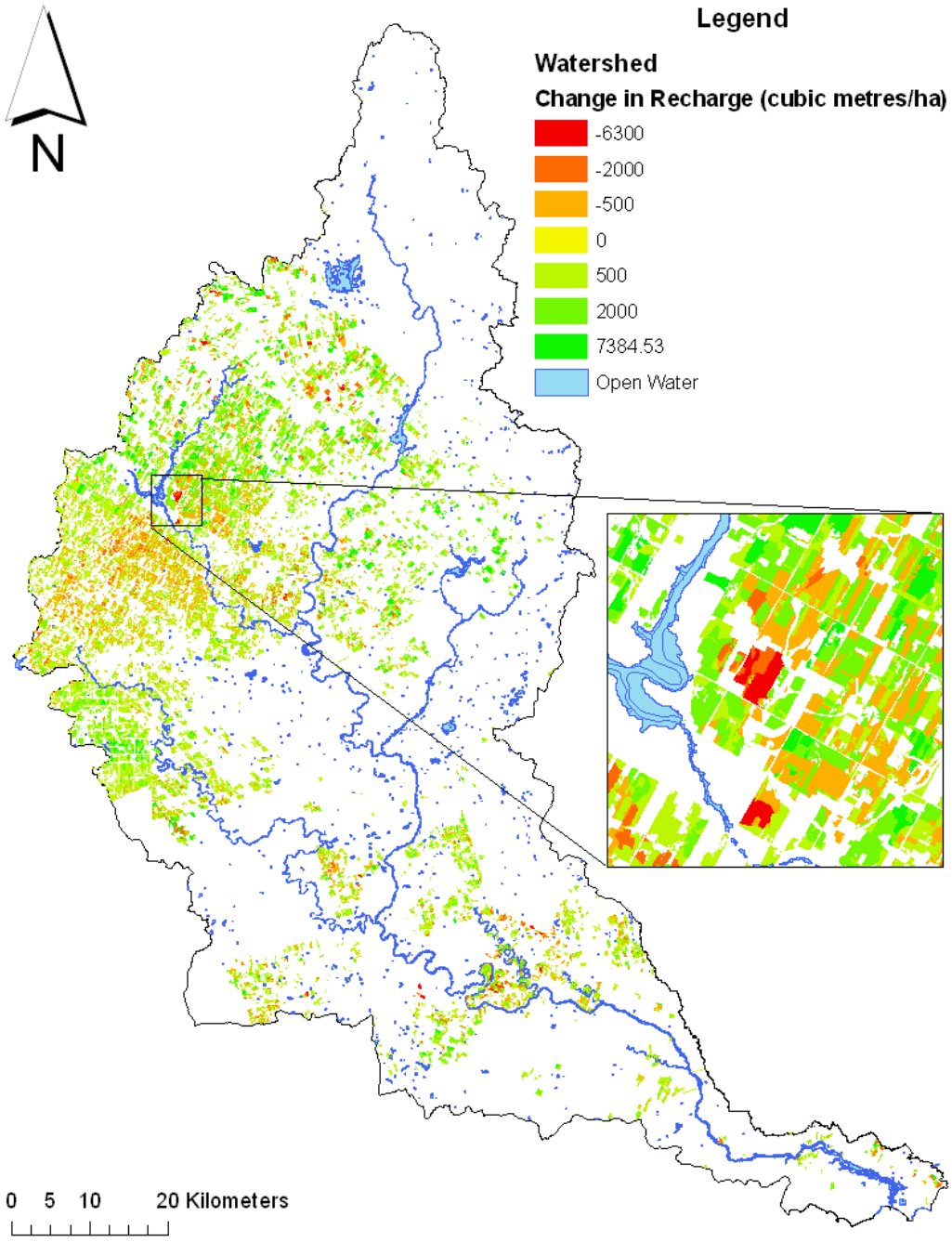

Figure 4.36: Change in recharge (m^3/ha) in April for the A2 scenario

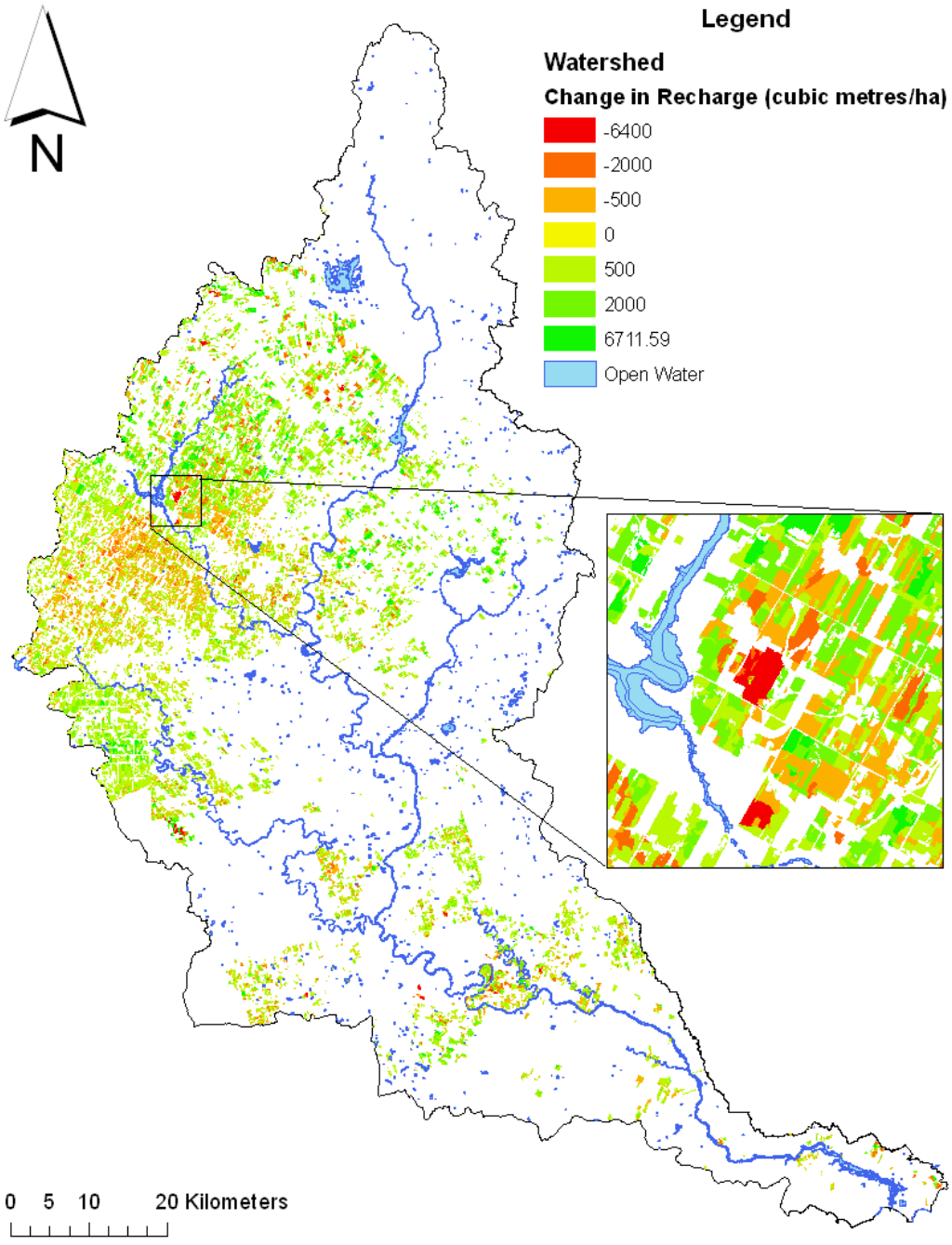

Figure 4.37: Change in recharge (m^3/ha) in April for the A1B scenario

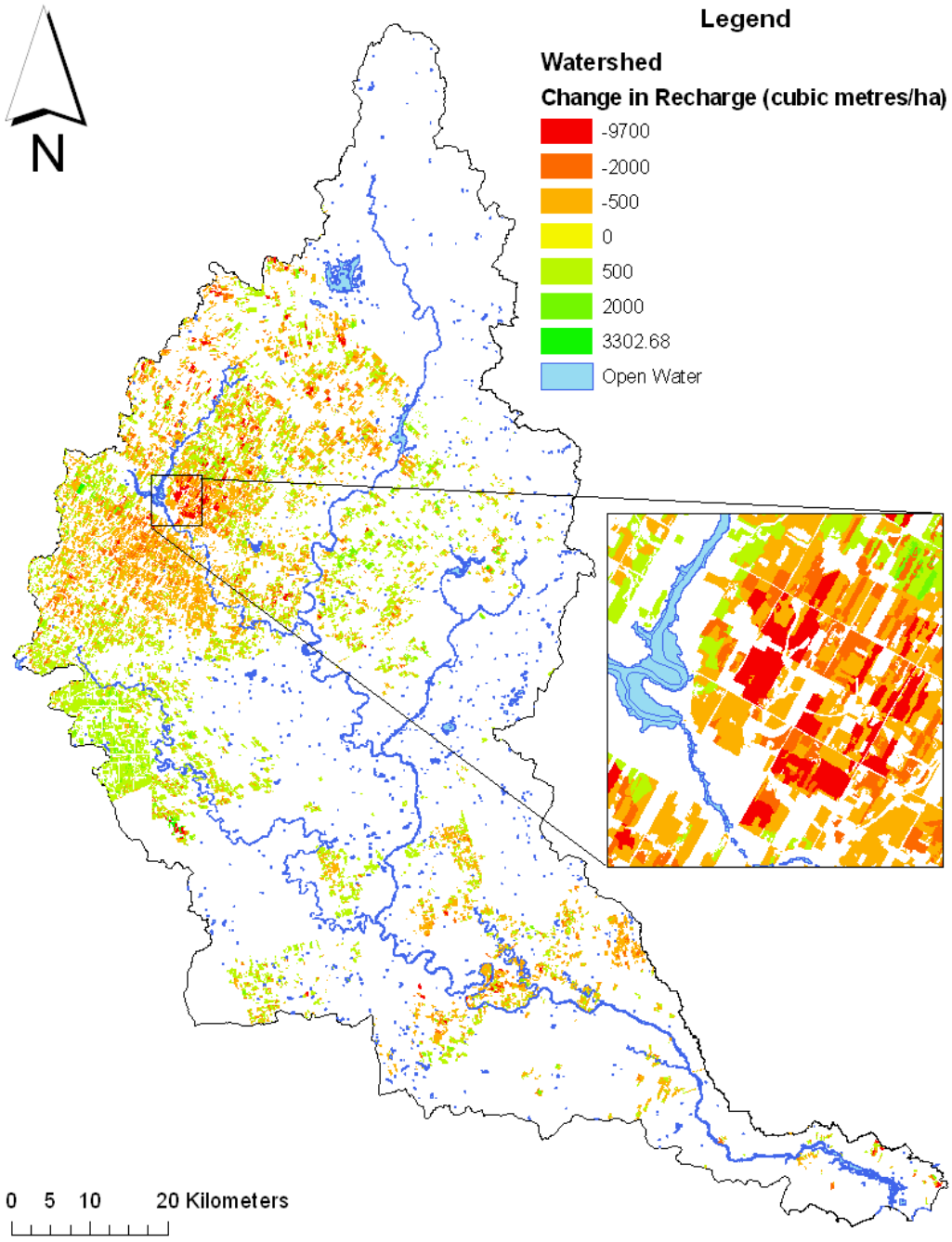

Figure 4.38: Change in recharge (m^3/ha) in April for the B1 scenario

April. The orange and red areas indicate where recharge has decreased in the month of April.

Surface runoff in the month of April for the A2 scenario as compared to the base-case analysis ranged from -100 m^3/ha to 667 m^3/ha. The surface runoff for the A2 scenario had an average decrease of approximately 16 m^3/ha with a total decrease of 1,140,000 m^3 for the month of April. Surface runoff in the month of April under the A1B scenario ranged from -100 m^3/ha to 977 m^3/ha. The surface runoff for the A1B scenario as compared to the base-case analysis had an average decrease of approximately 15 m^3/ha and a total decrease in surface runoff of approximately 1,120,000 m^3 for the month of April. Surface runoff in the month of April under the B1 scenario as compared to the base-case analysis ranged from -100 m^3/ha to 972 m^3/ha. The surface runoff for the B1 scenario had an average increase of approximately 0.89 m^3/ha on average with a total increase of approximately 64,000 m^3. Figures 4.39, 4.40, and 4.41 illustrate the change in surface runoff for the respective climate change scenario in April.

The green areas indicate an increase in surface runoff for the month of April. The orange and red areas indicated a surface runoff decrease for the month of April.

The change in evapotranspiration in the month of April under the A2 scenario as compared to the base-case analysis ranged from 0 m^3/ha to 29,000 m^3/ha. The evapotranspiration for the A2 scenario had an average increase of approximately 317 m^3/ha with a total increase of approximately 23,000,000 m^3 for the month of April. Evapotranspiration in the month of April under the A1B scenario as compared to the base-case analysis ranged from -55 m^3/ha to 17,000 m^3/ha.The evapotranspiration for the A1B scenario showed an average increase of approximately 292 m^3/ha with a total increase of approximately 21,200,000 m^3 for the month of April. Evapotranspiration in the month of April under the B1 scenario ranged as compared to the base-case analysis from -1,200 m^3/ha to 10,000 m^3/ha. The evapotranspiration for the B1 scenario showed an average increase of approximately 49 m^3/ha with a total increase of approximately 3,580,000 m^3 for the month of April. Each subsequent scenario has less precipitation and temperature increases. This results in less of an increase for the evapotranspiration. Figures 4.42, 4.43, and 4.44 illustrate the change in evapotranspiration for the respective climate

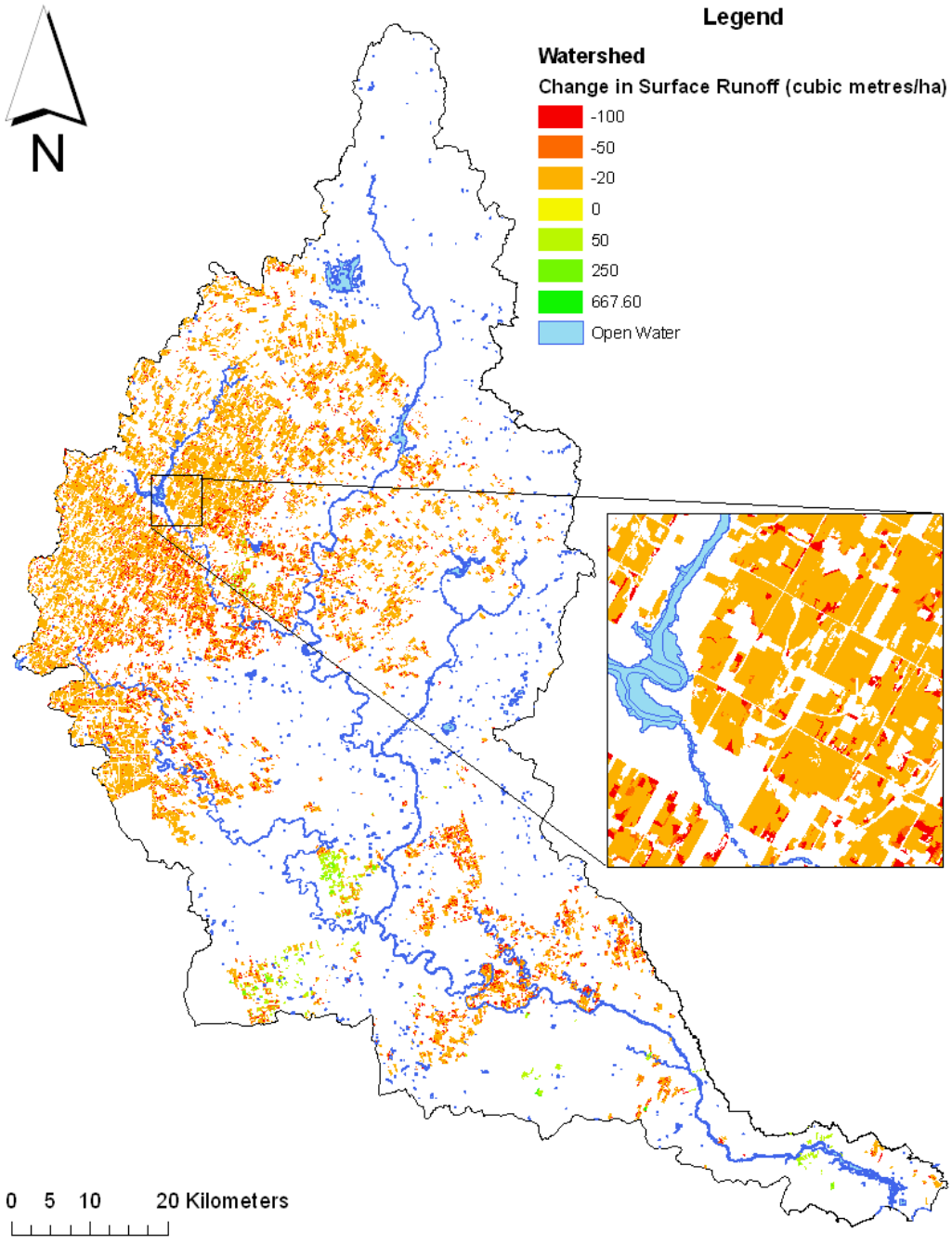

Figure 4.39: Change in Surface Runoff (m^3/ha) in April for the A2 Scenario

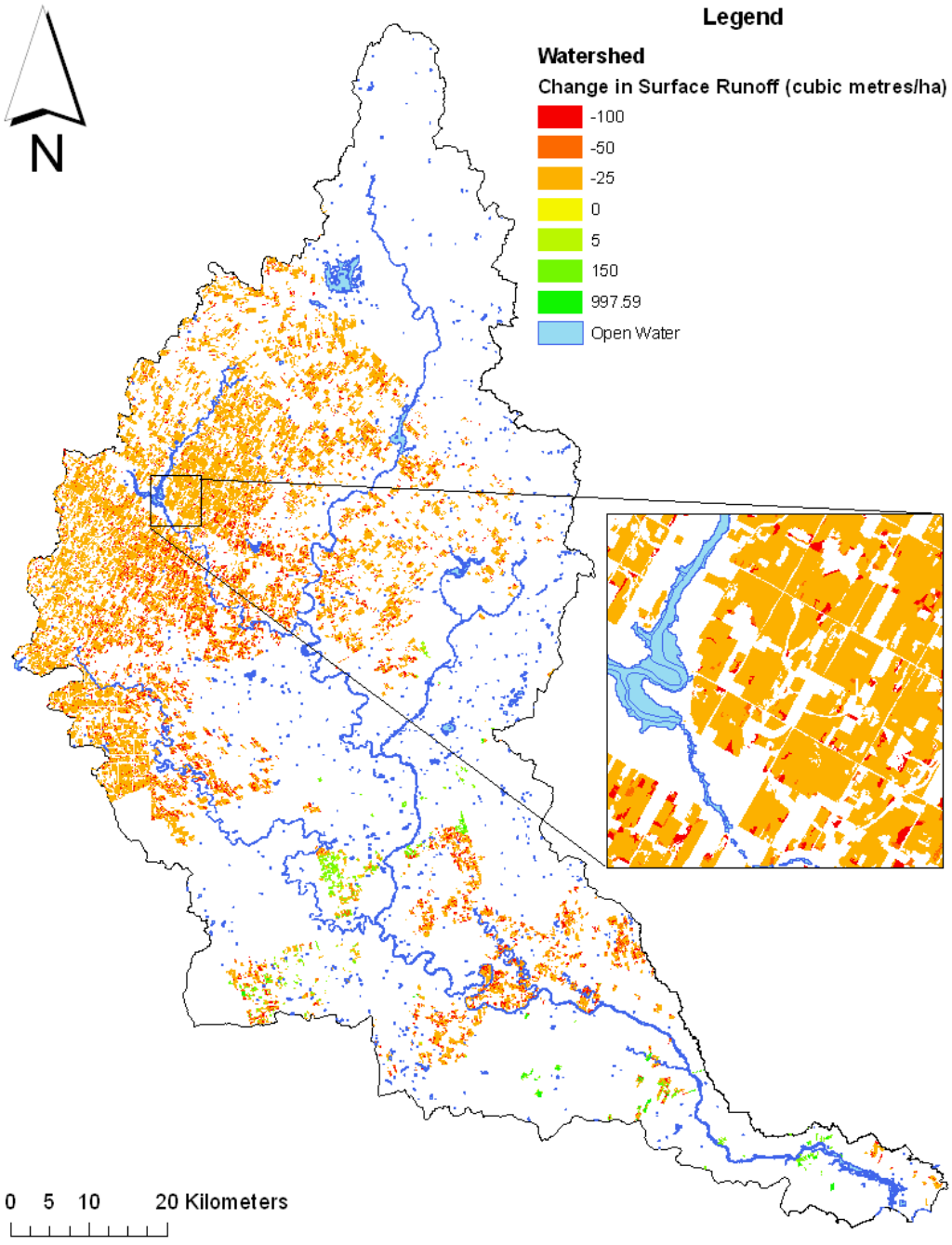

Figure 4.40: Change in Surface Runoff (m^3/ha) in April for the A1B Scenario

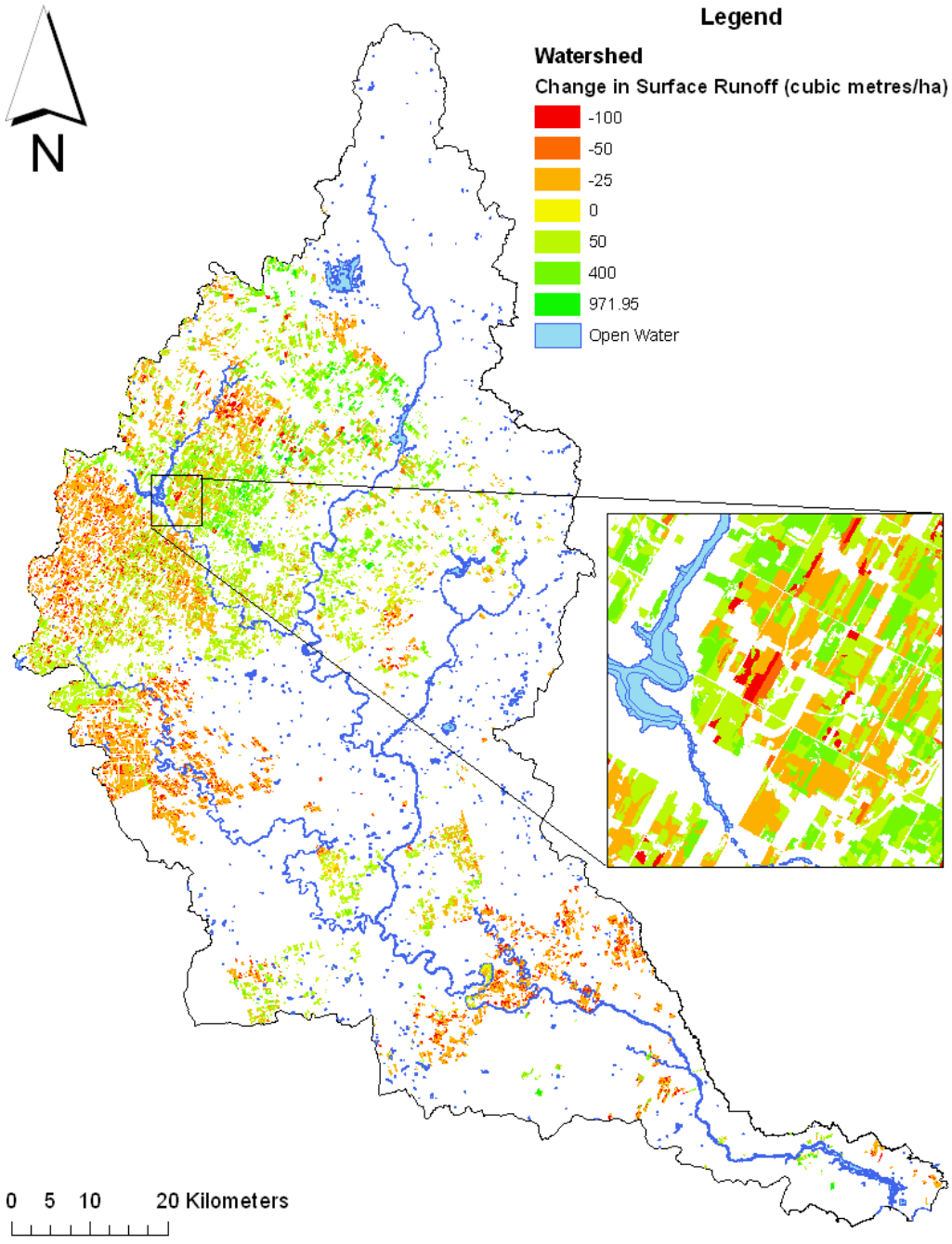

Figure 4.41: Change in Surface Runoff (m^3/ha) in April for the B1 Scenario

change scenario in April.

The green areas indicate an increase in evapotranspiration for the month of April. The orange and red areas indicated a evapotranspiration decrease for the month of April.

4.3.7 Climate Change April Summary

The climate change scenarios had an impact on the hydrological processes for the tiled cells in April. Table 4.3 summarizes the change that each of the scenarios had on the base-case in April 1999. Precipitation (Precip), surface runoff (Runoff), evapotranspiration (Evapo), tile drainage (Drainage), and groundwater recharge (Recharge) is reported as (mm/month). The climate change scenarios are reported as a forecast for 2039 because the climate change scenarios were simulated as if the they would instantly begin after 1999.

Table 4.3: Climate Change April Summary

Scenario	Precip (mm/mth)	Runoff (mm/mth)	Evapo (mm/mth)	Drainage (mm/mth)	Recharge (mm/mth)
Base-case 1999					
Avg	53.7	11.4	53	0.012	53
Max	85.1	65	91	1.4	143
Min	38.1	0.07	29	0	0
2039 A2					
Δ Avg	8.5	-4.7	22.3	0.0005	5.1
Δ Max	13.4	8	39	1.0	37
Δ Min	5.8	-46	1.5	-1.2	-35
2039 A1B					
Δ Avg	7.22	-4.6	20.5	0.0002	4.5
Δ Max	11.3	11	38	1.0	36
Δ Min	5	-42	-1.7	-1.3	-29
2039 B1					
Δ Avg	0.45	-0.58	3.3	-0.0009	-2.0
Δ Max	0.9	9.6	20	-1.3	21
Δ Min	0	-39	-8.6	1.1	-44

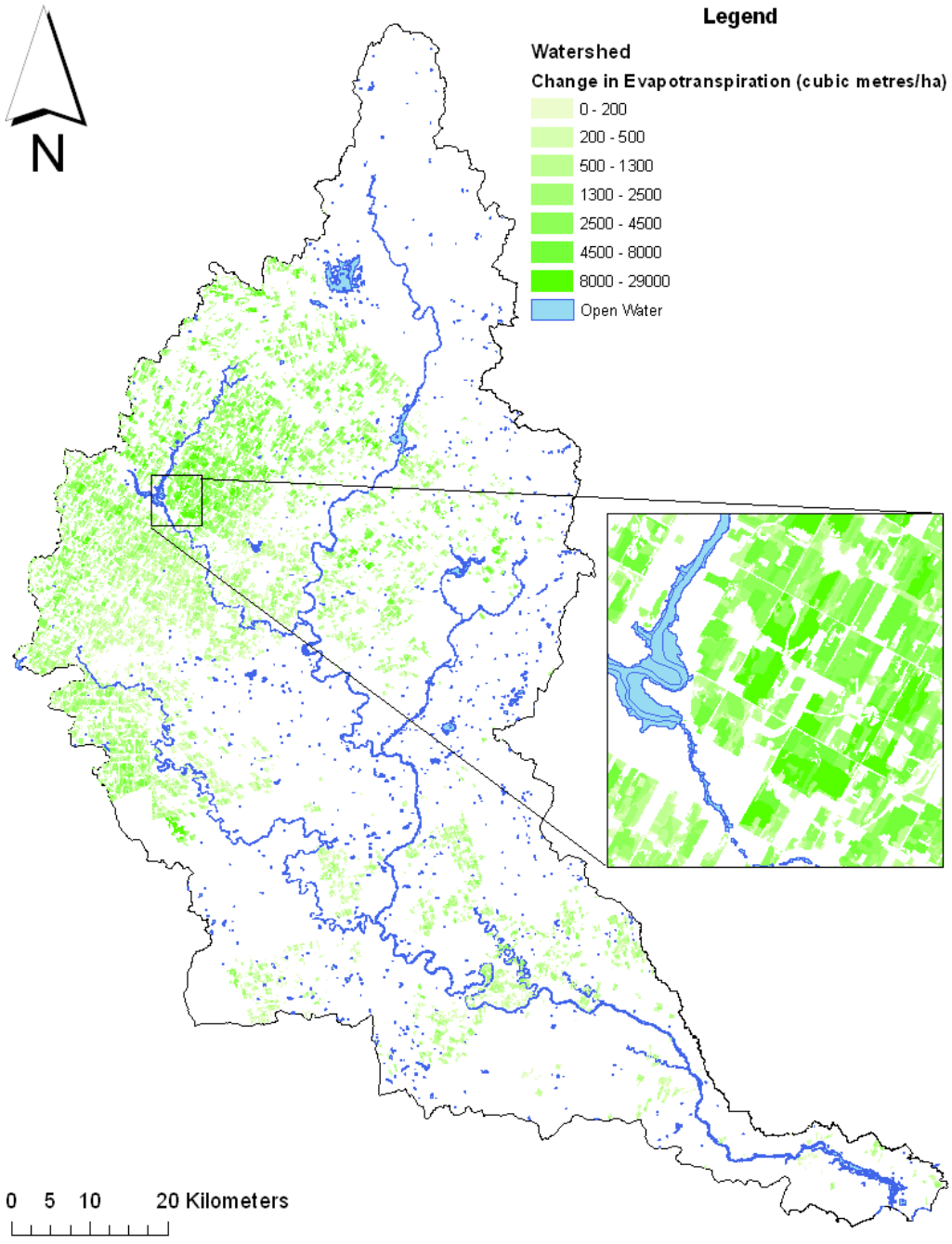

Figure 4.42: Change in evapotranspiration (m^3/ha) in April for the A2 scenario

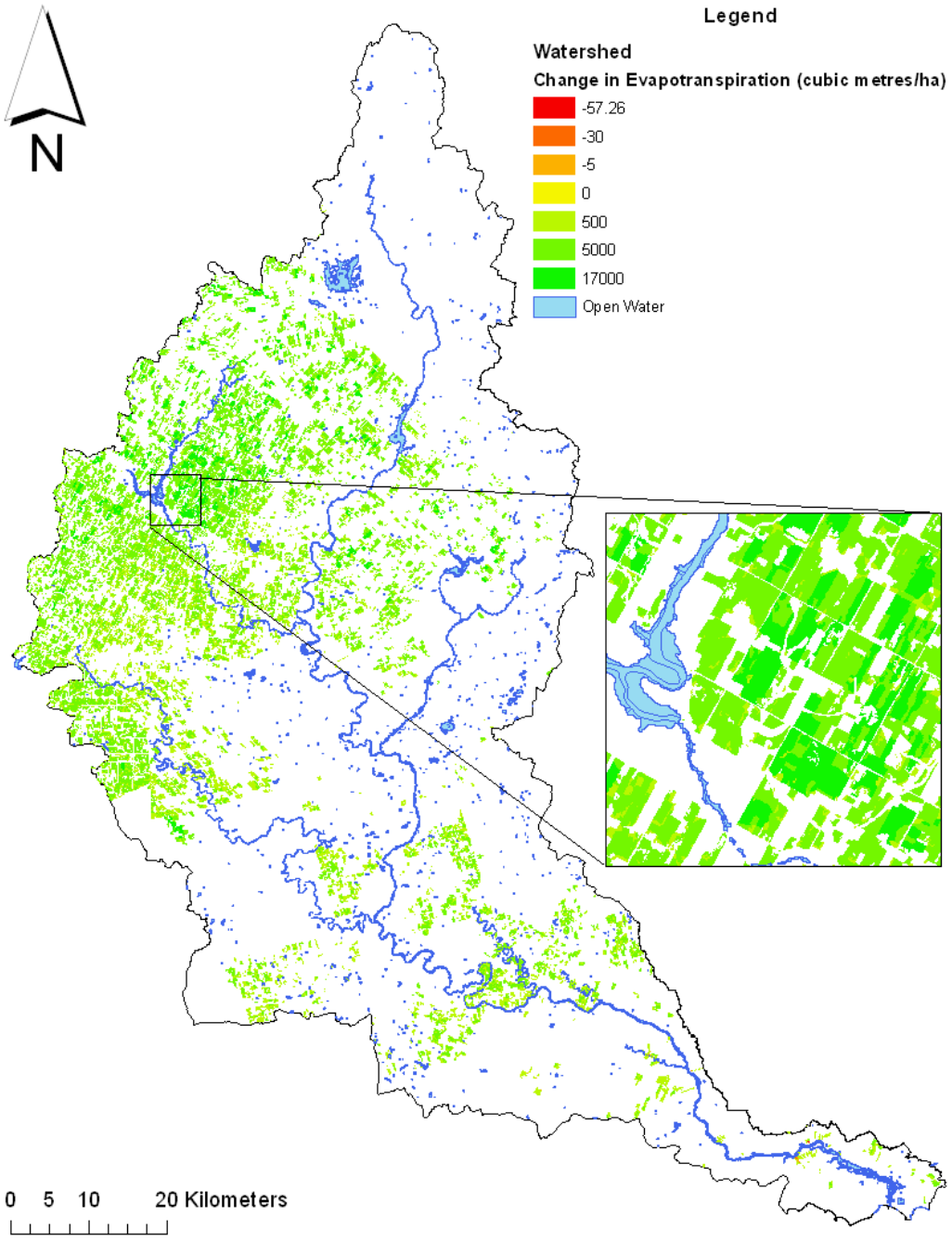

Figure 4.43: Change in evapotranspiration (m^3/ha) in April for the A1B scenario

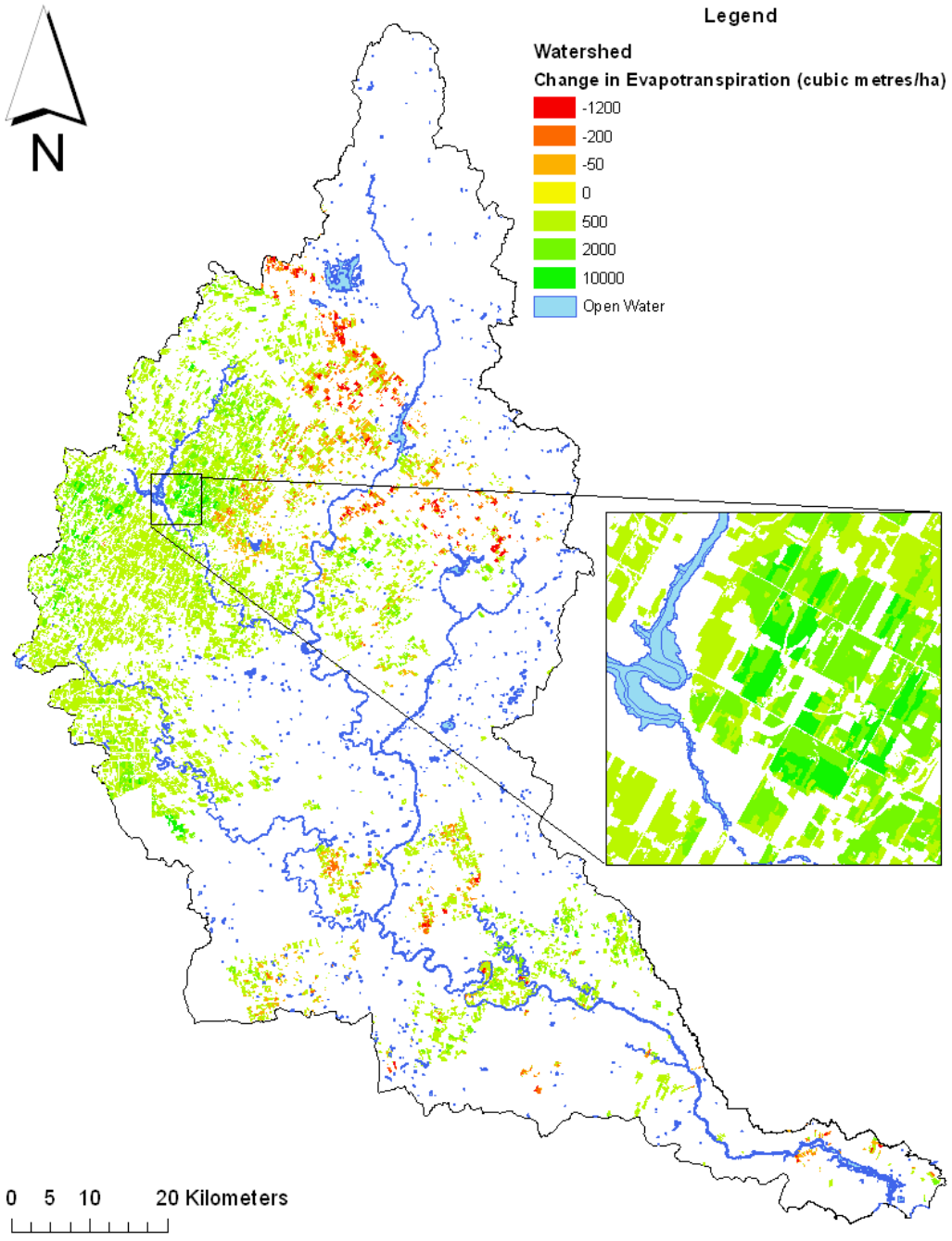

Figure 4.44: Change in evapotranspiration (m^3/ha) in April for the B1 scenario

Chapter 5

Conclusions

Estimating the temporal volume of water that is discharged from tile drains can potentially be a useful excercise for examining the local recharge and the potential for contaminants to be released into adjacent surface waters. Using the physically based HELP3 model and integrating ArcMap GIS and database software, a spatially distributed tile drainage estimate was calculated for the Grand River Watershed. Approximately 15% (99,800 ha) of the watershed has tile drains. These areas were modelled to incorporate tile drainage technology. For simplicity, all of the tile drains were located at a common depth, common spacing, and had a common slope.

Tile drains can be simulated using HELP3 to extract excess water out of the subsurface. The discharge from the tiled cells on a watershed scale was approximated with the available information. Along with drainage, the recharge, surface runoff and evapotranspiration were also approximated for the tiled cells in the watershed. Conditions of the soil type, meteorological data, and land use/land class can determine if tile drains may be active once or multiple times in a year. The results have indicated that tile drains and climate change can have a significant impact on the watershed hydrological processes.

The base-case model was simulated for 40 years using meteorological data for the watershed. The results from the modelling indicate that, as expected, the tile drains extract water from the subsurface. For the 1999 results approximately 16,100 m^3 or an average of 0.028% per cell of the precipitation that falls annually is extracted by the tiled cells. Generally the tile drains are most

effective in the spring and fall months. However, the bulk of the precipitation that is collected in the tile drains is in April. This is because of the spring melt that occurs and the influx of melted water into the subsurface during April. November generally is the second most active month for the tile drains in the GRW. In the fall months, rain falls frequently due to large tropical storms and hurricanes that land in the southern United States. The storm system dissipates as it moves north over the continent, but they can eventually reach the GRW. It is evident that in the summer and winter months the tile drains are not collecting very much water. *Macrae et al.* (2007) did observe that peak discharge times occurred during April during the spring melt and again in the fall. The same trend was also observed in the results from the simulations for the tiled cells.

There was an estimated increase in groundwater recharge when comparing the un-tiled scenario to the tiled scenario of approximately 104 m^3/ha in 1999. A total annual increase of approximately 7,503,000 m^3 was estimated to reach the groundwater recharge when comparing the tiled and un-tiled scenarios for 1999. When the tiles are simulated there are decreases in the annual surface runoff and evapotranspiration for the tiled cells in 1999. When the tile drains are simulated, the annual decreases were estimated to be approximately 3,060,000 m^3 and 1,480,000 m^3 for surface runoff and evapotranspiration, respectively.

Climate change scenarios were simulated and compared to the base-case analysis. Incorporating the tile drains into climate change model was accomplished to examine any impacts of the tile drains. The meteorological data was modified using the IPCC climate change scenario projections (*IPCC*, 2007c). The same cells were used in the climate change scenarios to simulate the impact on the tile drains and the hydrological processes of the GRW.

The three climate change scenarios that were chosen for simulation were A2, A1B, and B1. Each scenario was chosen because of the projected potential temperature and precipitation increases for the GRW. These climate change scenarios produced annual drainage totals of 17,700 m^3, 17,600 m^3, and 14,500 m^3 for the A2, A1B, and B1 scenarios respectively. These volumes can be compared to the annual total drainage for 1999 of the base-case, which had a total annual drainage of approximately 16,100 m^3.

Along with the drainage changes, the recharge in the GRW tiled cells was

also impacted by the tile drains and the climate change scenarios. The tiled cells had annual increases in recharge of 18,300,000 m^3 (+10% increase over the 1999 base-case) and 14,200,000 m^3 (+7%) for the A2 and A1B scenarios respectively. However, the B1 scenario had an annual decrease in recharge of approximately 8,230,000 m^3 (-4%). The 1999 base-case scenario total groundwater recharge was estimated to be 186,000,000 m^3 for the tiled cells.Results found by *Croley II and Luukkonen* (2003) agree with the results presented in this thesis. The groundwater recharge may increase or decrease from the base-case depending on the climate change scenario that is modelled. Unlike the results found by *Rosenburg et al.* (1999), groundwater recharge did not decrease for all climate change scenarios that were modelled.

Surface runoff and evapotranspiration were also impacted by the simulated change in climate conditions. The total annual surface runoff was increased by 12,040,000 m^3 (+100% increase over the 1999 base-case), 11,600,000 m^3(+96%) and 4,360,000 m^3 (+36%)for the A2, A1B and B1 scenarios respectively. The 1999 base-case scenario total surface runoff was estimated to be 12,008,000 m^3 for the tiled cells. The evapotranspiration increased for the A2, A1B and B1 scenarios. These increases were 79,500,000 m^3 (+16% increase over the 1999 base-case), 69,100,000 m^3 (+14%)and 7,920,000 m^3 (+2%), respectively. The 1999 base-case scenario total evapotranspiration was estimated to be 514,000,000 m^3 for the tiled cells.

Depending on the climate change scenario, the simulation can have great impact on the drainage, recharge, surface runoff, and evapotranspiration for the tiled cells in the watershed. The A2 scenario was modelled as the "worst case" scenario with the highest increase in temperatures and precipitation rates. The results from the A2 scenario indicated the highest increases in drainage, recharge, surface runoff, and evapotranspiration. The A1B scenario was modelled as an intermediate increase in temperature and precipitation. The results from the A1B scenario indicate increased drainage, recharge, surface runoff, and evapotranspiration. The B1 scenario was modelled as the lowest increases in precipitation and temperatures; this resulted in a major decrease in drainage, recharge, and surface runoff but an increase in evapotranspiration from the watershed tiled cells.

Chapter 6

Recommendations

A study of the GRW has been conducted and a recharge model has been developed for this thesis. For further study on this subject, it is recommended that water that has been discharged from the tile drains be routed to the nearest surface water body. This can give the discharged water a time line from when it was extracted to the time it is discharged into the surface water. If there are any contaminants in the discharged water they will be delivered from the groundwater to the surface water, in a shorter period of time. Both sources of water are used in the GRW for drinking water supply.

Another extension would be to couple the nitrogen transport model that was also developed at the University of Waterloo (*Scott*, 2006) with the recharge model developed in this thesis. With the tile drained recharge model and the nitrogen transport model, potential mass loading of nitrates to the surface waters from the tile drains could be estimated. Incorporating a form of crop rotation for the agricultural fields would also be of benefit because the agricultural fields receive different forms of fertilizer and at different doses depending on what crop is being grown for a given growing season. A second extension of this concept could be to implement the climate change model that was developed by *Jyrkama and Sykes* (2007) and modified in this thesis to accommodate the tile drains to examine how climate change and tile drains may impact nitrogen loading.

Finally, another recommendation that could be implemented based on this thesis, would be to use updated tile drain spatial data. More tile drainage data for the watershed was recently published by Natural Resources and Values

Information System (NRVIS) in May of 2008 and made available at the UW map library. The tile drainage data used for this thesis was produced by the Ontario Ministry of Natural Resources in 2002. The new data can be implemented in the same fashion and the analysis that is outlined in this thesis can be repeated with the new information. Using more recent data can provide more accurate results on the total area of the watershed that is impacted by tile drains.

References

(2007), *ArcGIS 9.2 Desktop Help*, Environmental Systems Research Institute (ESRI), Inc.

Ahmad, K., P. W. Gassman, and R. Kanwar (2002), Evaluation of the tile flow component of the SWAT model under different management systems.

Akbari, H., L. S. Rose, and H. Tha (2003), Analyzing the land cover of an urban environment using high-resolution orthophotos, *Landscape and Urban Planning*, *63*, 1–14.

Anderson, J. H., L. Schluter, and G. Aetebjerg (2006), Coastal eutrophication: recent developments in definitions and implications for monitoring strategies, *Journal of Plankton*, *28*(7), 621–628.

ArmTec (2008), Products - agricultural drainage, `http://www.armtec.com/products_agricultural.html`.

Badiella, P. (2008), Photography and drawings, `www.telefonica.net/web2/pbadiella/photo.htm`.

Biocrawler (2005), The nitrogen cycle, `http://www.biocrawler.com/encyclopedia/Nitrogen_cycle`.

Bohdziewicz, J., B. Michal, and W. Ewa (1999), The application of reverse osmosis and nanofiltration to the removal of nitrates from groundwater, *Desalination*, *121*, 139–147.

Böhlke, J. K., R. Wanty, M. Tuttle, G. Delin, and M. Landon (2002), Denitrification in the recharge area and discharge area of a transient agricultural nitrate plume in a glacial outwash sand aquifer, minnesota, *American Geophysical Union*, *38*(7), 10–1–10–6.

Borah, D. K., and M. Bera (2003), Watershed-scale hydrologic and nonpoint-source pollution models: Review of mathematical bases, *American Society of Agricultural Engineers*, *46(6)*, 1553–1566.

Brooks, R. H., and A. T. Corey (1964), Hydraulic properties of porous media, *Hydrology Papers*, *3*, 27.

Burkart, M. R., and D. E. James (1999), Agricultural - nitrogen contributions to hypoxia in the gulf of mexico, *Journal of Environmental Quality*, *28*(3), 850–859.

Busse, T., and R. Hinkelmann (2006), Hydrodynamic-numerical modelling of surface flow in interaction with different hydrological processes, technische Universität Berlin, Institute of Civil Engineering, Department of Modeling of Hydrosystems.

Byre, K. R., J. M. Norman, L. G. Bundy, and S. T. Gower (2001), Nitrogen and carbon leaching in agroecosystems and their role in denitrification potential, *Journal of Environmental Quality*, *30*, 58–70.

Campbell, J. B. (2006), *Introduction to Remote Sensing, Fourth Edition*, The Guilford Press.

Carlier, J. P., C. Kao, and I. Ginzburg (2007), Field-scale modeling of subsurface tile-drained soils using an equivalent-medium approach, *Journal of Hydrogeology*, *341*, 105–115.

Colding, L. (1872), Om lovene for vandets bevaegelse i jorden, *Natur v. og math*, *9B*, 563–621.

Corporation, S. I. (2006), Msds: Anhydrous ammonia, `http://www.fertilizerworks.com/html/msds_anhyd.html`.

Croley II, T., and C. Luukkonen (2003), Potential effects of climate change on groundwater in lansing michigan, *Journal of the American Water Resources Association*, *39*, 149–163.

David, M., G. L.E., D. Kovacic, and K. M. Smith (1997), Nitrogen balance in and export from an agricultural watershed, *Journal of Environmental Quality*, *26*, 1038–1048.

Davis, D. M., D. J. Gowda, D. J. Mulla, and G. W. Randall (2000), Modeling nitrate leaching in response to nitrogen fertlizer rate and tile drain depth or spacing for southern minnesota, usa, *Journal of Environmental Quality*, *29*, 1568–1581.

Drinkwater, L. E., P. Wagoner, and M. Sarrantonio (1998), Legume-based cropping systems have reduced carbon and nitrogen losses, *Nature*, *396*, 262–265.

Eckhardt, K., and U. Ulbrich (2003), Potential impacts of climate change on groundwater recharge and streamflow in a central european low mountain range, *Journal of Hydrology*, *284*, 244–252.

Finch, J. W. (2001), Estimating change in direct groundwater recharge using a spatially distributed soil water balance model, *Quarterly Journal of Engineering Geology and Hydrogeology*, *34*, 71–83.

Flere, J. M., and T. C. Zhang (Eds.) (2001), *National Conference on Environment and Engineering*, 344–349.

Forchheimer, P. (1930), Hydraulik, *Introduction to soil physics*, *3*.

Goddard, L., S. J. Mason, S. E. Zebiak, C. F. Ropelewski, R. Basher, and M. A. Cane (2001), Current approaches to seasonal-to-interannual climate predictions, *International Journal of Climatology*, *21*, 1111–1152.

Grand River Conservation Authority (2008), Grand river conservation authority, `http://www.grandriver.ca/`.

Holysh, S., J. Pitcher, and D. Boyd (2000), Regional groundwater mapping: An assessment tool for incorporating groundwater into the planning process, *Tech. rep.*, Grand River Conservation Authority.

Hooghoudt, S. (1940), Bijdragen tot de kennis van eenige natuurkundige groothen van den grond, 7. algemeene beschouwing van het probleem ven de detail ontwatering en de infiltrate door middel van parrallel loopende drains, grepples, slooten en kanalen, *Versl. Landb. Ond. Algemeene Landsdrukkerij*, *46*, 515–707.

Hunter, W. J. (2001), Use of vegetable oil in a pilot-scale denitrifying barrier, *Journal of Conatiminant Hydrology*, *53*((1-2)), 119–131.

Intergovernmental Panel on Climate Change (IPCC) (2001), Climate change 2001: The scientific basis, Cambridge Univerity Press.

IPCC (2007a), Working group i report "the physical science basis" chapter 11: Regional climate projections, *Tech. rep.*, Intergovernmental Panel on Climate Change.

IPCC (2007b), Regional climate change projections, *Tech. rep.*, Intergovernmental Panel on Climate Change.

IPCC (2007c), Climate change 2007: Synthesis report, *Tech. rep.*, Intergovernmental Panel on Climate Change.

Irvine, D. G., K. Robertson, W. J. Hader, and R. West (1993), Applied geochemisrty, *Environmental Geochemistry*, *2*, 235–240.

Jaynes, D. B., T. S. Colvin, K. D. L., C. C. A., and D. W. Meek (2001), Nitrate loss in subsurface drainage as affected by nitrogen fertilizer rate, *Journal of Environmental Quality*, *30*, 1305–1314.

Jyrkama, M. I., and J. F. Sykes (2007), The impact of climate change on groundwater, *The Handbook of Groundwater Engineering 2nd Edition*, *2*, 28–1–28–42.

Jyrkama, M. I., J. F. Sykes, and S. D. Normani (2002), Recharge estimation for transient ground water modeiling, *Ground Water*, *40*, 638–648.

Kladivko, E. J., J. Grochulska, R. F. Turco, G. E. Van Scoyoc, and J. D. Eigel (1999), Pesticide and nitrate movement into subsurface tile drains on a silt loam soil in indiana, *Journal of Environmental Quality*, *20*, 264–270.

Kladivko, E. J., J. R. Frankenberger, J. D. B., D. W. Meek, and J. B. J. (2004), Nitrate leaching into subsurface drains as affected by drain spacing and changes in crop production system, *Journal of Environmental Quality*, *33*, 1803–1813.

Knutssen, G. (1988), Humid and arid zone groundwater recharge: a comparative analysis. estimation of natural groundwater recharge., *NATO ASI Series C*, *222*, 493–504.

Kovar, D. D., and J. Jorgensen (2004), Remote sensing, `http://maps.unomaha.edu/Peterson/gis/notes/RS2_files/optical.gif`.

Kyveryga, P. M., A. M. Blackmer, J. W. Ellsworth, and R. Isla (2004), Soil ph effects on nitrification of fall-applied anhydrous ammonia, *Soil Science of America Journal*, *68*, 545–551.

Le Maitre, D. C., D. F. Scott, and C. Colvin (1999), A review of information on interactions between vegetation and groundwater, *Water South Africa*, *25*, 137–152.

Lerner, D., A. S. Issar, and I. Simmer (1990), Groundwater recharge: a guide to understanding and estimating natural recharge, *International Contributations to Hydrogeology*, *8*, 208–214.

Loaiciga, H. A., J. B. Valdes, R. Vogel, J. Garvey, and H. Schwarz (1995), Global warming and the hydrologic cycle, *Journal of Hydrology*, *174*(1), 83–127.

Macrae, M., M. English, S. L. Schiff, and M. Stone (2007), Intra-annual variability in the contribution of tile drains to basin discharge and phosphorus export in a first-order agricultural catchment, *Agricultural Water Management*, *92*, 171–182.

Manabe, S., and R. T. Wetherland (1987), Large-scale changes in soil wetness induced by an increase in carbon-dioxide., *Journal of Atmospheric Science*, *44*(1), 1211–1235.

McGregor, J. L. (1997), Regional climate modeling, *Meteorology and Atmospheric Physics*, *63*, 105–117.

Ministry of the Environment (MOE) (2002), *Ontario Drinking Water Quality Standards (O. Reg 169/03)*, Ministry of the Environment (MOE).

Moody, W. (1966), Nonlinear differential equation of drain spacing, *Journal of Irrigation Drainage*, *92(2)*, 1–9.

Murphy, A. (1991), Chemical removal of nitrate from water, *Letters to Nature*, *350*, 223–225.

Muttiah, R. S., and R. A. Wurbs (2002), Scale-dependent soil and climate variability effects on watershed water balance method of the swat model, *Journal of Hydrology*, *256*, 264–285.

National Oceanic and Atmospheric Administration (NOAA) (2004), Gulf of mexico hypoxia watch, `http://www.ncddc.noaa.gov/ecosystems/hypoxia`.

National Oceanic and Atmospheric Administration (NOAA) (2008), National hurricane center, `http://www.nhc.noaa.gov/`.

NOLA.com (NOLA) (2007), Despite promises to fix it, the gulf's dead zone is growing, `http://blog.nola.com/times-picayune/2007/06/despite_promises_to_fix_it_the.html`.

North American Space Agency (NASA) (), Technical and historial perspectives of remote sensing, `http://rst.gsfc.nasa.gov/Intro/Part2_1.html`.

Ohio State University (1991), Ohio state university extension fact sheet: Nitrogen and the hydrologic cycle, `ohioline.osu.edu/aex-fact/0463.html`.

Ontario Ministry of Agriculture Food & Rural Affairs (OMAFRA) (2008), Tile drainage outlets, `http://www.omafra.gov.on.ca/english/engineer/facts/90-223.htm`.

Oosterbaan, R. (1994), Agricultural drainage criteria, *Drainage Principles and Applications*, *16*(2), 1–49.

Peck, A. J. (1978), Salinzation of non-irrigated soils: a review, *Australian Journal of Soil Research*, *16*, 157–168.

Prakasa Rao, E., and K. Puttanna (2000), Nitrates, agriculture and environment, *Current Science*, *79*(9), 1163–1168.

Presant, E. W., and R. E. Wicklund (1971), The soils of waterloo county, *The Ontario Soil Survey*, *44*, 1–147.

Rabalais, N. N., R. E. Turner, and W. J. Wiseman Jr. (2001), Hypoxia in the gulf of mexico, *Journal of Environmental Quality*, *30*, 320–329.

Ramanathan, V., and W. Collins (1991), Thermodynamic regulation of ocean warming by cirrus clouds deduced from oberservations of the 1987 el niño., *Nature*, *351*(1), 27–32.

Rosenburg, N. J., D. J. Epstien, L. Vail, R. Srinivasan, and J. G. Arnold (1999), Possible impacts of global warming on the hydrology of the ogallala aquifer region, *Climatic Change*, *42*, 677–692.

Rushton, K. R. (1988), Numerical and conceptual models for recharge models for recharge estimation in arid and semi-arid zones. estimation of natural groundwater recharge, *NATO ASI Series C*, *222*, 223–238.

Schroeder, P. R., C. M. Lloyd, P. A. Zappi, and N. M. Aziz (1994), *THE HYDROLOGIC EVALUATION OF LANDFILL PERFORMANCE (HELP) MODEL USER'S GUIDE FOR VERSION 3*, U.S. Environmental Protection Agency (EPA) Office of Research and Development, Washington, DC.

Scott, M. (2006), Grand river watershed analysis of nitrate transport as a result of agricultural inputs using a geographic information system, Master's thesis, University of Waterloo.

Singh, J., V. Knapp, J. Arnold, and M. Demissie (2005), Hydrological modeling of the iroquois river watershed using hspf and swat, *Journal of the American Water Resources Association*, *41(2)*, 343–360.

Singh, P., and R. S. Kanwar (1995), Modification of rzwqm for simulating subsurface drainage by adding tile flow component, *American Society of Agricultural Engineers*, *38*(2), 489–498.

Sklar, F. H., and J. A. Browder (1998), Coastal environmental impacts brought about by alterations to freshwater flow in the gulf of mexico, *Environmental Management*, *22*(4), 547–562.

Sloan, P., and I. Moore (1984), Modeling subsurface stormflow on steeply sloping forested watersheds, *Water Resources Research*, *20(12)*, 1818–1812.

Stillman, J. S., N. W. Haws, R. S. Govindaraju, and P. S. C. Rao (2006), A semi-analytical model for transient flow to a subsurface tile drain, *Journal of Hydrogeology*, *317*, 49–62.

Tilman, D. (1998), The greening of the green revolution, *Nature*, *396*, 211–212.

Toghi, H., T. Abe, K. Yamazaki, T. Murata, C. Isobe, and E. Ishizaki (1998), The cerebrospinal fluid oxidized NO metabolites, nitrite and nitrate, in alzheimer's disease and vascular dementia of binswanger type and multiple small infarct type, *Journal of Neural Tranmission*, *105*, 1283–1291.

Vitousek, P. M., J. D. Aber, R. W. Howarth, G. E. Likens, P. A. Matson, D. W. Schindler, W. H. Schlesinger, and D. G. Tilman (1997), Human alterations of the global nitrogen cycle: Sources and consequences, *Ecological Applications*, *7*(3), 737–750.

Walker, G. R., L. Zhang, T. W. Ellis, T. J. Hatton, and C. Petheram (2002), Estimating impacts of changed land use on recharge: review of modelling and other approaches appropriate for management of dryland salinity, *Hydrogeology Journal*, *10*, 68–90.

Wang, X., J. R. Frankenberger, and E. J. Kladivko (2006), Uncertainties in drainmod predictions of subsurface drain flow for an indiana silt loam using the glue methodology, *Hydrological Processes*, *20*, 3069–3084.

Wilby, R., and T. Wigley (1997), Downscaling general circulation model output: a review of methods and limitations, *Progress in Physical Geography*, *21*, 530–548.